

Distribution Agreement

In presenting this thesis or dissertation as a partial fulfillment of the requirements for an advanced degree from Emory University, I hereby grant to Emory University and its agents the non-exclusive license to archive, make accessible, and display my thesis or dissertation in whole or in part in all forms of media, now or hereafter known, including display on the world wide web. I understand that I may select some access restrictions as part of the online submission of this thesis or dissertation. I retain all ownership rights to the copyright of the thesis or dissertation. I also retain the right to use in future works (such as articles or books) all or part of this thesis or dissertation.

Signature:

Shala L. Thomas

Date

Analysis of the EF24-modulated signaling pathways for the development of
novel cancer combination therapies

By

Shala L. Thomas
Doctor of Philosophy

Graduate Division of Biological and Biomedical Science
Molecular & Systems Pharmacology

Haian Fu, PhD
Advisor

Dennis Liotta, PhD
Committee Member

Shi-Yong Sun, PhD
Committee Member

Lily Yang, MD
Committee Member

Accepted:

Lisa A. Tedesco, PhD
Dean of the Graduate School

Date

Analysis of the EF24-modulated signaling pathways for the development of
novel cancer combination therapies

By

Shala L. Thomas
B.S., Xavier University of Louisiana, 2003

Advisor: Haiyan Fu, PhD

An abstract of
A dissertation submitted to the Faculty of the Graduate School of Emory
University in partial fulfillment of the requirements for the degree of
Doctor of Philosophy

Molecular and Systems Pharmacology
Graduate Division of Biological and Biomedical Sciences

2009

Abstract

Analysis of the EF24-modulated signaling pathways for the development of
novel cancer combination therapies

By Shala L. Thomas

This dissertation seeks to uncover the cellular mechanisms of the curcumin analog EF24 that are responsible for its anticancer activity and differ from the parent compound. Additionally, this study highlights signaling pathways induced by EF24 that ultimately interferes with its therapeutic effect. We suggest that identifying these major pathways and inhibiting survival signaling will enhance the anticancer activity of EF24. We provide evidence that inhibiting p38 with pyridinyl imidazole compounds potentiates EF24-mediated inhibition of cancer cell proliferation and induction of apoptosis. Additional studies suggest that one way in which EF24-induced p38 activation promotes survival is through the specific transcriptional up-regulation of Hsp70, a heat shock protein strongly up-regulated in response to stress. Moreover, we show that EF24 treatment results in microtubule polymerization, leading to the inhibition microtubule-dependent pathways like HIF. p38 inhibition further enhanced microtubule polymerization, suggesting this anti-tubulin activity is involved in the synergistic nature of the EF24 and p38 inhibitor combination. The collective findings presented herein provide insight into the mechanisms by which EF24 promotes cancer cell death, the cellular response to EF24, and potential strategies in the form of combination therapies to exploit of these cellular activities.

Analysis of the EF24-modulated signaling pathways for the development of
novel cancer combination therapies

By

Shala L. Thomas
B.S., Xavier University of Louisiana, 2003

Advisor: Haian Fu, PhD

A dissertation submitted to the Faculty of the Graduate School of Emory
University in partial fulfillment of the requirements for the degree of
Doctor of Philosophy

Molecular and Systems Pharmacology
Graduate Division of Biological and Biomedical Sciences

2009

Table of Contents

	<u>Page</u>
I. Introduction	1
a. Curcumin	3
i. Historical uses	4
ii. Chemical properties	5
iii. Biological activity	7
iv. Inhibition of nuclear factor kappa-B (NF- κ B)	14
v. Curcumin-based clinical trials	20
vi. Development of curcumin conjugates and analogs	21
b. p38 Mitogen-activated protein kinase (MAPK) pathway	25
i. Identification and isoforms of p38	27
ii. Regulation of p38 activity	28
iii. Functional role of p38	30
iv. Involvement in heat shock protein 70 (Hsp70)	33
v. Small molecule p38 inhibitors	36
c. Microtubule	41
i. Structure and dynamics	41
ii. Regulation of microtubules	44
iii. Microtubule function	47
iv. Targeting microtubules for cancer therapy	50
v. Downstream hypoxia inducible factor-1 (HIF-1) pathway	56

II. Materials and Methods	64
III. Enhancing the anticancer activity of EF24 with p38 MAPK inhibitors	73
a. Rational	74
b. Results	76
c. Conclusions	105
IV. Induction of Hsp70 by EF24-mediated p38 signaling confers cancer survival advantage	110
a. Rational	111
b. Results	113
c. Conclusions	127
V. EF24 disrupts the microtubule cytoskeleton and inhibits HIF-1	130
a. Rational	131
b. Results	132
c. Conclusions	157
VI. Discussion	163
VII. References	169

Index of Figures

	<u>Page</u>
Figure 1.1 – Structure of curcumin	5
Figure 1.2 – Three major curcuminoids in turmeric	7
Figure 1.3 – NF- κ B-mediated target genes	15
Figure 1.4 – Canonical NF- κ B pathway	17
Figure 1.5 – Structure of EF24, a novel fluorinated analog	22
Figure 1.6 – EF24 is more potent against a panel of cancer cell lines than curcumin	24
Figure 1.7 – Regulation of the MAPK pathway	26
Figure 1.8 – Hsp70 prevent caspase-dependent and caspase-independent apoptotic signaling	35
Figure 1.9 – Commonly used pyrimidyl imidazole p38 MAPK inhibitors	36
Figure 1.10 – Organization and assembly of microtubule polymer	43
Figure 1.11 – The importance of microtubules in chromosome segregation and cell division	48
Figure 1.12 – Proposed drug binding sites on tubulin	51
Figure 1.13 – Hypoxic regulation of HIF-1 α controls the HIF-1 pathway	59

Figure 3.1 – The effect of curcumin and EF24 on A549 cell viability and the activation of the MAPKs	77
Figure 3.2 – Inhibition of p38 enhances EF24-induced growth inhibition	81
Figure 3.3 – Effect of SB203580 on dose-response growth curves of EF24 and curcumin	84
Figure 3.4 – Scheduling of the EF24 and SB203580 combination	87
Figure 3.5 – Knockdown of p38 sensitizes A549 cells to EF24-induced cytotoxicity	89
Figure 3.6 – Combination of EF24 and SB203580 synergistically induces apoptosis	92
Figure 3.7 – EF24 and SB203580 show a synergistic effect on the inhibition of A549 colony formation	95
Figure 3.8 – EF24 does not potentiate SB203580-mediated inhibition of p38 activity <i>in vitro</i>	98
Figure 3.9 – Combination of the specific IKK inhibitor and SB203580 does not cause a dramatic effect on cell viability	101
Figure 4.1 – EF24 specifically induces Hsp70 protein levels in a dose-dependent and time-dependent manner	115
Figure 4.2 – EF24 induces Hsp70 protein levels through increased transcription	117

Figure 4.3 – Inhibition of EF24-induced Hsp70 expression inhibits cancer cell viability	119
Figure 4.4 – Decrease in caspase-mediated apoptosis linked to EF24-induced Hsp70	122
Figure 4.6 – Inhibition of p38 MAPK downregulates EF24-induced Hsp70	1245
Figure 5.1 –EF24 induced mitotic arrest and stabilized interphase microtubules	134
Figure 5.2 – EF24, but not curcumin, induced microtubule stabilization	137
Figure 5.3 – Weak inhibition of tubulin assembly by EF24	142
Figure 5.4 – Inhibition of p38 MAPK pathway enhances EF24-induced microtubule stabilization	145
Figure 5.5 – EF24 and curcumin downregulate HIF-1 α and HIF-1 β levels and impair the transcriptional activity of HIF	148
Figure 5.6 – Curcumin and EF24 inhibit HIF-1 α in a VHL protein-dependent but proteasome-independent manner	152
Figure 5.7 – Curcumin, but not EF24, inhibits <i>HIF-1α</i> gene expression	155
Figure 6.1 – Working model of EF25-mediated cellular activity and proposed EF24-based combinations to elicit potentiated therapeutic effects	166

Index of Tables

	<u>Page</u>
Table 3.1 – EF24 and SB203580 cooperate to create cytotoxic synergism in multiple lung cancer cell lines	103
Table 5.1 – EF24 and curcumin both retain cytotoxic activity against a panel of β -tubulin mutants specific for the taxane and the epothilone binding sites	140

List of Abbreviations

17-AAG	17-allylamino-17-demethoxygeldanamycin
17-DMAG	17-dimethylaminomethylamino-17-demthoxygeldanamycin
2ME2	2-methoxyestradiol
AIF	apoptosis inducing factor
Ang	angiopoietins
AP-1	activating protein-1
ARNT	aryl hydrocarbon receptor nuclear translocator
ATP	adenosine triphosphate
Curc	curcumin
EGF	epidermal growth factor
ENO1	enolase 1
EPO	erythropoietin
ERK	extracellular signal-regulated kinase
FIH	factor inhibiting HIF-1 α
GSH	glutathione (reduced)
GSSG	glutathione disulfide (oxidized)
GST	glutathione-S-transferase
H ₂ O ₂	hydrogen peroxide
HIF-1	hypoxia inducible factor-1
HRE	hypoxia response element
HSE	heat shock response element
HSF1	heat shock transcription factor-1

Hsp	heat shock protein
IGF-1	insulin growth factor-1
JNK	c-Jun N-terminal kinase
LDHA	lactate dehydrogenase A
MAPK	mitogen-activated protein kinase
MAP	microtubule associated protein
MKK (MAP2K)	MAPK kinase
MKKK (MAP3K)	MAPK kinase kinase
MTOC	microtubule organizing center
NF- κ B	nuclear factor kappa-B
NO	nitric oxide
NSCLC	non-small cell lung cancer
ODD	oxygen-dependent degradation
PHDs	prolyl-4-hydroxylases
PI	propidium iodide
PI3K	phosphatidylinositol 3-kinase
PKA	protein kinase A
PKC	protein kinase C
PTX	paclitaxel
pVHL	Von Hippel-Lindau protein
RCCs	renal cell carcinomas
ROS	reactive oxygen species
SOD	superoxide dismutase

SRB	sulforhodamine B
TGF β	transforming growth factor-beta
TNF α	tumor necrosis factor-alpha
VCR	vincristine
VEGF	vascular endothelial growth factor
VEGFR	vascular endothelial growth factor receptor
VHL	von Hippel Lindau
$\Delta\Psi_{mt}$	mitochondrial membrane potential

CHAPTER 1

Introduction

Recently, much attention has been given to the development of anticancer pleiotropic agents, molecules that are not designed to target one specific protein, enzyme, or signaling pathway with great affinity but instead modulates a unique set of cellular factors leading to activity against cancer but not normal cells. Commonly, these are molecules isolated from natural sources, or complete or partial synthetic analogs of the aforementioned molecules, and have been used traditionally as medicinal agents for a variety of disease states or disorders because of their promiscuous therapeutic activity. Instead of the forward pharmacology approach of determining a molecular target and using medicinal chemistry to design molecules that specifically interact with a particular target, a reverse pharmacological approach is utilized. Potential chemotherapeutics are determined by extensively studying the efficacy of natural agents against particular cancer populations, and molecular biology is then used to determine the mechanism of action of these agents. By evaluating recent research data, this introduction seeks to summarize the development of the synthetic analog EF24 from the natural product curcumin and our current understanding of the mechanisms of contributing to its cellular activity involving the NF- κ B, p38 MAPK, Hsp70, HIF-1 and the microtubule cytoskeleton.

CURCUMIN

Curcumin is a naturally occurring polyphenolic compound isolated from turmeric, the spice extracted from the root of the East Indian *Curcuma Longa* plant. Curcumin is the principal yellow component of all curry powders and pastes and has been used in Eastern traditional medicine to treat liver disease, rheumatoid arthritis, and insect bites for centuries, demonstrating its high tolerability. Due to the established connection between chronic inflammation and cancer, curcumin has been tested as a potential chemopreventative agent and chemotherapeutic in Phase I/II clinical trials. Presently, however, the complete mechanisms of action are not completely understood. Data suggests that curcumin has powerful antioxidant capabilities as well as inhibits the cytosolic activation of nuclear factor of kappa-B (NF- κ B) by blocking its nuclear translocation. There are also reports that link curcumin-mediated apoptosis to the attenuation of other important transduction pathways involved in cell survival and growth including the protein kinase C (PKC) and mitogen-activated protein kinases.

Though curcumin represents an ideal chemotherapeutic and chemopreventative agent due to its low molecular weight and low toxicity, its low potency and poor absorption pose important concerns regarding its clinical efficacy. Thus, the compound's poor bioavailability in humans has prompted investigation of curcumin as a lead structure in the development and synthesis of analogs with enhanced pharmacokinetic profiles and activity. One such compound is the fluorinated curcumin analog EF24, synthesized at Emory and shown to be the most active among 100 novel synthetic

curcumin analogs tested for antiangiogenic and anticancer activity. In addition, even though EF24 appears to be one of the most active of the synthetic curcumin analogs, it remains less toxic *in vivo* than the commonly prescribed chemotherapeutic agents such as cisplatin.

1.1. Historical uses

Compounds made by plants and microproducts or modified versions of these compounds have historically been used as a rich source of medicinal agents for ailments and diseases (1, 2). Oral administration of curcumin has known to treat the common cold, liver diseases, urinary tract infections, and cancer while topical treatment helps to heal wounds, parasitic skin infections, and acne. The origin of curcumin (diferuloylmethane) is from turmeric, a spice isolated is the *Curcuma Longa* plant that is native to India and also cultivated in south and southeast tropical Asia (3). Turmeric is comprised of three major curcuminoids, the major component being curcumin (4). Eastern cuisine, including curried food, is usually seasoned heavily with turmeric and gives it its spicy favors and color. The average intake of turmeric in India is approximately 2-2.5g daily based on normal diets (5). Epidemiological data shows lower cancer rates for people in these eastern regions possibly due to high curcumin-content diets (5, 6). To support this claim, the cancer rates have been shown to then become similar in second generation immigrants who have migrated to the west. Adaption of a more western lifestyle, lacking curcumin, by the same group of people is thought to contribute to this higher incidence of cancer (5).

1.2. Chemical properties

Curcumin, or diferuloylmethane, is a α , β -unsaturated ketone which comprises about 2-8% of turmeric by weight and exists as an orange-yellow crystalline powder. The molecular weight of curcumin is 368.4 g/mol, and the melting point is 179-183°C. The chemical structure of curcumin was first described in 1973 and includes two methoxyl groups, two phenolic hydroxyl groups, and three double conjugated bonds. The bis-keto form of curcumin predominates under neutral and acidic aqueous conditions but exists in equilibrium with its enol tautomer especially at room temperature (Fig 1.1).

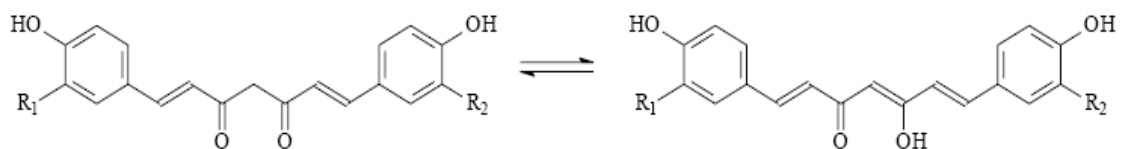


FIG 1.1. Structure of curcumin. Curcumin contains two carbonyl groups which forms a diketone. The diketone switches between the stable enol (protonated) and enolate (deprotonated) forms.

Ortho-substituted α , β -unsaturated ketones are the most potent antioxidants, which may contribute to the ability of curcumin to scavenge damaging free radicals (7). In the keto form, the heptadienone linkage between the two methoxyphenol rings contains a highly activated carbon atom. Also, the α , β -unsaturated β -diketone moiety acts as Michael acceptors which is thought to be important to the curcumin-induced

cytotoxicity (8). In a Michael addition, a carbanion nucleophile attacks an active and susceptible α , β -unsaturated carbonyl compound, such as curcumin, at the β carbon.

Curcumin is unstable at $\text{pH} > 7$ and degrades readily though research studies have found that this degradation is blocked by the presence of serum or human blood or with the addition of antioxidants such as ascorbic acid, *N*-acetylcysteine, or glutathione. Degradation of curcumin has also been found to be much slower under acidic conditions. Curcumin is an extraordinarily potent H-atom donor at low pH but mainly acts as an electron donor at basic pH. Curcumin is insoluble in water but it is soluble in acetone, ethanol, and dimethylsulfoxide. Curcumin's photochemical instability makes it particularly sensitive to light, and maximum light absorption occurs at 420nm (9).

Curcumin is commercially available but most commonly not in pure form (10). This preparation contains a mixture of the three curcuminoids of turmeric which are extracted from the roots of the *Curcuma Longa* plant: curcumin [1], desmethoxycurcumin [2], and bisdesmethoxycurcumin [3] (Fig 1.2). Like curcumin, the other curcuminoids are polyphenols, however, they are less active when isolated from turmeric extracts (11). Curcumin is the major curcuminoid, about 70-75% of the curcuminoid content in turmeric. Demethoxycurcumin comprises the second largest amount of curcuminoid composition (15-20%) while bisdemethoxycurcumin only makes up about 5%.

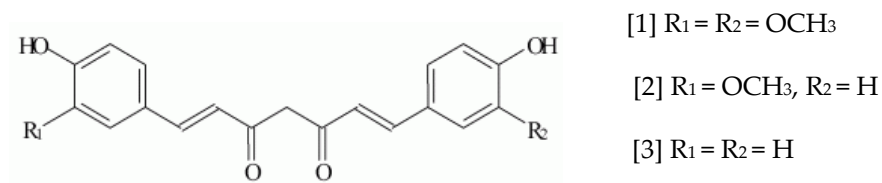


FIG 1.2. Three major curcuminoids in turmeric. Curcumin is the major component of the spice turmeric with two other structurally-related curcuminoids demethoxycurcumin and bis-demethoxycurcumin.

1.3. Biological activity

Curcumin has been studied extensively in pre-clinical *in vitro* models and has been described in the literature to have potential as both a chemopreventative agent and a chemotherapeutic. These research efforts include providing scientific evidence for its traditional use in medicine. Since curcumin has often been described as the “miracle spice”, due to its pharmacological activity against not only cancer but countless other disease states including HIV, cystic fibrosis, and Alzheimer’s, the molecular targets of curcumin has been of interest. After years of investigation, curcumin is believed to target and modulate multiple gene products, which contribute to its biological activity. These gene products include inflammatory cytokines, biotransformation enzymes, transcription factors, and other molecular factors involved in cancer survival, proliferation, and metastasis. Curcumin modulates the activity of these proteins by inhibiting their enzymatic activity or increasing or decreasing expression. Due to its

molecular activity, curcumin has also been shown to sensitize cancer cells that are otherwise chemoresistant and radioresistant to cancer therapy.

Chemopreventative activity

Chemoprevention is defined as intervening in the major stages of cancer development - initiation, promotion, and progression - to prevent carcinogenesis or reduce the risk of cancer formation (12). Like other polyphenols (i.e. isoflavanone, resveratrol), curcumin has garnered attention due to its chemopreventative activity (13). Epidemiological studies across human populations show a negative correlation between the dietary consumption of curcumin and the incidence of common cancers, such as breast, prostate, colon, and lung (14). Curcumin also was able to decrease the number of pre-malignant lesions in a number of patients with a predisposition to cancer. This is consistent with data demonstrating that most chemopreventative agents are natural products derived from plant extracts (15, 16).

As a chemopreventative agent, curcumin is thought to protect against cancers induced by environmental chemicals and other toxic carcinogens. Data from rodent models of these cancers showed prevented the onset of cancer induced by carcinogens like 7,12-dimethylbenz[a]anthracene (DMBA) and benz(a)pyrene based on the reduction in the number of tumors formed and the reduction in tumor size (11, 17-20). Additionally, studies show that curcumin not only effectively inhibited the incidence of diethylnitrosamine-induced hepatocarcinogenesis in rodents according to

histopathological examination but also caused a reduction in multiplicity (21). It is postulated that the chemopreventative ability of curcumin may in part be due to its oxidant scavenging capabilities, induction of endogenous intercellular antioxidants, and modulation of biotransformation enzymes which are known to metabolize carcinogens.

Many natural products and derivatives from these agents have shown considerable promise as chemopreventative agents by reducing oxidative stress, the imbalance of the oxidant to antioxidant ratio. It is accepted that high levels reactive oxygen species play a key role in carcinogenesis and that reversal of the malignant phenotype of cancer cells can be accomplished by reducing or preventing ROS formation. If this is beyond the normal intercellular antioxidant capacity of the metabolites ascorbic acid (vitamin C), glutathione, and ubiquinol (coenzyme Q), oxidation reactions can produce free radicals which can damage and mutate DNA and other cell structures, leading to aberrant cell growth. Thus, antioxidant agents can be used to revert pre-cancerous cells to a normal appearance, normalize growth curves, and decrease the tumor-producing ability of these cells when injected in immunocompromised mice.

The antioxidant potential of curcumin has been demonstrated in *in vitro* cell models where curcumin is an effective free radical scavenger by directly reacting with radical species. Because of this scavenger activity, oxidative DNA damage has been shown to be inhibited with curcumin treatment (22). Additionally, curcumin lowers lipid peroxidation by enhancing the activity of antioxidant enzymes like catalase,

superoxide dismutase, and glutathione peroxidase (23). The high antioxidant potential of curcumin is evident when you consider how curcumin has been found to have a 100-fold greater antioxidant capacity than vitamin E (24). In an oxidative stress mouse model, oral pretreatment of curcumin protected against cadmium-induced oxidative damage of lipids (25). Indirectly, curcumin also acts as an antioxidant by upregulating the levels of the endogenous antioxidant system metabolites like the tripeptide glutathione, an antioxidant important in cellular adaptation to stress. This is achieved through the induction of glutathione-S-transferase, possibly through the increase of glutathione-S-transferase (GST) mRNA (26).

Metabolism of xenobiotics to a more soluble entity is typical in the body. This is accomplished by the work biotransformation enzymes in the liver or gut, divided into phase I and phase II pathways, which modify the compound by chemical reactions or conjugations. Though metabolism of xenobiotics that enter the body may enhance the elimination of these compounds, often times phase I enzymes activate the compound to harmful carcinogens. Curcumin has been found to inhibit metabolizing enzymes which bioactivate carcinogens that are normally inactive (27). This includes alkylation reactions catalyzed by the cytochrome P450 isozymes 1A1, 1A2, and 2B1 in cell and animal models. In one study, curcumin was found to decrease cytochrome P450 and aryl hydrocarbon hydroxylase (AHH) activity, resulting in the decrease in the bioactivation of benzo[a]pyrene and ultimately in DNA-adduct formation (11). Curcumin even induce conjugating phase II enzymes like GSTs and quinone reductases

which deactivate normally active carcinogens (28). The activity of curcumin on biotransformation enzymes is heavily dependent on concentration. However, curcumin contributes to the decrease activation and deactivation of harmful carcinogens and potentially decrease the risk of carcinogenesis in this way (29).

Induction of cell cycle arrest and apoptosis

Curcumin globally induces apoptosis, or programmed cell death, in a variety of cancer cell lines from the breast, cervix, prostate, lung, skin, and lymph nodes (30, 31). Classic characteristics of cancer including DNA fragmentation, cell shrinkage, and membrane blebbing were all observed following curcumin treatment of cell cultures. The induction of apoptosis by curcumin is almost exclusively in cancerous cells with normal cells being left relatively unaffected (30). It is for this reason in animal models (i.e. mice, rats, monkeys, guinea pigs) that administration of curcumin causes very little to no toxicity noted by changes significant weight loss or adverse events to the liver or kidneys. The mechanism of how curcumin induces apoptosis varies but is thought to be through modulation of pathways leading to the mitochondrial release of cytochrome c and downstream caspase activation (32). Documented reports describing curcumin-induced apoptosis point to this compound activating only the intrinsic apoptotic pathway and not the extrinsic pathway (33). However, curcumin, though its induction of mitochondrial apoptosis, has been shown to sensitize malignant and chemotherapeutic-resistant cell lines to factors that induce extrinsic apoptosis (i.e. TRAIL, FasL) (34).

Curcumin is also reported to arrest cancer cells in the G₁/S or G₂/M phase of the cell cycle depending on the origin of the cell line, which also diverts cells into the apoptotic pathway (20, 35, 36). One mechanism by which curcumin induces cell cycle arrest is by the downregulation the expression of cyclin E and D, proteins which are involved heavily in the progression of cells through the cell cycle by regulating cyclin-dependent kinases. Recently a connection was found between the induction of apoptosis by curcumin and the ability of curcumin to inhibit the cell cycle. Genetic inhibition of the cyclin-dependent kinase (Cdk) inhibitor p21, which is induced by curcumin, blocks curcumin-induced apoptosis (37).

Anti-inflammatory activity

Based on its historical uses, curcumin has widely been used as an effective anti-inflammatory agent, which may also contribute to its anticancer activity. A connection between chronic inflammation and cancer has long been proposed. The potent anti-inflammatory activity of curcumin is believed to be mediated through the inhibition of prostanoids and alteration of eicosanoid metabolism, which mediate the inflammatory response (38). Pharmacological inhibition of prostanoids has been a known strategy to reduce inflammation. Prostanoids, including prostaglandins and prostacyclins, are synthesized by the conversion of arachidonic acid by cyclooxygenase (COX). Data suggests that curcumin decreases the catalytic activity of phospholipase A₂ (PLA₂), leading to a decrease in arachidonic acid release from the phospholipid membrane (39). Curcumin also intervenes in this pathway by blocking the chemical modification of

arachidonic acid through its inhibition of COX. The ability of curcumin to inhibit COX, as well as pro-inflammatory cytokines like tumor necrosis factor-alpha ($\text{TNF}\alpha$), is most likely through downregulation of nuclear factor of kappa-B (NF- κ B), the transcription factor that controls expression of these proteins. In order to demonstrate that curcumin inhibits the action of arachidonic acid, studies showed that topical application of curcumin inhibited edema of mouse ears induced by arachidonic acid (40).

Molecular targets

Curcumin has found to have many different molecular targets which may be important for its biological activity. Another major target of curcumin is the c-jun N-terminal kinase (JNK) signaling pathway apparent from the curcumin-mediated downregulation of activating protein-1 (AP-1), a downstream effector of JNK (41, 42). Curcumin inhibits a range of enzymes (i.e. protein kinase C (PKC), epidermal growth factor receptor (EGFR), telomerase (hTERT)) and alters the expression of proteins involved in signaling and cellular regulation (i.e. c-myc, cyclin-dependent kinases (CDKs), telomerase (hTERT)) (32, 43, 44). Modulating all of these intercellular factors may contribute to the anticancer properties of this natural product and may even explain the efficacy of curcumin against models of other disease states including cystic fibrosis, Alzheimer's disease, arthritis, diabetes, and cardiovascular disorders (14, 45-48).

1.4. Inhibition of nuclear factor of kappa-B (NF- κ B)

The anticancer properties of curcumin are majorly attributed to its ability to inhibit the activation of the transcription factor NF- κ B induced by a variety of stimuli (49, 50). Numerous published reports demonstrate the blockage of NF- κ B activation mediated by curcumin (41, 42). Suppression of NF- κ B has been found to inhibit proliferation, cause cell cycle arrest, and lead to apoptosis, which are all activities shown to be caused by curcumin treatment.

NF- κ B was discovered in 1986 as a factor in the nucleus of B cells that binds to the 10-base pair enhancer region of the kappa light chain of immunoglobulins. This factor was believed to be only central to the immune system since it was activated by a variety of pathogens. However, NF- κ B now represents a family of transcription factors that are found in almost every mammalian cell type. The NF- κ B pathway is highly involved not only in the inflammatory response but also in cell proliferation and suppression of apoptosis. NF- κ B binds to its specific consensus sequence on DNA and controls the transcription of over 200 genes such as survivin, XIAP, cyclin D1 and Bcl-2 which help to control the fate of a cell (Fig 1.3). The eventual outcome of NF- κ B signaling depends on not only the heterodimer involved, but also the cellular stimuli that lead to NF- κ B pathway activation.

Members of the NF- κ B family include c-Rel, Rel A (p65), Rel B, NF- κ B-1 (p105 processed to p50), and NF- κ B-2 (p100 processed to p52), which all share a 300-amino

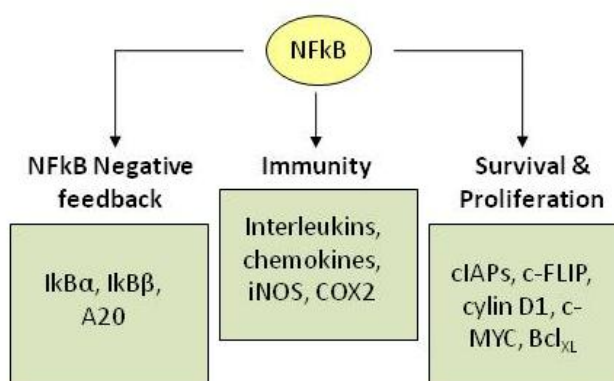


FIG 1.3. NF- κ B-mediated target genes. The transcription factor NF- κ B controls the transcription of over 200 target genes involved in aspects of immunity, cell proliferation and invasion from apoptosis, and factors that participate in NF- κ B pathway regulation.

acid Rel homology domain (RHD) in the N-terminal protein. These NF- κ B family members dimerize through the RHD and normally exist as heterodimers or homodimers in the cytoplasm. Stimulatory transcriptional pairs contain RelA, c-Rel, or Rel-B which have C-terminal transcriptional activation domains (TAD), enabling NF- κ B to activate gene expression. Homodimers of p50 and p52, which are processed from the larger precursors p105 and p100 respectively, can not stimulate transcription since they do not contain TADs and are known to repress transcription.

Canonical NF- κ B pathway

The major regulator of the cytokine transcription is the canonical NF- κ B pathway, in which NF- κ B is comprised primarily of the p50 and p65 subunits (Fig 1.4). Generation of p50 from the larger precursor p105 is a constitutive process involving the

proteasomal degradation at the ankyrin repeats of the C-terminal region. Under low stimulus conditions, the p50/p65 complex is retained in the cytoplasm by its interaction with the inhibitor of NF- κ B (I κ B). I κ B α , an ankyrin domain containing protein, masks the nuclear localization sequence (NLS) by virtue of its ankyrin repeats, preventing NF- κ B import into the nucleus. Though there are many members in the I κ B family known to act as endogenous NF- κ B inhibitors (i.e. I κ B β , I κ B γ , I κ B ϵ), I κ B α is the one of which the most is known. When this canonical pathway responds to activating stimuli such as cytokines, radiation and inflammation, I κ B α is phosphorylated on two key serines (Ser³² and Ser³⁶ on human I κ B α) by the I κ B kinases, or IKK. IKK is a trimeric complex of two catalytic subunits (IKK α and IKK β) and one regulatory subunit (IKK γ or NF- κ B essential modulator, NEMO). Though studies have shown that both IKK α and IKK β have similar catalytic activities, IKK β is more important to the activation of the canonical pathway than IKK α . Although the signaling upstream of IKK is not completely dissected, IKK is known to be directly phosphorylated and activated by various kinases including Akt. Once I κ B is phosphorylated, it is marked for ubiquitination on Lys²¹ and Lys²² and is then subsequent degradation by the 26S proteasome. Phosphorylation and ubiquitination of I κ B precedes the dissociation of I κ B from NF- κ B. Degradation of I κ B releases NF- κ B and it is then free to translocate to the nucleus in order to stimulate transcription of NF- κ B-mediated target genes.

The exact target of curcumin in the NF- κ B pathway is still in question though it is believed to inhibit pathway activation some where upstream of I κ B α phosphorylation,

preventing the degradation of I κ B α and NF- κ B nuclear translocation (41, 42). Many published reports explain the anti-NF- κ B activity of curcumin by suggesting IKK β as a direct target in cancer cell models though recent data from our lab using immunoprecipitated IKK β in an *in vitro* kinase assay refutes those claims (51, 52). As a consequence of NF- κ B downregulation by curcumin, expression of inflammatory cytokines involved in the inflammatory response and metastasis are also decreased (53, 54).

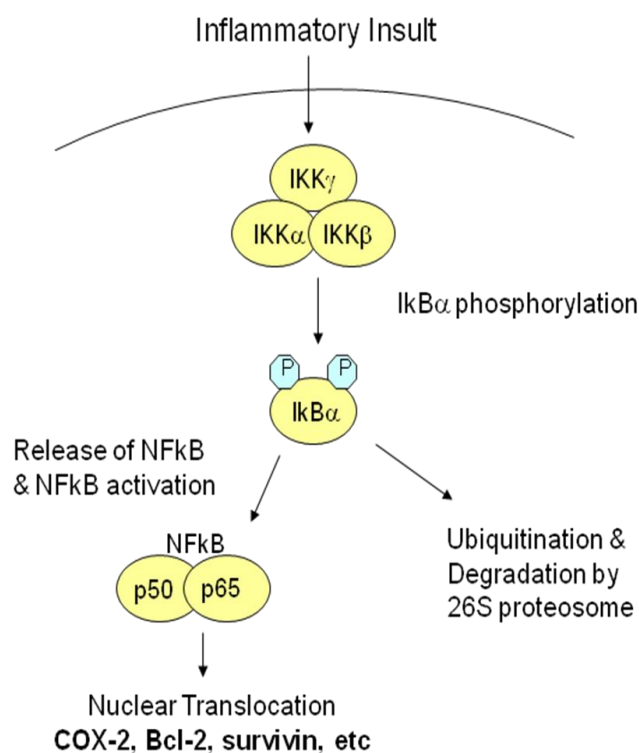


FIG 1.4. Canonical NF- κ B pathway. The kinase IKK mediates signaling through the canonical NF- κ B pathway. Activation of NF- κ B occurs through phosphorylation and degradation of the I κ B inhibitory subunit, freeing the RelA-p50 complex to translocate to the nucleus and binding κ B DNA sequences.

Non-canonical NF- κ B pathway

In the non-canonical pathway, NF- κ B-transcription is mediated through Rel B and p52. This pathway is mainly involved in the development of lymphoid organs responsible for the generation of B and T lymphocytes and is found to be activated by stimulating factors at the B cell-activating factor receptor, lymphotoxin-beta receptor, and latent membrane protein-1 (LMP-1) receptor. Receptor stimulation then leads to the activation of the NF- κ B-inducing kinase (NIK) which then phosphorylates and activates a two IKK α subunit complex. The p100 subunit, which is bound to Rel B in the cytoplasm and prevents the heterodimer from nuclear localization, is phosphorylated by this IKK α homodimer. Phosphorylation targets p100 for processing by the proteosomal degradation down to the p52 subunit. The Rel B/p52 heterodimer is then free to translocate to the nucleus and bind to κ B sites to regulate transcription.

Oxidative stress-induced NF- κ B

The NF- κ B pathway responds positively to oxidative stress, an increase in pro-oxidants over antioxidants. Direct addition of H₂O₂ has been found to activate NF- κ B in certain cell lines. Since many agents that induce NF- κ B activation seem to simultaneously induce increases in intracellular levels of ROS, it has also been proposed that agents that induce NF- κ B activation do so through production of ROS. This activation of the NF- κ B pathway seems primarily to be due to IKK, which has been found to be a redox-sensitive kinase and becomes activated readily by hydrogen

peroxide and other ROS second messengers. Consistent with this idea, activation of IKK has been found to be attenuated by antioxidants and by inhibition or overexpression of enzymes that affect intracellular ROS levels. The mechanism for oxidative stress-induced activation of IKK is still under investigation and may be cell-type specific.

Other anti-NF- κ B strategies

Inhibition of the NF- κ B pathway is thought to be beneficial to many disease states but especially cancer where NF- κ B has been found to be constitutively active in most cancer cell lines and also patient samples of hematopoietic and solid tumors compared to normal tissue. This is especially true for cancers that overexpressed EGFRs and over activation of the Akt pathway. The cause of this continuous activation may possibly be through mutations in I κ B α that prevent NF- κ B binding, enhanced proteasomal degradation of I κ B α , or increase cytokine expression.

Many strategies for NF- κ B inhibition have been proposed. Proteasome inhibitors like MG132, which is used for exclusively experimental purposes, and PS-321 (velcade, bortezomib), which has had mild success in the clinic, have been found to block NF- κ B activity (39, 55). These inhibitors are thought to decrease activation of NF- κ B by inhibiting I κ B proteolysis. Clinical studies looking at combining these proteasome inhibitors with chemotherapeutics that are known to induce NF- κ B are currently underway. Other compounds including glucocorticoids, hsp90 inhibitors, and PPAR γ antagonists have been shown to decrease NF- κ B activity by various mechanisms (56).

More targeted approaches to the NF- κ B pathway like using small inhibitory RNA (siRNA) against p65 NF- κ B and inhibitors against kinases upstream of NF- κ B activation has shown some efficacy in inhibiting cancer cell proliferation and sensitizing cells to other chemotherapeutics *in vitro* (57). Currently, the most attention is being given to developing inhibitors to the canonical pathway that directly target IKK β . Publish reports hint that inhibiting the activity of IKK β induces cell death melanoma and multiple myeloma as well as leads to chemosensitivity in cancer cell models.

1.5. Curcumin-based clinical trials

Based on encouraging pre-clinical experimental data, several human trials have been initiated and are enrolling patients. The safety of curcumin has been demonstrated in studies with healthy volunteers, showing no significant changes to liver and kidney functions and blood counts (58). A few preliminary studies observing the clinical efficacy of curcumin in different populations of individuals who are at high risk for cancer have been conducted (59). The effects of curcumin have also been studied in patients with HIV, rheumatoid arthritis, cancer, chronic pancreatitis, and psoriasis (60). Indications of the maximal tolerated dose (MTD) and bioavailability of curcumin have been reported from phase I/II clinical studies and dose escalation studies (61). One clinical study suggests that there is no treatment-related toxicity at up to 8,000 mg/day of curcumin but show a peak plasma concentration at that dose of only $1.77 \pm 1.87 \mu\text{M}$ (59). Furthermore, when two grams of oral curcumin is ingested, very low steady-state levels or even undetectable levels were found in the serum. Though curcumin has a poor

bioavailability profile, Phase II clinical trials do report some biological activity which also confirms the pre-clinical reports that curcumin is an anti-NF- κ B agent. Curcumin down-regulated NF- κ B-regulated biomarkers like IL-6 and COX-2 in peripheral blood mononuclear cells from pancreatic cancer and colon cancer patients.

Additionally, human subjects appear to be able to tolerate curcumin at a higher dose than preclinically-tested animals. The difference between animal and human test subjects may be due to variations in metabolism manifested by the differential expression and/or activity of p450s and other metabolizing enzymes. It has been a question whether the activity of curcumin is exerted by the compound itself or metabolite(s). Low systemic bioavailability following oral administration thought to be due to first pass metabolism and some degree of intestinal metabolism (62). Conjugates of curcumin like curcumin glucuronides and curcumin sulfates were found in the circulation as well as hexahydrocurcumin, formed from the reduction of curcumin (63). Tests show that these metabolites have less biological activity than curcumin.

1.6. Development of curcumin conjugates and analogs

To address the issues of curcumin's poor bioavailability when given orally (64), methods such as co-supplementation of curcumin with piperine to increase absorption have been used. Different methods of encapsulation in liposomes, polymeric nanoparticles, and other lipid-based nanoparticles have also shown some preclinical potential (65). Since curcumin lacks water solubility, a factor that contributes to its poor

absorption, efforts to create curcumin conjugates that will make the compound more water soluble have been attempted. Conjugation of curcumin with such molecules as poly(ethylene glycol) has had limited success.

More attention has been given to optimizing the structure of curcumin to design curcumin analogs with better bioavailability, solubility, and activity *in vitro* and *in vivo* (65). The structure of curcumin has proven to be a good starting point for drug discovery based on the large amount of preclinical and clinical data available. Three areas of have been focused on to improve on the efficacy of curcumin – aromatic rings, beta-diketone moiety, two flanking double bonds. Extensive structure-activity relationship studies have been conducted to explore mono-carbonyl derivatives and diarylpentanoids for its anticancer activity. Over 100 compounds were synthesized by our collaborators using curcumin as the lead structure. This panel of compounds included the very potent EF24, a fluorinated curcumin analog (Fig 1.5).

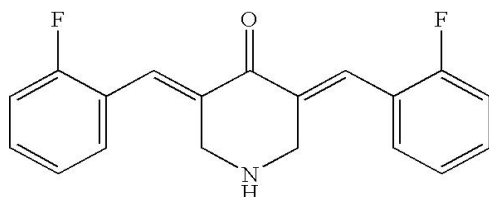


FIG 1.5. Structure of EF24, a novel fluorinated analog. Curcumin was used as a lead compound in the design of analogs to address the solubility and bioavailability issues of the parent compound. EF24 was found to be one of the most active compounds.

EF24 exhibits over 10 times more biological anticancer activity than curcumin in cell culture when comparing IC₅₀ values (Fig 1.6) and shows good oral bioavailability and pharmacokinetics in mouse models (66, 67). The *in vitro* activity of EF24 includes potent cytotoxicity and induction of apoptosis as measured by cell viability, cell cycle analysis, caspase 3 activation, and phosphatidylserine externalization (66, 68, 69). EF24 is also more effective than curcumin in reducing tumor size and volume in mouse models (67). Though this activity *in vivo* is possibly due to the ability of EF24 to inhibit cancer cell proliferation, it also may be due to its increased solubility and absorption.

Like the parent compound curcumin but with greater potency, EF24 effectively suppresses NF- κ B activation upstream of I κ B phosphorylation. However these compounds differ in their anti-NF- κ B mechanism of action (52). Recent data suggests that EF24 directly targets IKK while curcumin does not. Though EF24 may also affect other points in the NF- κ B pathway, this study indicates that IKK is a major target of EF24. EF24 also shares with curcumin the ability to act as a Michael acceptor and reacts with endogenous GSH, affecting the intercellular levels glutathione (69). This redox-mediated activity has been proposed to alter mitochondria function and contribute to EF24-induced apoptosis (69). EF24 has even been reported to be effective against chemotherapeutic-resistant cell lines, indicating its potential use against drug resistance to other agents in the clinic (68).

Furthermore, conjugates with EF24 have proven even more effective against cancer models and is used to specifically target EF24 to tumor cells (67). Recently, a

specific drug delivery system comprised on EF24 chemically conjugated to coagulation factor VIIa (fVIIa) through a tripeptide-chloromethyl ketone was found to significantly reduce tumor size in breast cancer xenografts compared to curcumin and even to unconjugated EF24 (70). Further investigation into the molecular mechanism of EF24 will benefit the clinical development of this agent as a potential anticancer therapy.

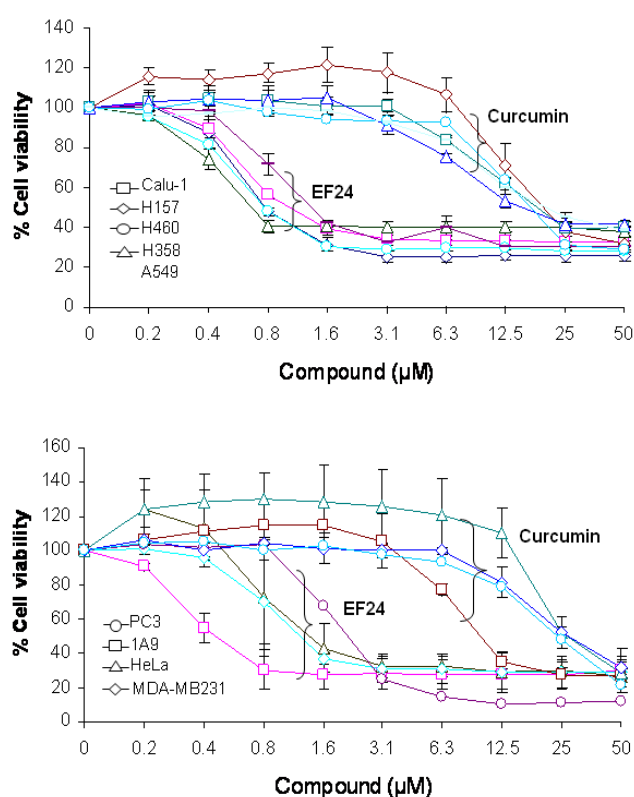


FIG 1.6. EF24 is more potent against a panel of cancer cell lines than curucmin. Results from SRB cell viability assess with a panel of lung cancer cells: (**Top**) A549, H358 (adenocarcinoma), H460 (large cell carcinoma), H157 (squamous cell carcinoma), and Calu-1 (epidermoid carcinoma). (**Bottom**): breast (MDA-MB231), cervical (HeLa), prostate (PC3), and ovarian (1A9) cancer cell lines.

P38 MAPK

p38 MAPK is one of the three major mitogen-activated protein kinases (MAPKs), along with initial member extracellular-regulated kinase (ERK) and the c-jun N-terminal kinase (JNK), which has been found to exist in the majority of eukaryotes (Fig 1.7). Discovered in yeast as HOG1, the p38 MAPK pathway has been found to be tightly controlled by a system of cellular pathways. Like other members of the MAPK family, p38 responds to stimuli acting through diverse receptors and intercellular molecules and is activated by phosphorylation of its specific Thr/Tyr motif. Characteristically, p38 is activated by stress stimuli and mediates a cellular stress response. Through phosphorylation of its substrates, p38 MAPK coordinates the activation of gene transcription, protein synthesis, cell proliferation and differentiation. p38 is known to modulate the activity of factors important for cellular regulation including p53, heat shock protein 27 (hsp27), and activating transcription factor (ATF). Signaling through p38 is terminated by dephosphorylation of p38 by MAPK-specific phosphatases. Though p38 is majorly considered a pro-apoptotic kinase, publish reports hint at possible pro-survival functions for p38, depending on the particular cell stimuli and temporal activation.

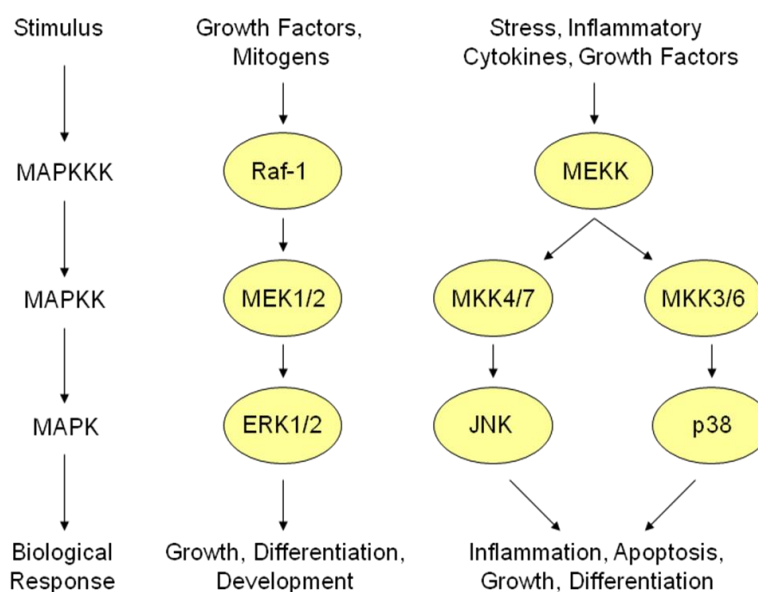


FIG 1.7. Regulation of the MAPK pathways. MAPK pathways are three-tiered kinase pathways that are activated by dual phosphorylation and signal to transcription factors which control the transcription of factors involved in growth & differentiation, inflammation, and apoptosis.

The p38 MAPK pathway acts in concert with the NF- κ B pathway, linking this MAPK with the propagation of inflammation. Experimental use of the pyridinyl imidazole class of p38 MAPK inhibitors has connected the p38 MAPK pathway to the synthesis of cytokines, mediators of the inflammatory response. Development of inhibitors to p38 is in the forefront of clinical research into agents to treat inflammatory diseases with the prototypical pyridinyl imidazole compounds used in the design of these therapeutic agents. Chronic inflammation has been associated with tumors or even may be considered an initiator of the cancer development. Due to this, p38 MAPK

inhibitors have been tested for potential use in cancer therapy with some promising compounds entering clinical trials.

2.1. Identification of p38 MAPK

P38 MAPK (also referred to as reactivating kinase, or RK) was first identified in murine pre-B cells as a protein of 38-kDa that responded to LPS stimulation and osmotic shock (71). The polypeptide was eventually isolated and purified by anti-phosphotyrosine immunoaffinity chromatography. Molecular cloning revealed a 40-50% similarity to the MAPK family of protein kinases. Many groups also identified that this was a kinase involved in the cell's response to physiological stress. Around the same time, p38 was discovered as the target of the pyrimidyl imidazole compounds which were known to inhibit cytokine biosynthesis. The corresponding ortholog, the Hog1 pathway, was found in *S. Cerevisiae* which also was tyrosine phosphorylated in response to osmolarity and represented the only stress kinase found in fission yeast (71).

Four isoforms of p38 exist – p38 α , p38 β , p38 γ , p38 δ – with approximately 60% homology between these isoforms. These isoforms differ in tissue expression, often times in upstream and downstream activators, and in their roles in inflammation (72, 73). The p38 α and p38 β isoforms are ubiquitously expressed while the other isoforms have limited tissue expression. The expression of p38 γ is mainly confined to skeletal muscle where it plays a prominent role in muscle differentiation. Conversely, p38 δ is expressed in tissues in the lung, kidney, pancreas, testis, and small intestine, and may

have a function in developmental processes. p38 α also may a role in development since inactivation of this isoform is embryonic lethal around embryonic day 11. All isoforms of p38 have similar activation profiles, but seems to have different kinetics and levels of activation.

2.2. Regulation and catalytic mechanism of p38 signaling

The pathways involving MAPKs were first delineated by the discovery of ERK and were found to be heavily regulated three-tiered kinase pathways. MAPKs have a conserved Thr-x-Tyr activating motif in the activation loop of the kinase that is specific to each family member. The MAPKs are activated by reversible Tyr and Thr phosphorylation by dual specific MAPK kinases (MKKs). These MKKs are themselves activated via Ser/Thr phosphorylation by MAPK kinases kinases (MKKKs or MAP3Ks). Once activated, MAPKs directed to their substrates by proline residues, though specific MAPK docking sites on the substrates allow for specificity. Inactivation of MAPKs is mediated by phosphatases, proteins that dephosphorylate both Thr and Tyr residues of all the three major MAPKs. The most common of these phosphatases include pp1, pp2C or the MKP family of MAPK-specific phosphatases.

The p38-specific activation sequence is Thr-Gly-Tyr (TGY) corresponding to Thr¹⁸⁰ and Tyr¹⁸², which is primarily phosphorylated by MKK3/6 in response to cytokines, heat shock, and mitogenic activating stimuli (74). Upstream activation of MKK3/6 often occurs through the apoptosis-related kinase-1 (ASK-1), MEKKs, and Tak1.

Signaling components to the MAPK pathways are often have more than one biological function and regulation (Fig 1.5). This is the case with the p38 and JNK pathways which, in many cases, run parallel to each other yet are at times independent and differentially activated. p38 and JNK typically share MKKKs based on experiments where overexpression of particular MKKKs and even some specific stimuli leads to co-activation JNK and p38 (75). Under physiological conditions, p38 MAPK activation, like the activation of the other MAPKs, is transient. p38 is dephosphorylated by all the major MAPK phosphatases though the MKP family of phosphatases acts primarily on the alpha and beta isoforms, with the other isoforms being resistant to inactivation by MKP. Published reports also suggest a feedback mechanism in which phosphorylated p38 may also activate dual-specific phosphatases, threonine phosphatases, and tyrosine phosphatases in order to terminate p38 signaling.

As all other kinases, p38 uses ATP to transfer a phosphate group to a specific targeted substrate. The ordered sequential kinetic mechanism of p38 involves the initial substrate binding which is then required for ATP to bind strongly (76). This was based on the use of ATF as the p38 MAPK substrate yet it is possible that specific substrates may affect the catalytic mechanism of p38. However, this is first reported as a unique mechanism for Ser/Thr kinases.

2.3. Functional role of p38 MAPK

Activation of p38 was first revealed to be a common event triggered by pro-inflammatory cytokine receptor activation and one that is essential for inflammation. Evidence also links p38 signaling to the control of cell homeostasis through modulation of transcription factors, cytoskeleton elements and other kinases. It is still controversial whether activation of p38 primarily leads to continued cell survival or cell death. However, data implies the p38 can function in both capacities, depending on the stimuli and ultimately the targets of p38 MAPK signaling. Subcellular localization of p38 may also impact the function of p38 (77). The outcome of p38 activation, however, is most likely dependent on how the balance between apoptosis and survival is shifted and which side is dominant.

Mediator of inflammation

Around the time when p38 was first cloned, it was also discovered to be the target of cytokine-suppressive anti-inflammatory drugs (CSAIDs) and often referred to as CSAID binding proteins (CSBPs) (78). CSAIDs exert their anti-inflammatory activity by inhibiting cytokine biosynthesis and were found to be potent and selective inhibitors of the p38 MAPK pathway. This finding connected p38 MAPK to cytokine production and the inflammatory response (79). Since then, p38 MAPK is thought to participate in the expression of pro-inflammatory mediators like the cytokine interleukin-6 (IL-6) and the inducible COX-2 via the NF- κ B-mediated transcription. Chemical stresses that are

known to induce COX-2 expression do so through a p38-dependent mechanism (80). Published reports suggest that p38 potentially acts at various points in the NF- κ B pathway since pharmacological inhibition of p38 MAPK has been shown to attenuate NF- κ B transactivation without affecting NF- κ B DNA binding (81, 82). p38 is known to phosphorylate the p65 subunit of NF- κ B in the transactivation domain and possibly up-regulate transcription in this manner (83, 84). Another mechanism that has been proposed suggests that p38 phosphorylates transcriptional co-activations like CREB needed for NF- κ B-mediated transcription (85).

p38 has also plays a role in the mRNA stability of cytokines. Cytokine mRNAs typically have a short half-life due to the 3' untranslated region (UTR) AU rich elements where AU rich element binding proteins (ARE-BPs) bind and target the mRNA for degradation. In basal control conditions of p38 MAPK, transcript stability is low but increase with the activation of the p38 pathway. This stabilizing activity is thought to occur through a MAPKAPK-2-dependent mechanism where the ARE-BPs are phosphorylated, inhibiting their repressive activity.

Role in induction of apoptosis

Investigations into the role of MAPK pathways in the activity of chemotherapeutic agents are common (86). Some studies show that p38 activation mediates cancer cell death initiated by particular anticancer agents. In these situations, activation of p38 may or may not be in concert with JNK activation. Treatment with

paclitaxel and other microtubule-targeting agents have been reported to show concurrent activation of p38 and JNK, and by inhibiting activity of these kinases with specific inhibitors, drug-mediated apoptosis was blocked (87). Retinoids seem to require p38 activation for its anticancer properties in ovarian carcinoma cell lines (88). p38 has also been demonstrated to directly activate the tumor suppressor p53 by phosphorylation, leading to cell cycle arrest and potentially apoptosis (89). In most of these cases, MAPK activation is prolonged rather than transient, which dictates the apoptosis-inducing signaling.

p38-mediated tumor progression

Though immense evidence puts p38 in the apoptotic pathway, there is also proof that p38 can mediate survival signaling and has a role in tumor progression. Inhibition of p38 is known to cause growth inhibition in particular cancers like follicular lymphomas (90). Elevated levels of p38 expression and activity discovered in breast carcinoma cells in pleura effusions and are believed to confer growth advantage to these cells (91). Many non-small cell lung cancer (NSCLC) cell lines like A549 have constitutively active p38 compared to wild-type cells (92). This data also corresponded to clinical studies looking at tumor and normal lung tissue where p38 activation was inversely correlated with patient survival. This survival signaling is thought to be propagated through the downstream effectors of the p38 pathway like Hsp27, which lies downstream of the p38 substrate MAPKAPK-2, and provides protection against stresses to cells and often correlated with tumorigenesis when phosphorylated (93). Activation of

expression of the NF- κ B-regulated anti-apoptotic gene products also appears to require p38 activity, solidifying a relationship between p38 and the pro-survival NF- κ B pathway and suggesting a role of p38-dependent NF- κ B transcriptional activity (81, 82). Data also suggests that in many instances p38 acts in concert with the ERK pathway to increase cell proliferation, migration and invasion (94).

2.4 Involvement in heat shock protein 70 (Hsp70)

Several published reports provide evidence that MAP kinases such as p38 MAPK coordinate genetic responses to external cellular stresses through the phosphorylation of transcription factors. p38 has been postulated to participate in the induction of Hsp70 protein levels through its interactions with the heat shock transcription factor-1 (HSF1), the major regulator of the Hsp70 gene (95). Several phosphorylation sites (Ser³⁰³, Ser³⁰⁷) on HSF1 have been identified *in vitro* and appear to be a consensus sites for p38 (96). These phosphorylation sites are inducible and are thought to increase the binding of HSF1 to heat shock response elements (HSE) in the 5' regulatory regions of the gene. This then ultimately up-regulates the transcription of Hsp70 .

Hsp70 is a member of the heat shock protein family which generally strongly up-regulated by toxic agents or cellular stress (97). This family is classified based on their size and include hsp100, hsp90, Hsp70, hsp60 and small heat shock proteins (15 to 30kD). Several Hsp70 proteins are known ranging from 66kD to 78kD and differ mainly in localization and expression. The most closely studied is the cytosolic stress-induced Hsp72 transcribed from *HSPA1A*.

Hsp70 assists in the folding process of over 20% of cellular proteins after they are released from ribosomes, which is one of the main mechanisms of all heat shock proteins (97, 98). Protein folding is accomplished by interacting with the hydrophobic peptide segments to shield the protein from intermolecular interactions in an ATP-assisted fashion. Energy of ATP is then used to induce the conformational changes in the client protein and to drive the ATPase cycle. This chaperone activity is on the order of minutes or longer. Hsp70 also plays a role in the prevention of protein aggregation especially of partially-synthesized peptides.

There are three major functional domains of Hsp70 that work to complex with protein substrates and mediate protein folding (77, 97). The N-terminus contains the ATPase domain of 45kD which binds ATP and drives the conformational changes in other domains. Hsp70 normally has very weak ATPase activity when only bound to ATP. ATP-bound Hsp70 then freely associates with client peptides at the substrate binding domain. Peptides up to seven amino acids in length interact with Hsp70 at a time, which ultimately stimulates the ATPase activity of Hsp70. The 25kD C-terminus domain contains a lid for the substrate binding domain. It is ATP binding that allows opening of the lid as well as peptide binding and rapid release. Conversely, ADP binding closes the lid so after peptides interact with Hsp70, they are captured and are tightly bound.

Published reports suggest that Hsp70 has an important role as a survival factor, inhibiting apoptosis by acting on caspase-dependent and caspase-independent

pathways (Fig 1.8). Caspase 3 activation is prevented by the direct binding of Hsp70 to Apaf-1 through its ATPase domain (99). Hsp70 also directly interacts with caspase 3/7 and prevents the cleavage into the active forms (100). In terms of caspase-independent apoptosis, Hsp70 has been shown to prevent this mode of apoptosis inducing factor (AIF)-mediated cell death even in the presence of caspase inhibitors (99, 101). This is accomplished through the interaction of Hsp70 with AIF and prevention of AIF from translocating to the nucleus (102). Subsequent downregulation of Hsp70 sensitizes cells to AIF-mediated cell death. Overexpression of Hsp70 also leads to increased resistance to apoptosis-inducing agents like TNF α , doxorubicin, and staurosporin (103-105).

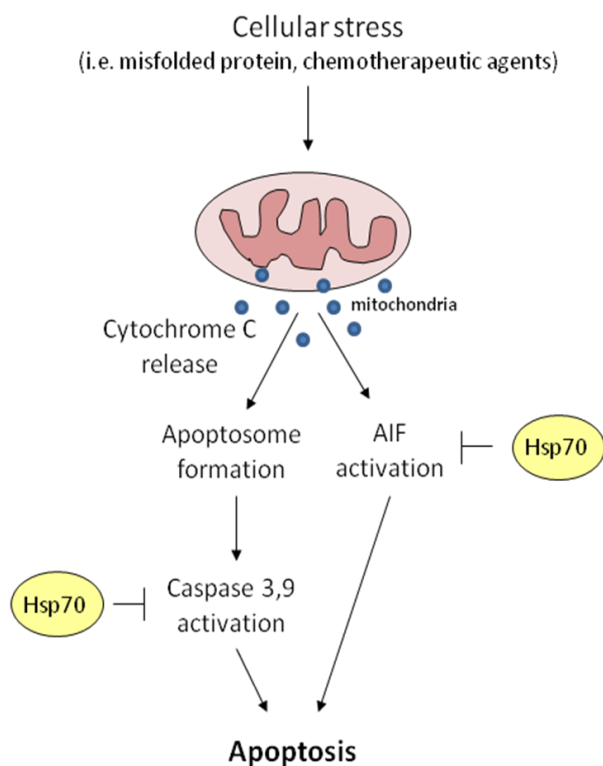


FIG 1.8. Hsp70 prevent caspase-dependent and casapase-independent apoptotic signaling. Besides protein folding, Hsp70 has been postulated to be involved in inhibiting the apoptotic response to chemotherapeutic and other cytotoxic agents at several points in the pathway.

2.5. Small molecule inhibitors of p38

In the last decade, protein kinases have become a very popular target for drug development especially in the treatment of cancer with p38 MAPK inhibitors representing the most extensive development efforts for inhibitors to the MAPK family. Currently, the most success has been made for identifying inhibitors to the alpha and beta isoforms of p38, though a few compounds the specifically target p38 γ have also been discovered. The utility of p38 MAPK inhibitors in the treatment of inflammatory diseases, from rheumatoid arthritis to cancer, illustrates how p38 represents a convergence point for signal transduction activated in inflammation ad cytokine production.

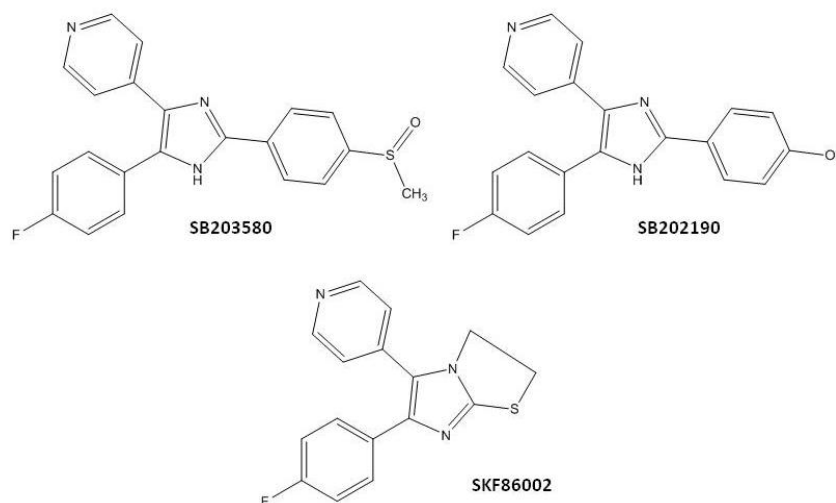


FIG 1.9. Commonly used pyrimidyl imidazole p38 MAPK inhibitors. Pyrimidyl imidazole compounds, including SKF86002, were the first agents discovered to inhibit p38 activation. Since then additional generations of pyrimidyl imidazole have been used in research (i.e. SB203580, SB202190) and clinical development.

The prototypical pyridinyl imidazole compounds

The connection between p38 and cytokine synthesis was not appreciated until p38 was identified as the molecular target for the pyridinyl imidazole class of compounds, or CSAIDs, known to inhibit the synthesis of cytokines (106). The first in this class to be reported was SKF 86002, a COX and LOX inhibitor. Subsequently, SB203580 and the closely related SB202190 were developed and are the most used inhibitors in research for studying the effects of p38 α/β inhibition because of its specificity for this kinase (107). Further studies show that these compounds not only inhibit the production of pro-inflammatory cytokines but also downregulate their actions, due to its potent inhibition of p38 *in vitro* and *in vivo* (108). The pyridinyl imidazole compounds have now become the standard for p38 inhibitors, and the structure of these agents is often used as a basis for the design of next generation drugs (Fig 1.9).

Mechanism of p38 inhibition

A vast majority of p38 inhibitors, especially the pyridinyl imidazole class of compounds, is competitive with ATP and thus is believed to interact with the kinase at the ATP binding site (109). Subsequently, this interferes with the phospho-transfer to the p38 substrates since ATP is not available due to decreased binding. What is unique about the pyridinyl imidazole inhibitors is that they seem to have a similar binding affinity to all forms of p38, whether active or inactive (110). In this instance, these

inhibitors were found to not be competitive with ATP for the low activity, unphosphorylated p38, since ATP binds inactive kinases poorly. This provides an explanation on why these inhibitors are effective in when intercellular concentrations of ATP is very low. Possibly as a consequence of binding the unphosphorylated form of p38, pyridinyl imidazoles appear to also interfere with p38 activation (111).

. The crystal structure of inactive p38 and SB203580 has been solved and it has been determined that these molecules interact with the same sites known for binding the adenine rings and phosphate groups of ATP (112). The amino acid residue at position 106 in the ATP binding site of human p38 kinase is crucial for determining sensitivity of this kinase to inhibitors. Binding occurs at the ATP pocket of p38 in a mode in which only threonine or small residues can accommodate the fluorophenyl ring of the pyridinyl imidazoles (112). The alpha and beta p38 isoforms have a threonine and are sensitive to submicromolar concentrations of pyridinyl imidazoles. p38 delta and gamma have a larger methionine residue, and JNK and ERK have even bulkier residues at the corresponding position, leaving these kinases unaffected by p38 inhibitors. This residue is known to confer selectivity of these inhibitors to p38 α and p38 β since mutating this residue in other kinases changes sensitivity to inhibition. For SB203580, the *in vitro* IC₅₀ values are 50nM and 500nM for p38 α and p38 β , respectively (113). This compound also inhibits kinases such as LCK, GSK3 β , PKB α but at values 100-500 fold higher than for p38. The specificity of SB202190 is similar, inhibiting p38 α and p38 β with an IC₅₀ of

50nM and 100nM though this inhibitor may be less selective and have additional targets (113).

Though most p38 inhibitors bind to the ATP site, a few have been found to bind to a site adjacent to this active site. Due to this unique interaction with the p38 molecule, these inhibitors are potentially allosteric modulators (114). The binding site, termed the “DFG-out” site, is associated with conformation changes in the conserved Asp-Phe-Gly motif in subdomain VIII of p38 at the start of the activation loop. Many of the compound that promote the DFG conformation prevents the activation of p38 by the upstream kinase MKK6, offering a new approach to inhibition of p38 beside competition with ATP (115).

Clinical implications for p38 inhibitors

Initially, because of the success of SB203580 *in vitro*, it was tested as a potential drug in whole animals. However, it did not make it as a first generation anti-inflammatory drug to due severe toxicity in the liver (116). With the development of more generations of agents, the testing of selective inhibitors to the p38 pathway has moved from animal models of inflammatory diseases to clinical trials for psoriasis, arthritis, and now for the treatment of cancer (117, 118). Recently, small molecules such as AMG 548, BIRB 796, VX 702, SCIO 469, and SCIO 323 have been developed and clinically tested by pharmaceutical companies (119). p38 inhibitors appear to have relevance in the treatment of rheumatoid arthritis since the underlying pathology

involves the destruction of the joints due to increase inflammation (120). High levels of activation of p38 have been detected in tissue from RA patients, primarily in the synovial microvessels and cells of the synovial lining layer. p38 inhibitors have also emerged as a potential therapy for cardiovascular disease. Stress kinases have been found to be activated by ischemia and reperfusion of the heart (121). This indicates that inhibiting this kinase will be beneficial for acute coronary syndromes. Additionally, investigations into the use of p38 inhibitors for the treatment of chronic obstructive pulmonary disease (COPD) and asthma show a reduced risk of disease progression of the airways (122, 123).

MICROTUBULES

Microtubules are a major component of the cellular cytoskeleton and are required for important functions in cell maintenance and growth. Built from the self-association of alpha/beta-tubulin monomers, these structures are highly dynamic and are regulated by evolutionary conserved post-translational modifications as well as microtubule-associated protein (MAPs). The significant role of microtubules in cell division, structure and support, and movement of organelles and cytoplasmic proteins have made it a great target for the development of anticancer agents for a variety of malignancies. The drugs that have been discovered to directly affect the integrity of microtubules, usually natural products, represent a chemically diverse group of compounds. These microtubule-targeting agents (MTAs) bind to tubulin and inhibit microtubule dynamics and/or stability without changing the molecular mass of microtubules. This class of compounds is arguably the most clinically successful class of anticancer agents and the numbers of compounds found to bind to microtubules are constantly expanding. The most well known agents in this class are the taxanes, which act by hyperstabilizing microtubules and leads to subsequent cell death after mitotic arrest.

3.1. Microtubules: Structure and dynamics

The basic structural units of the microtubule are α/β dimers, which are always found bound to each other. These dimers associate in a head-to-tail fashion, an alpha

subunit of one dimer contacting with a beta subunit of another, to form protofilaments. Each alpha and beta monomer has a binding site for a molecule of GTP. GTP provides the energy necessary for formation of a microtubule. When the heterodimer is assembled, the GTP on β -tubulin is partially exposed and can be hydrolyzed from GTP to GDP. After hydrolysis, the GDP can readily be exchanged for another GTP molecule and is said to be "exchangeable". However, the conversion of GTP to GDP is often following by protofilament formation and the nucleotide bound to β -tubulin becomes buried and is no longer exchangeable. Conversely, the GTP of the α -tubulin is buried in the intradimer interface and can not be hydrolyzed. Protofilaments then interact laterally, unusually in groups of 13, to form hollow cylindrical structures known as microtubules. The arrangement of protofilament have been found to create an imperfect helix with one turn containing 13 tubulin dimers from different protofilaments and has a diameter of approximately 25 nm.

Microtubules are highly dynamic structures and are in a constant state of instability (Fig 1.10). They have a length contingent of the continual lengthening and shortening of these structures, varying from 25 to 200 nm. The two ends of microtubules have varying polymerization rates dependent on the α -tubulin and β -tubulin ends. The ends with α -tubulin exposed have been shown to grow slower than the fast-growing β -tubulin ends. The shrinking of microtubules after growth is known as catastrophe while the opposite is called rescue. Tubulin adds onto microtubules only in the GTP state and if GDP is bound at the end, the microtubule is prone to depolymerization and the

dimers will fall off. Addition of GTP-bound tubulin creates a GTP cap at the ends which protects the microtubule from disassembly. The current model of microtubule polymerization is that if GTP hydrolysis is faster than nucleotide addition, the microtubules begins to shorten. However, if enough GTP can be added to the ends at a faster rate than hydrolysis, the microtubule growth resumes.

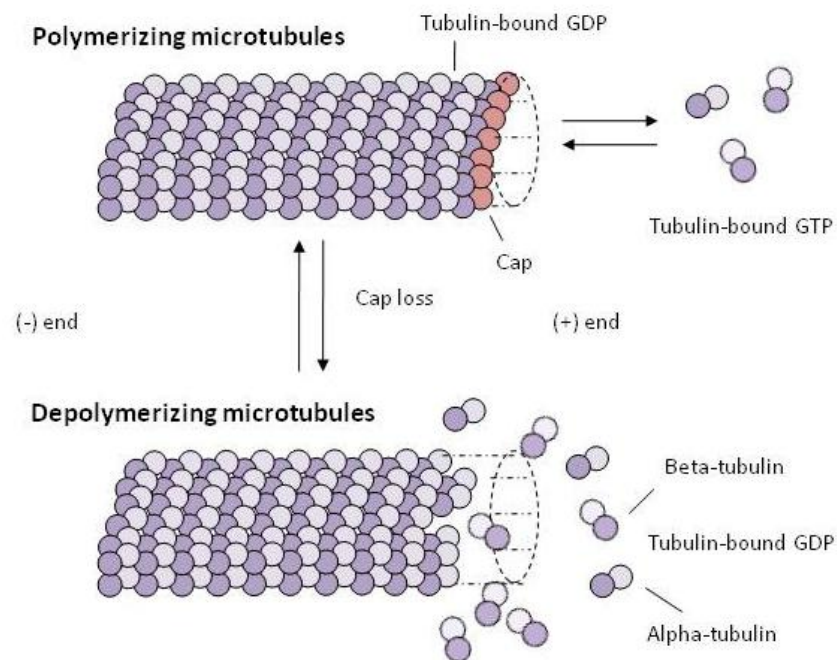


FIG 1.10. Organization and assembly of microtubule polymer. Microtubules are hollow cylinders comprised of the assembly of tubulin dimers (alpha- and beta-subunits). GTP bound to tubulin is hydrolyzed to GDP when tubulin is added during polymerization. The end containing tubulin-bound GTP is stable against depolymerization while tubulin-bound GDP end is destabilized and often results in catastrophe, or shortening of the microtubule.

Along with creating different rates of growth, the association of the heterodimers in microtubule also creates polarity. The β -tubulin ends extend out toward the periphery of the cell and are designated as the plus (+) end while the end with α -tubulin exposed is the minus (-) end. Minus ends of microtubules nucleate at the microtubule-organizing center (MTOC). MTOCs are thought to radiate from centrosomes, a structure organized by cellular organelles called centrioles, which exists in the cytoplasm near the nucleus. Within the centrosome is γ -tubulin, an isoform of tubulin unique to the pericentriolar area of the cell. Ultimately, nucleation is important in preventing random and spontaneous polymerization of microtubules in the cytoplasm and therefore creates a more organized network of microtubules.

In addition to dynamic instability, microtubules also undergo a process called treadmilling. Treadmilling is the process in which the net growth of one end of the microtubule is balanced by a net shortening at the other end. This creates a “treadmill” with no net loss in microtubule length. Treadmilling is due the flow of tubulin subunits from the minus ends to the plus ends. Both dynamic instability and treadmilling can occur simultaneously. The entire population of cellular microtubules is either undergoing one of these events or both.

3.2. Regulation of microtubules

The regulation of microtubules are not completely understood but is thought to be due to both post-translational modifications of tubulin and other regulatory

pathways involved in the polymerization and depolymerization states of microtubules. Cellular factors called microtubule associated proteins (MAPs) have been discovered to interact with microtubules and function to regulate tubulin assembly (124). Additionally, research studies show that expression of α - and β -tubulin isoforms could also affect microtubule dynamics. Taken together, these factors combine help to control the dynamic nature of microtubules within the cell.

MAPs are mainly known to regulate microtubule polymerization. These proteins bind to microtubules and stabilize them. Unlike the assembly of microtubules, this binding does not depend on the GTP/GDP state of microtubules but rather is electrostatic and involves the acidic C-terminal domain of tubulin subunits. The classical stabilizing MAPs include MAP1, MAP2, MAP4, and tau. They are negatively regulated by phosphorylation which reduces the affinity of these proteins with the microtubule network.

There are also a few destabilizing factors which reduce the net assembly of microtubules and increase microtubule turnover. Katanin functions as a severing factor at the ends of microtubules, generating new ends lacking the protective GTP cap, leading to massive disassembly. Depolymerizing kinesins bind to both ends of microtubules and forces protofilament peeling. Though this leads mainly to negative regulation of microtubule development, it is required for the formation and the dynamic nature of microtubules.

Isoforms of tubulin

Tubulin is encoded by a multigene family of proteins. The tubulin superfamily includes alpha, beta, gamma, delta, epsilon, and zeta. The cellular function of epsilon and zeta is still unknown. Gamma-tubulin is approximately 30% identical to the most common isoforms, alpha and beta. Distinct isotypes of α - and β -tubulin exists and are highly conserved, being the most variable in the last 10-15 amino acids of the C-terminus. The variability primarily affects the association of accessory proteins and not necessarily the polymerization of microtubules. In total, at least six isoforms of alpha and eight isoforms of beta are present in mammals. There is evidence that tubulin isotypes exhibit some tissue specificity since they are differentially expressed. In most instances, the isoforms seems functionally interchangeable and appear to coassemble *in vitro* (125). However, in the case of sensitivity of chemotherapeutics, *in vitro* studies show that certain isotypes may be affected by microtubule disrupting agents (MDAs) differently (126, 127).

Post-translational modification

Both the alpha and beta isoforms can be modified by acetylation, polyglutamylation, polyglycylation, tyrosination, phosphorylation, and palmitoylation (128). All but acetylation has been found to occur at the charged ends. Post-translational modifications is thought to influence the interactions of microtubules with

accessory proteins though the complete function of these modifications is still unknown (128).

3.3. Microtubule function

Microtubules have many cellular roles with its dynamic nature and polarity being key to these functions. Most notably, microtubules significantly participate in the division of a single cell into two daughter cells (Fig. 1.11). In the early stages of cell division, or prophase, centrosomes are replicated, split into two, and nucleate an array of microtubules at each end of the cell. This formation of microtubules is called an aster and fully develops in late prophase. The asters then form bipolar mitotic spindles in early metaphase, requiring different populations of microtubules and a high degree of regulation. Many MAPs and microtubule-based factors play a role in regulating the dynamics necessary to create such a structure. The astral microtubules that radiate from centrosomes are thought to contribute to the separation of the poles and orientation of the mitotic spindle. Polar microtubules function to stabilize and retain the bipolarity of the spindle. As the chromosomes align at the metaphase plate, populations of microtubules, called kinetochore microtubules, attach to the kinetochores of the chromosomes and connect them to the spindle. These microtubules also aid in segregating the sister chromatids into the two new genetically identical daughter cells.

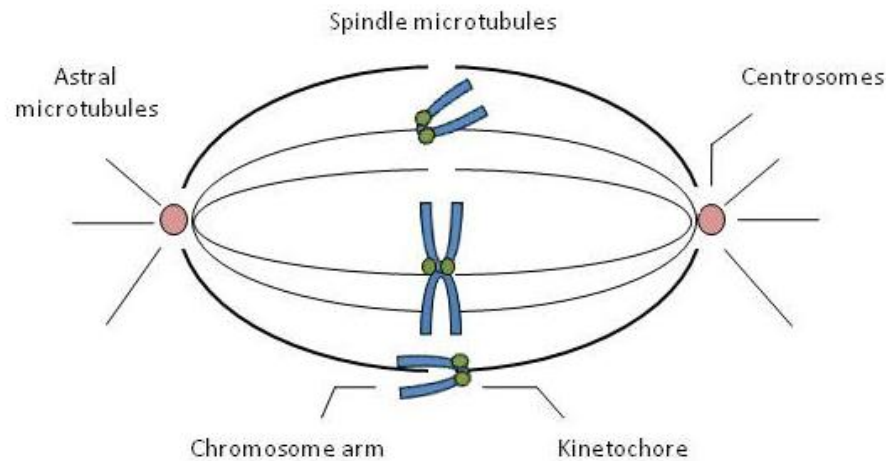


FIG 1.11. The importance of microtubules in chromosome segregation and cell division. Prophase of cell division is characterized by the formation of microtubule asters at each end of the cell. During early and late metaphase phase, spindle microtubules interact with condensed chromosomes, which are then aligned at the equator of the spindle. Under the control of microtubules, sister chromatids are separated during anaphase and move toward the asters in order to be packaged into the resulting daughter cells.

Microtubule polarity allows for the directional flow of molecules from one end of the cell to the other and is aided by microtubule-based motor proteins. These motor proteins use the energy of ATP hydrolysis to perform a step-like motion across the microtubule network and drive the movement of molecular cargo. The particular motor protein involved in this transportation is dependent on microtubule polarity. Dyneins are minus-end directed motor protein while plus-end directed kinesins move in the opposite direction. Dyneins are majorly responsible for the transport of organelles such

as ER-Golgi complexes, late endosomes, and chromosomes (129, 130). An important accessory factor called dynactin has been found to be necessary for the function dyneins (131, 132). On the other hand, kinesins are known to move mitochondria and smaller molecules (i.e. tumor suppressor proteins, translational factors, etc) away from the centrosomes (133, 134). Approximately 15-30% of mRNA is thought to be link with the cytoskeleton when associated with polysomes and may use the microtubule network to localize to the cytoplasm.

With the discovery of signaling molecules that interact with microtubules came the idea that intercellular signal transduction may possible have some dependence on microtubules (135). MDAs are known to cause multiple effects to signaling cascades dependent on their microtubule disrupting activities. It has been proposed that microtubules are possibly critical to signal transduction by sequestering molecules, acting as a protein scaffold, or even modulating the delivery of signaling factors. The NF- κ B/I κ B complex is thought to be sequestered to the microtubule surface and once the microtubules are modified or disrupted, this complex could then be released. Microtubules may also provide a surface for the interaction of two or more cellular factors which would otherwise have low affinity for each other. The binding of one factor to microtubules may also open up a potential binding site for a second factor. Large signaling cascades like the MAPK pathways have long been thought to be modulated by microtubules.

3.4. Targeting microtubules for cancer therapy

Agents that disrupt the microtubule cytoskeleton are probably the most effective class of chemotherapeutics to date (136). Initially, the essentialness of microtubules in cell division was the basis of the development for new generation of MTAs since the strategy was to inhibit cell division. Now, the success of MTAs is also attributed to the grave importance of this cytoskeletal protein in the maintenance of cell shape and polarity, intracellular transport and signal transduction. This has been validated by the extensive research into the mechanism of clinically successful MTAs including taxanes and the vinca alkaloids. Much attention has been given to the discovery of agents that also act to disrupt microtubules with a majority of these being natural products or compounds derived from them (137). Due to this, the MTAs represent one of the most diverse classes of molecules compared to other classes of anticancer agents.

Drug binding sites

Upon binding to tubulin, microtubule-targeting agents are known to block cell division. This activity leads to the accumulation of cells in the G₂/M phase of the cell cycle and ultimately mitotic arrest. Due the ability of these agents to inhibit cell division, these agents are often referred to as anti-mitotics. MTAs disrupt the microtubule network by both inducing microtubule polymerization through stabilizing microtubules and increasing the microtubule polymer mass or by inhibiting microtubule assembly. Though these activities are distinctly different, both induce mitotic arrest and

apoptotic cell death. Interestingly, the three well established drug binding sites for MTAs on tubulin all lie on the β -tubulin subunit. These sites include the taxane, vinca alkaloid, and colchicine binding sites. Recently, other sites on tubulin have been proposed though the validity of these findings is currently under investigation (Fig. 1.12).

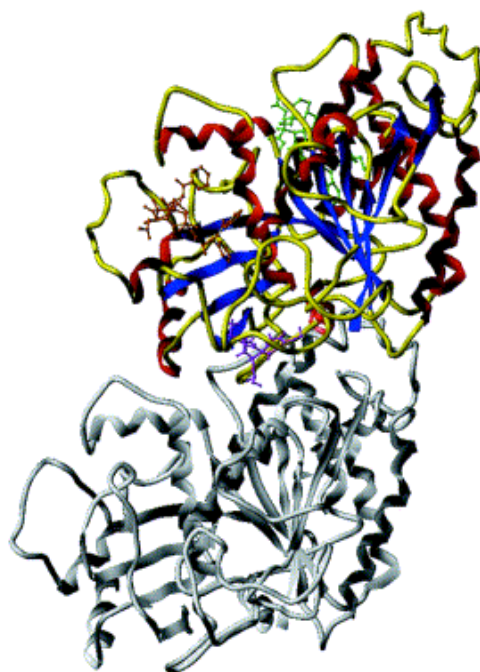


FIG 1.12. Proposed drug binding sites on tubulin. The hypothesized position of the three major MTAs are shown here: paclitaxel representing the taxanes (orange), vinblastine representing the vinca alkaloids (green), and colchicine (purple). Published reports suggests that all of these known sites lie on beta-tubulin (colored) and not on alpha-tubulin (grey).

Paclitaxel (taxol) is arguably the most successful member of the microtubule-targeting family of chemotherapeutics and has been used in the treatment of breast, ovarian, prostate, and non-small cell lung cancer (138). Isolated from the bark of the pacific yew *Taxus brevifolia*, paclitaxel possesses strong stabilizing abilities and induces

the formation of distinct microtubule bundles (139). At low concentrations, it suppresses microtubule dynamics. Paclitaxel is thought to accomplish these things by binding to a specific region of β -tubulin and stabilizing GDP-bound tubulin so even when hydrolysis reaches the end of the microtubule, no shrinking back of the microtubule occurs. After the discovery of the site to which paclitaxel and derivatives of taxol (i.e. docetaxel) bind, this binding pocket was named the taxane binding site. The taxane binding site lies next to a region of tubulin known as the M-loop. Taxol is believed to bind at the lateral interface between adjacent protofilaments from the terminal end of the microtubule. Other agents like discodermolide and epothilones have been found to also bind to the taxane site and induce microtubule stabilization in a similar fashion to taxol (140, 141). Additionally, laulimalide-induced reorganization of the microtubule network is also due to the formation of microtubule bundles (142). However, this agent does not interact with tubulin at the taxane binding site but may bind at a yet unidentified site.

The vinca alkaloids are a class of MTAs which includes the compounds vinblastine and vincristine and the semi-synthetic derivatives vindesine, vinorelbine, and vinflunine (143). The natural agents are commonly isolated from the leaves of the periwinkle *Catharanthus roseus* and are used primarily for the treatment of leukemias, lymphomas, and solid malignancies. Collectively, the vinca alkaloids induce microtubule depolymerization by binding at the polar, opposite side of beta-tubulin at

the plus end interface adjacent to the site where GTP is hydrolyzed, dissolving the microtubule network.

One of the earliest MTAs identified is colchicine. As with most microtubule-targeting agents, colchicine was initially isolated from a natural source, the meadow saffron *Colchicum autumnale*. Colchicine is postulated to bind at the intra-dimer interface between alpha- and beta-tubulin. Colchicine and other agents that bind at this site induce microtubule depolymerization and further prevents the formation of microtubule polymers (144). For instance, 2ME2, a natural metabolite of estrodial, binds to the colchicine site and inhibits microtubule assembly (145). Treatment with colchicine has been found to cause very high toxicity to normal tissues which has hindered the development of colchicine as a clinical agent. In addition to colchicine, other agents that bind to this site have been discovered.

Drug-induced side effects

Since cells depend heavily on the dynamic nature of microtubule and the formation of the mitotic spindle for cell division, the initial thought was that targeting the microtubule cytoskeleton would preferentially and selectively kill rapidly dividing cancer cells, which are thought to be more rapidly dividing. However, the use of MTAs has proven this is not the case. Due to the involvement of microtubule in various cellular processes important to the survival of all cells, MTAs are known to specifically affect, in a dose-limiting manner, cells of the nervous and immune systems. Most often,

neurological side effects lead to peripheral neuropathies and are manifested as numbness, motor weakness, and loss of reflex at the feet and ankles (146). Cranial and autonomic neuropathies also may frequently occur. This is primarily due to the drug-induced disruption of axonal microtubules, which are important for the transportation of cellular information in the nervous system. Microtubule-targeting agents also cause hematological toxicity. In addition to these specific side effects of MTAs, these agents also induce the more common side effect known to be caused by most chemotherapeutics including severe nausea, diarrhea, and alopecia.

Mechanisms of drug resistance

Drug resistance is a natural response to drug-induced pressures, challenging the survival of cancer cells. Due to this, drug resistance stands as one of the most significant impediments to the successful and long-term treatment of cancer as well as other disease states. As with all resistance to therapeutic agents, this can be due to intrinsic properties of the drug target, cell, or whole organism, or resistance may be due to acquired or developed changes. Though factors such as the pharmacokinetics and metabolism of a drug affects the ability of the drug to reach and kill cancer cells, modifications within the targeted cells extensively contributes to tumor resistance. Chemotherapeutic resistance commonly caused by microtubule-targeting agents can arise from various mechanisms including the upregulation of protein drug efflux pumps, changes in expression of protein tubulin isoforms, and modification to the structure of tubulin. Though many of these mechanisms of MTA-induced resistance have been discovered *in vitro*, some

clinical studies have failed to link the contribution of these cellular alterations to *in vivo* models of cancer.

The overexpression of p-glycoprotein (P-gp) and other plasma membrane-bound, ATP-dependent drug transporter proteins is a common mechanism of drug resistance and has been correlated to an increased risk of failure to the response to particular chemotherapeutics. Normally, the role of these transporters, found in both tumorigenic and normal cells, is to protect against excessive intracellular concentrations of foreign toxins. Upon binding of a chemical compound to P-gp, the energy from ATP hydrolysis causes a conformation change that releases the compound out of the cell. However, cancer cells take advantage of this process by upregulating expression of these transporters, reducing the ability of these cells to accumulate certain cytotoxic agents and leading to resistance to multiple drugs. Taxanes and vinca alkaloids are known substrates of these drug efflux pumps and show high susceptibility to this tumor-resistance mechanism.

Other scientific studies have identified resistance to MTA due to specific mutations of tubulin at the corresponding binding sites for particular agents, hindering any potential MTA-tubulin interactions. Several alterations in the structure of β -tubulin have been identified in the taxane and colchicine binding sites and replicated *in vitro* in order to determine approaches to circumvent drug resistance.

Alternate expression of tubulin isoforms is another proposed mechanism for MTA-resistance though some *in vivo* studies show that this may not be the case. Increased expression of the β -tubulin III isotype conveys insensitivity to paclitaxel binding, potentially due to the reduced stability of this isoform thought to counteract paclitaxel-induced microtubule stabilization. Consequently, β -tubulin III has been used as a biomarker for paclitaxel resistance in the clinical setting.

3.4. Downstream hypoxia-inducible factor-1 (HIF-1) pathway

Recently, microtubule-targeting agents (MTAs) have been found to share the property of downregulating HIF-1 α , an instrumental factor in the oxygen-regulated angiogenesis and tumor growth. Importantly, inhibition of HIF-1 is downstream of microtubule disruption and is primarily believed to be through inhibition of the translation of HIF-1 α (147).

Low oxygen tension, or hypoxia, is a critical characteristic of approximately 50-60% of advanced solid tumors. Hypoxia is a result of increased energy demand and diminished and abnormal vascular supply. Intratumoral hypoxia results when cells are located too far from functional blood supply for the diffusion of an adequate amount of oxygen. The presence of hypoxic regions of tumors was first postulated based on observations of the necrotic areas of tumors away from blood vessels (148). These hypoxic regions also result in a shift from oxidative metabolism to glycolysis, increased

mutation rates, and upregulation of transcription for genes to deal with this anaerobic environment (149).

Induction of HIF-1 represents the major response to reduced oxygen levels within a cell. HIF-1 is the name given to the heterodimeric complex comprised of the HIF-1 α and HIF-1 β subunits. HIF-1 α is highly regulated in both an oxygen-dependent and oxygen-independent manner and was originally discovered as a protein that binds DNA at high-affinity when the hypoxia-mediated induction of the EPO gene was being investigated in 1995 (150). This discovery gave way to a molecular target for the presence of hypoxic regions in solid tumors. Since then, HIF-1 has been found to act as a transcription factor in many cell types (151). HIF-1 acts by localizing to the cis-acting hypoxia-responsive element and stimulating the transcription of more than 40 genes in response to hypoxia (152, 153). Many of these HIF-1 regulated genes result in an increase in glucose metabolism and angiogenesis, necessary for cellular survival in low oxygen tension. A deficiency in this complex results in developmental arrest, which is manifested as neural tube defects and cardiovascular malformations, and embryonic lethality (154, 155). HIF-1 also controls the transcription of survival factors and invasion factors, and overexpression of HIF-1 can lead to tumorigenesis. Additionally, upregulation of HIF-1 is correlated with a resistance to chemotherapy. Since the identification of the role of HIF-1 in cancer development, therapeutic strategies against HIF-1 have been developed including small molecule inhibitors to directly target the

HIF-1 pathway, topoisomerase inhibitors, Hsp90 inhibitors, and even microtubule-targeting agents.

Regulation of HIF-1

While HIF-1 β (aryl receptor nuclear translocator or ARNT) is constitutively expressed, the tight regulation of HIF-1 α is primarily due to posttranscriptional modification. This represents an evolutionarily controlled system in the response to changes in the external cellular environment like hypoxia or non-oxygen related stresses.

Under the normal oxygen level, which is nearly 21% O₂, HIF-1 α is degraded and maintained at very low levels through a highly controlled process (Fig. 1.13). This process is mediated by a family of HIF prolyl-4-hydroxylases (PHDs) (156-158). Using oxygen along with iron as cosubstrates for the enzymatic reaction, PHDs hydroxylate HIF-1 α at residues 402 and 564 found in the oxygen-dependent degradation domain (ODD) (159). The ODD contains two PEST motifs which are a signature of rapid intercellular degradation. This hydroxylation allows the interaction of HIF-1 α with the Von Hippel Landau (VHL) protein, which acts as an E3 ubiquitin ligase and targets HIF-1 α for degradation by the 26S proteasome. PHDs have an oxygen-sensing function so in low oxygen tension, activity of this enzyme is inhibited since oxygen is not available (159, 160). Half maximal induction of HIF-1 α have been demonstrated between 1.5-2% oxygen with maximum induction at approximately 0.5% O₂. In addition, removal of

ODD, the central region of HIF-1 α , results in a stable protein which is no longer induced by hypoxia.

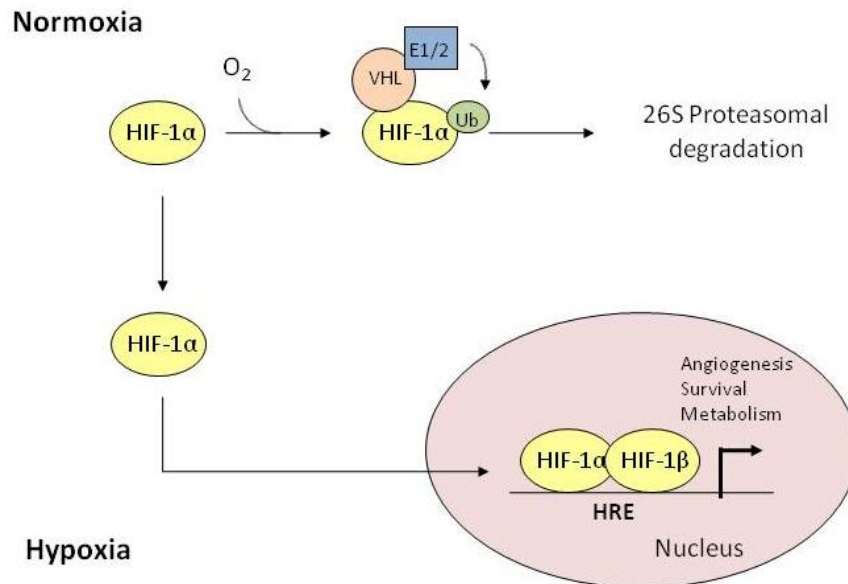


FIG 1.13. Hypoxic regulation of HIF-1 α controls the HIF-1 pathway. Under normoxic conditions, HIF-1 α is targeted for degradation by a post-transcriptional hydroxylation on Pro⁴⁰² and Pro⁵⁶⁴ by PHDs. This allows recognition of HIF-1 α by VHL, which ubiquitinates HIF-1 α . In hypoxic environments, oxygen which is necessarily for the hydroxylation reaction by PHD, is in low quantities and HIF-1 α is therefore stabilized.

HIF-1 α protein levels are also controlled by signaling pathways activated by growth factors including the PI3K and MAPK pathways (161). These pathways lead to an increase in the rate of HIF-1 α synthesis and have found to stimulate the function of the transactivation domain through phosphorylation. For instance, ERK is known to

phosphorylate HIF *in vitro* and in whole cells which increases the transcriptional activity of the complex. Reactive oxygen species (129) like superoxide and nitric oxide have also been shown to induce HIF-1 α expression similar to the oxygen-dependent mechanism of HIF regulation but under normoxic conditions (162, 163). The exact mechanism is still under investigation but it has been proposed that ROS stabilizes HIF by inducing s-nitrosylation of critical cysteine residues of the ODD domain and inhibiting PHD activity. Under hypoxia, mitochondria produce a burst of ROS that is also necessary and sufficient to stabilize HIF-1 α (164). It has also been suggested that p53 regulates HIF transcriptional activity by controlling HIF binding to its coactivator p300/CBP (165).

HIF-1 regulated genes

There are more than 80 putative HIF-1 target genes that have been identified. Hypoxia-induced genes represent an estimated 1-2% of the entire genome. These groups of genes are not only involved in global cell survival and proliferation but also glucose metabolism (i.e. LDHA, ENO1), angiogenesis (i.e. vascular epithelial growth factor or VEGF), and extracellular matrix metabolism. Conversely, HIF-1 α deficiency has been associated with decreased expression of at least 13 different genes encoding glucose transporters and glycolytic enzymes. Expression of the genes controlled by hypoxic conditions relies on the functional interaction between HIF-1 and its coactivators, determined by developmental and physiological programming. This process tends to also be cell specific. Though these genes are instrumental in the

adaption and survival of normal tissues, hypoxia-inducible genes are relevant to the growth and behavior of cancer.

HIF-1 and cancer

Overexpression of HIF-1 α and subsequently of HIF-1 dependent genes contributes to the phenotype of many solid tumors. Greater than 70% of human cancers across more than 13 tumor types have to found to have overexpressed HIF-1 (166, 167). Moreover, there is a negative correlation between HIF-1 α overexpression and patient survival especially in the case of breast, endometrial, and esophageal cancers (168-172). This overexpression is typically due to genetic alterations. Loss of function of the tumor suppressor PTEN can augment the expression of HIF-1 α and therefore can increase HIF-1-mediated gene expression (173, 174). Gene deletion or inactivating deletion of p53 also further enhances HIF-1 α accumulation. Additionally, gain-of-function mutations in the P13K and MAPK pathways upregulate HIF-1. In most of these cases, upregulation of HIF-1 activity seem to occur in the earliest detectable stages of neoplastic lesions (175).

The greatest effects of HIF-1 regulation are observed in most renal cell carcinomas (RCCa), which have lost functional VHL and therefore have constitutively expressed HIF-1 α . Lost of VHL is caused by inactivating mutations and is common in hereditary cancer syndromes, particularly in central nervous system hemangioblastomas and solid tumors including renal carcinomas (176). VHL-disease is commonly

associated with the sporadic formation of tumors. Reintroduction of VHL into renal carcinoma cell lines reverses tumorigenicity.

Therapeutic anti-HIF strategies

The high extent of HIF-1 regulation highlights its importance in cellular responses and cancer biology. Due to the many mechanisms of HIF-1 upregulation in response to hypoxia and cellular stress, several strategies have been postulated to inhibit the HIF-1 pathway. These strategies include inhibiting HIF-1 mRNA or protein expression by decreasing the rate of protein synthesis and/or increasing the rate of degradation, inhibiting the binding of HIF-1 to DNA, or inhibiting the transcriptional activity of the HIF-1 complex. A majority of the focus in preventing the induction of the HIF-1 pathway is on small molecule development (177, 178). This has taken the form of agents like the natural product echinomycin which specifically targets HIF-1 DNA binding or chetomin, which disrupts the interaction between HIF-1 and its coactivator p300. Additional efforts have been ongoing to develop small molecule inhibitors that hinder the dimerization of the alpha and beta HIF-1 subunits. Currently, there are no specific HIF-1 inhibitors in clinical development. However, other nonselective small molecules like Hsp90 inhibitors have been found to interfere with HIF protein folding and stability, inducing HIF degradation (179-181). Additionally, non-steroidal anti-inflammatory drugs (NSAIDs) downregulate the HIF-1 pathway, though the detailed mechanism is unknown (182, 183). Though an appropriate approach to inhibiting HIF may be developed, it is important to note that inhibition of HIF may not enough alone to

halt angiogenesis and tumor growth. The combination of HIF-1 inhibitors with other chemotherapeutic agents may be necessary for the adequate treatment of cancer and also the overcoming of clinical drug resistance.

CHAPTER 2
Materials and Methods

Chemicals and antibodies - Curcumin, purchased from Sigma-Aldrich (St. Louis, MO), was found to be a mixture of three different curcuminoids. Curcumin was purified by column chromatography over silica gel to remove the minor metabolites (20%) and provide pure curcumin as pictured in Figure 1.1. EF24 was synthesized as previously described (184). Stock solutions (0.01 mM) were made in dimethyl sulfoxide (DMSO) and stored in aliquots at 4°C. The pyridinyl imidazole compounds SB203580 (Promega; Madison, WI) and SB202190 (Biosource; Camarillo, CA) were used as p38 α/β MAPK inhibitors. The IKK-2 inhibitor IV was obtained from Calbiochem (San Diego, CA). The compounds were diluted in cell culture medium immediately prior to each experiment. Vincristine was from Eli Lilly (Indianapolis, Indiana), paclitaxel from Sigma-Aldrich, MG-132 (Z-Leu-Leu-Leu-aldehyde) from Alexis Biochemicals (San Diego, California), and the rhodamine phalloidin used in the immunofluorescence studies was from Molecular Probes (Eugene, OR). In addition, the following primary antibodies were used for immunofluorescence: α -tubulin (Chemicon International, Temecula, CA), HIF-1 α (BD Biosciences, San Diego, CA), HIF-1 β and actin (Santa Cruz Biotechnology, Santa Cruz, CA). Secondary antibodies were horseradish peroxidase-conjugated (Amersham, Piscataway, NJ), Alex Fluor 488 goat anti-mouse (Molecular Probes), and Alex Fluor 568 goat anti-rat (Molecular Probes). Antibodies against total and phospho-JNK (Thr¹⁸³/Tyr¹⁸⁵), total and phospho-p38 MAPK (Thr¹⁸⁰/Tyr¹⁸²), total and phospho-ERK (Thr²⁰²/Tyr²⁰⁴), PARP (full length and cleaved fragments), caspase 3 (full length and cleaved fragments), and Hsp70 were all purchased from Cell Signaling (Beverly, MA).

Additionally, the antibody against Hsp90 was obtained from Santa Cruz. RPMI 1640 medium was from Sigma-Aldrich and fetal bovine serum (FBS) was from CellGro (Manassas, VA).

Cell lines - Human cancer cell lines MDA-MB-231 (breast), PC3 (prostate), and A549 (NSCLC) were grown in RPMI-1640, 10% FBS; 1A9 human ovarian carcinoma cells and paclitaxel-, epothilones-resistant cell lines derived from the 1A9 line (1A9/PTX10, 1A9/A8, respectively) were also cultured in RPMI-1640, 10% FBS. Human breast cancer MCF-7 cells with green fluorescent protein-(GFP)-tubulin were cultured in RPMI-1640, 10% FBS with G418 sulfate solution. All media was supplemented with 1% penicillin/streptomycin. Cells were maintained at 37°C in an atmosphere containing 10% CO₂.

Immunoblot analysis - Cells were lysed in 1% NP-40 buffer supplemented with protease inhibitor tablet (Roche, Indianapolis, IN). Proteins (25–60 µg/lane) from whole cell extracts were resolved by 7.5% or 12.5% SDS-PAGE, electrotransferred to nitrocellulose or PDVF membranes, and blocked with 5% nonfat dry milk in TBS-Tween 20. The blots were then incubated with the indicated primary antibodies, followed by horseradish peroxidase-conjugated secondary antiserum. Immunoreactivity was visualized by enhanced chemiluminescence reagent (Amersham Biosciences, Piscataway, NJ). For sequential blotting with additional antibodies, the membranes were stripped of antibodies using a 2 M NaOH solution or a strip buffer with 2-

mercaptoethanol (1:1000), and the same blots were reprobbed with different primary antibodies.

***In vitro* cytotoxicity assay** – Cells were plated at a density of 5,000 cells/well in a 96-well plate and allowed to adhere overnight. The following day the cells were treated with drug for 48 hours in triplicate. To accurately obtain the IC₅₀ values, the sulforhodamine B assay was performed. Cells were fixed with 50µl of 10% TCA at 4°C for 1hr. The plates were washed with water and stained with 4% SRB (100 µl). Acetic acid (1%) was then used to wash the plates. Lastly, 10mM unbuffered Tris was added to solubilize the dye. Absorbance at 490 nM was recorded using a 96-well plate reader. The mean value and standard error for each treatment were determined and the % cell viability relative to control (0.5% DMSO) was calculated. The IC₅₀ is defined as the concentration of drug that kills 50% of the total cell population as compared to control cells at the end of the incubation period.

Clonogenic assay – A549 cells were plated in low density (450 cells/well) in a 12-well plate and were allowed to adhere overnight. The cells were treated with test compounds the following day and every 3 days thereafter. On day 10 after colonies were formed, cells were fixed using 10% TCA for 30 min at 4°C. The wells were washed with water, stained with sulforhodamine (SRB), and then washed with 1% acetic acid. An image of each well was taken. Colonies were counted using Image Processing and Analysis in Java (Image J, Research Service Branch, NIH). Large colonies were defined

as colonies with a diameter greater than or equal to 2 mm. Small colonies were defined as though <2 mm in diameter.

Flow cytometry analysis – Apoptosis was examined by flow cytometry of propidium iodide (PI)-stained cells. A549 cells were treated with a single agent or drug combination for 48hr. Attached and unattached cells were then collected, washed with 1%BSA/PBS and fixed with 75% cold ethanol for at least 1hr. PI (50 μ g/ml) was then used to stain the cells, and the DNA content of these stained cells was measured by a FACScan cytometer equipped with Cell Quest software (BD Biosciences).

Cell health assay – A549 cells which were cultured in 96-well plate, were stained with Hoechst 33342 (5 μ g/ml), PI (2.5 μ g/ml) and YO-PRO-1 (0.1 μ M) at 4 °C for 30 min and analyzed by ImageXpress system (Molecular Devices). PI-single positive and YO-PRO-1-single positive cells are recognized as necrotic and early apoptotic cells, respectively, whereas PI/ YO-PRO-1-double positive cells are referred to as late apoptotic cells (185). The percentages of viable cells and dying/dead cells, which consist of necrotic, early and late apoptotic cells were analyzed.

siRNA transfection – A549 cells were transiently transfected with oligonucleotide p38 MAPK siRNA (Cell Signaling, Beverly, MA) using oligofectamine transfection reagent (Invitrogen, Carlsbad, California) or DharmaFECT reagent (Dharmacon, Chicago, IL) according to the manufacturer's instructions. For the oligofectamine transfection, cells were transfected on the first day and subsequently transfected again on the following day

before the addition of drugs into the culture media. For DharmaFECT transfection, cells only underwent a single round of transfection.

***In vitro* p38 kinase assay** – The p38 recombinant kinase (Invitrogen, CA) was preincubated with test compound for 30 min. The test compounds are SB203580 (0.078–40 μ M) with or without EF24 (0.078–40 μ M). p38 was then incubated with a mixture of [γ - 32 P] ATP (0.8 μ Ci; Amersham Pharmacia Biotech) and the exogenous substrate MBP (0.4 mg/ml) at 30°C for 15 minutes. The reactions were stopped by spotting 20 μ l of the reaction mixture onto individual pre-cut strips of phosphocellulose P81 paper (Whatman, U.K.). The phosphocellulose paper was then washed with phosphoric acid (0.5%) to remove unincorporated [γ - 32 P] ATP. Incorporated [γ - 32 P] ATP in MBP was measured using liquid scintillation counting.

HIF reporter gene assay - 1A9 cells were transfected with 1 μ g/well of a luciferase reporter plasmid (pBI-GL V6L) containing six HREs elements from the VEGF promoter as previously described (186, 187). Enzymatic activity was measured by a chemiluminescent assay and normalized to the total protein in the cellular extracts.

Isolation and analysis of RNA - Total RNA was isolated using the RNase Easy Mini Kit (Qiagen, Inc., Valencia, CA) or a TRI Reagent RNA extraction protocol (Ambion, Invitrogen, Carlsbad, CA). Northern blotting was performed with probes designed specifically for human HIF-1 α , β -actin (Ambion, Inc., Austin, TX) as previously described (150). A DNA probe for Hsp70 was designed from a Hsp70-HA plasmid

construct, cutting exon 1 into a approximately 500 kb fragment using Sac II and Nae I restriction enzymes.

Immunofluorescence and confocal microscopy - Exponentially growing cells were plated on 12 mm glass coverslips (Fisher Scientific, Pittsburgh, PA) in 24-well plates, and the cells were allowed to attach overnight. The following day, the cells were treated with the indicated drugs for 16 h and subjected to hypoxia for an additional 4 h. Cells were then washed and fixed onto the coverslips with PHEMO buffer (PIPES 0.068 M, HEPES 0.025 M, EGTA 0.015 M, MgCl₂ 0.003 M, 10% DMSO, pH 6.8) containing 3.7% formaldehyde, 0.05% glutaraldehyde, and 0.05% Triton-X-100 for 10 min at room temperature. Coverslips with fixed cells were blocked in 10% goat serum/PBS for 10 min and processed for immunofluorescence with rat anti- α -tubulin. Secondary antibodies Alexa Fluor 488 and Alexa Fluor 615 goat anti-rat antibody were added next, for visualization of primary antibody. Sytox green was used for DNA staining. In order to visualize actin fibers, rhodamine phalloidin was used. Stained coverslips were mounted onto glass slides and examined using a Zeiss LSM510 point-scanning confocal microscope.

Tubulin *in vitro* polymerization assay - The assembly of purified bovine brain tubulin, prepared as described previously (188), was evaluated as described in detail elsewhere (189). Briefly, 10 μ M tubulin was preincubated for 15 min at 30°C in 0.8 M monosodium glutamate (2 M stock solution adjusted to pH 6.6 with HCl) and 4% (v/v) DMSO and compounds as indicated. Samples were chilled on ice, and GTP (0.4 mM) was added.

(All concentrations are expressed in terms of the final reaction volume.) The samples were transferred to 0°C cuvettes in a temperature-controlled Beckman DU7400 spectrophotometer. Assembly was followed turbidimetrically, with apparent absorbance monitored at 350 nm.

Quantitative RT-PCR - To quantify mRNA levels, we used a highly sensitive, quantitative RT-PCR method. Total mRNA was isolated from cultured cells using TRIZOL (Invitrogen, Carlsbad, CA), and the concentrations were verified. All real-time RT-PCR reactions were performed in duplicate in a 20 μ l mixture containing 1 \times IQ SYBR Green supermix (BioRad, Hercules, CA), 0.2 μ M of each primer and 2 μ l of cDNA templates. The primers for *HIF-1 α* were 5'-TGGTGACATGATTTACATTTCTGA-3' and 5'-AAGGCCATTTCTGTGTGTAAGC-3', and the primers for glyceraldehyde 3-phosphate dehydrogenase (*GAPDH*) were 5'-GGAGTCAACGGATTTGGTCG-3' and 5'-CTTGATTTTGGAGGGATCTCG-3'. Real-time quantification was performed using the BIO-RAD iCycler iQ system (BioRad) under the following cycling conditions: (step 1) 94°C (2 min); (step 2) 50 cycles of 94°C (15 s), 60°C (60 s). The fluorescence threshold value was calculated using the iCycle iQ system software. The standard curves for *HIF-1 α* and *GAPDH* were generated, and the concentrations of the unknown samples were calculated by setting their crossing point to the standard curve. The relative expression level of *HIF-1 α* was normalized by comparative reference with the *GAPDH* gene value.

Co-Immunoprecipitation - Total protein lysate (240 μ g) in 1% NP-40 buffer supplemented with protease inhibitors was incubated at 4°C overnight on a tube rotator

with 10 μ l of anti-Hsp70 antibody (Santa Cruz Biotechnology) or 3 μ l of anti-capsase 3 antibody (Cell Signaling). Following overnight incubation, 25 μ l of protein G bead slurry was added, and the tube was allowed to rotate for an additional 2h. Following three washes with lysis buffer, the beads were collected at the bottom of the tube by centrifugation. Protein bound to the beads was eluted in 15 μ l of 6x SDS loading buffer, and the samples were resolved by SDS-PAGE and analyzed by western blot.

CHAPTER 3

Enhancing the anticancer activity of EF24 with p38 MAPK inhibitors

Rationale

Our hypothesis for this study is that concurrent inhibition of the NF- κ B pathway activation and p38 MAPK signaling leads to an increased cytotoxicity against cancer cells. This hypothesis was formulated based on the rationale stated below:

1. Preliminary data show that EF24 induces the dual Thr/Tyr phosphorylation and activation of all three of the major mitogen-activated protein kinases (MAPKs) including p38 MAPK, which in some instances has a pro-survival function.
2. Combination of EF24 and pyridinyl imidazole p38 MAPK inhibitors elicited cytotoxic synergy, leading to an approximate 40% drop in IC₅₀ below the additive effect of the two agents
3. Like the parent compound curcumin, EF24 has been found to inhibit TNF α -induced activation of the NF- κ B pathway, suggesting that the anticancer activity induced by EF24 may be, in part, mediated by its inhibition of the NF- κ B pathway. Published reports propose p38 activation is necessary for NF- κ B transactivation so

This study attempts to determine the consequences and potential mechanism of the EF24 and p38 MAPK inhibitor synergy. To investigate this, our objectives are to I) determine whether the combination of these agents lead to a synergistic induction of apoptosis and inhibition of longer term cancer cell proliferation, II) determine whether p38 inhibition

specifically enhances the anticancer activity of EF24, and III) investigate whether other approaches to inhibit NF- κ B in combination with p38 inhibition is also synergistic.

Results

EF24 induces the activation of three MAPK pathways: EF24 is more potent than the parent compound curcumin (Fig. 3.1A) in inhibiting A549 cell viability, consistent with the previous report (Fig 3.1B) (52). In order to understand the mechanism that may contribute to this potent anti-cancer activity of EF24, we analyzed pathways that may be modulated upon treatment with this agent. Previously, we demonstrated that EF24 down-regulates TNF α -induced NF- κ B activation by negatively regulating the activity of the upstream kinase of I κ B, IKK. Cross talk is known to exist between the NF- κ B pathway and other important mediators in regulating cell survival and proliferation including the three-tiered MAPK signaling pathways. To determine whether EF24 modulates any of the three well studied MAPKs, we monitored the activation states of ERK, p38 MAPK and JNK in response to EF24 or curcumin (30 min). Interestingly, we found that EF24 induces the activation of each of the MAPKs in a dose-dependent manner revealed by their upregulated phosphorylation (Fig. 3.1C). ERK, as well as p38, were also activated by curcumin as well as p38 MAPK, however at higher concentrations than EF24 (20 μ M vs 0.4 μ M and 50 μ M vs 0.8 μ M). At the time and doses used, no phosphorylation of JNK was detected with curcumin treatment while activation of JNK was detected after treatment of cells with EF24 (5 μ M). The lack of induction of JNK by curcumin is consistent with published data that curcumin inhibits, instead of activates, the signal transduction pathways leading to JNK activation (190, 191).

FIG 3.1. The effect of curcumin and EF24 on A549 cell viability and the activation of the MAPKs. (A) A549 cells were grown in a 96 well plate and treated with EF24 (0.4 μ M) or curcumin (8 μ M) for indicated times. Cell viability was assessed by the sulforhodamine B (SRB) method and is expressed as percentage of vehicle-treated control (0.5% DMSO) (n = 3). (B) A549 cells were treated with increasing EF24 or curcumin for 30 min before the status of ERK, p38 MAPK, and JNK were determined using phospho-specific antibodies for the Thr/Tyr activation motifs.

Inhibition of ERK and JNK activation does not dramatically affect EF24-induced cytotoxicity: Since ERK participates in a mitogenic pathway that promotes cell survival and proliferation and EF24 induces activation of ERK, we determined whether this pathway is important for the potency of EF24, and if inhibition of ERK would further augment the loss of cell viability of EF24-treated cells. A low dose of EF24 (0.4 μ M) was chosen for this experiment since it only induces a low level of growth inhibition (15-25%) of A549 cells after 48 h of treatment. The chemical inhibitor U0126 was used to selectively inhibit ERK by targeting the upstream kinase MEK. The concentrations of U0126 used in this study were determined to inhibit EF24-induced ERK phosphorylation. When the viability of cells with either agent alone was compared to those with the combination of EF24 and U0126, no significant change in cell viability with inhibition of ERK was observed.

Similarly, we determined if JNK inhibition would affect EF24-induced cytotoxicity. Several recent reports implicate JNK in the regulation of the apoptotic response in which activated JNK mediates the induction of cell death (192). We hypothesized that inhibition of JNK would attenuate EF24-induced cell death. A549 cells were treated with a combination of EF24 and a JNK inhibitor, SP600125, for 48h. JNK inhibition did not attenuate the loss of cell viability by EF24 but only caused a slightly additive drop in cell viability.

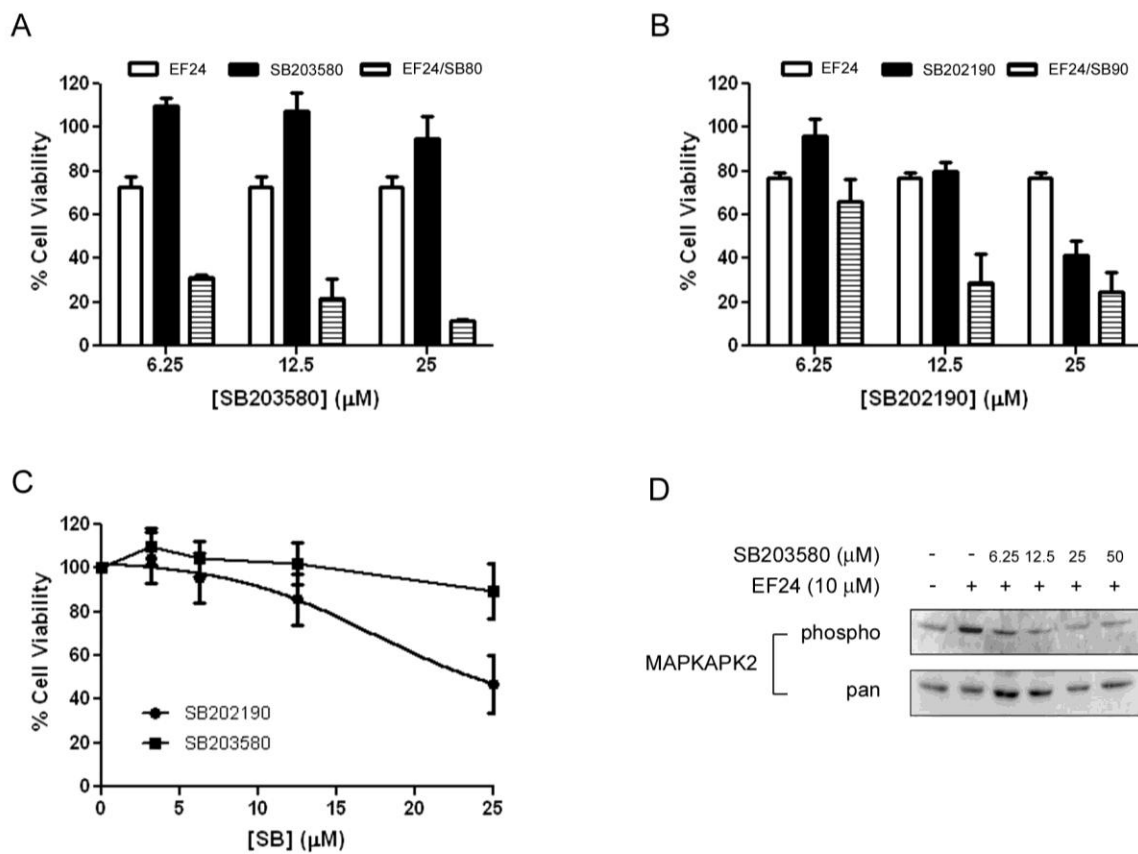
p38 inhibitors enhance EF24-induced A549 cytotoxicity: We then evaluated the effect of p38 MAPK inhibition on EF24-induced cytotoxicity (Fig. 3.2A&B). The same low dose

of EF24 (0.4 μM) was used as in the previous experiments with MEK and JNK. We combined EF24 with increasing concentration of a pyridinyl imidazole p38 MAPK inhibitor, (SB203580 or SB202190). These p38 inhibitors alone did not significantly inhibit A549 cell viability at the test concentrations. When SB203580 was combined with EF24, the percentage of growth inhibition was significantly greater than the effects of each compound alone (Fig. 3.2A). The combination of SB202190 (12.5 μM) and EF24 also had a dramatic effect on cell viability (Fig. 3.2B), showing an approximate 30% reduction in cell viability below the additive effects of the combination.

The synergistic effect of EF24 and p38 inhibitors was not observed when 6.25 μM and 25 μM of SB202190 were combined with EF24. To determine whether this is due to inherent cytotoxicity of this agent possibly due to off-target effects, the dose-dependent effect of both pyridinyl imidazoles on A549 cell growth was compared. SB203580 was found to have little effect on cell survival of A549 cells with the highest concentration tested (25 μM) only leading to a 10% loss in cell viability and an IC_{50} of approximately 50 μM (Fig. 3.2C). However, from the same analysis, the IC_{50} of SB202190 was determined to be approximately 25 μM . The inhibition of p38 MAPK activity by SB203580 was also demonstrated by monitoring at the phosphorylation of MAPKAPK-2, an immediate downstream effector of p38 (Fig. 3.2D). Again, inhibition of p38 by this compound significantly enhanced the EF24 effect. Since SB203580 has the least effect on A549 viability alone while still inhibition p38 activity, this compound was used for the remainder of the experiments.

FIG 3.2. Inhibition of p38 enhances EF24-induced growth inhibition. Cell viability was assessed using the SRB assay as the percentage of vehicle-treated (0.5% DMSO) control. Combination treatment of A549 with EF24 (0.4 μ M) and SB203580 (**A**) or SB202190 (**B**). Cells were treated with SB203580 and SB202190 for 48 h (**C**). (**D**) A549 cells were pretreated with SB203580 for 1h before treatment with EF24 (10 μ M) for 30 min. Cells were subjected to western blotting to access phosphorylation and protein expression of MAPKAPK-2 as a p38 substrate.

FIG 3.2 (continued). Inhibition of p38 enhances EF24-induced growth inhibition.



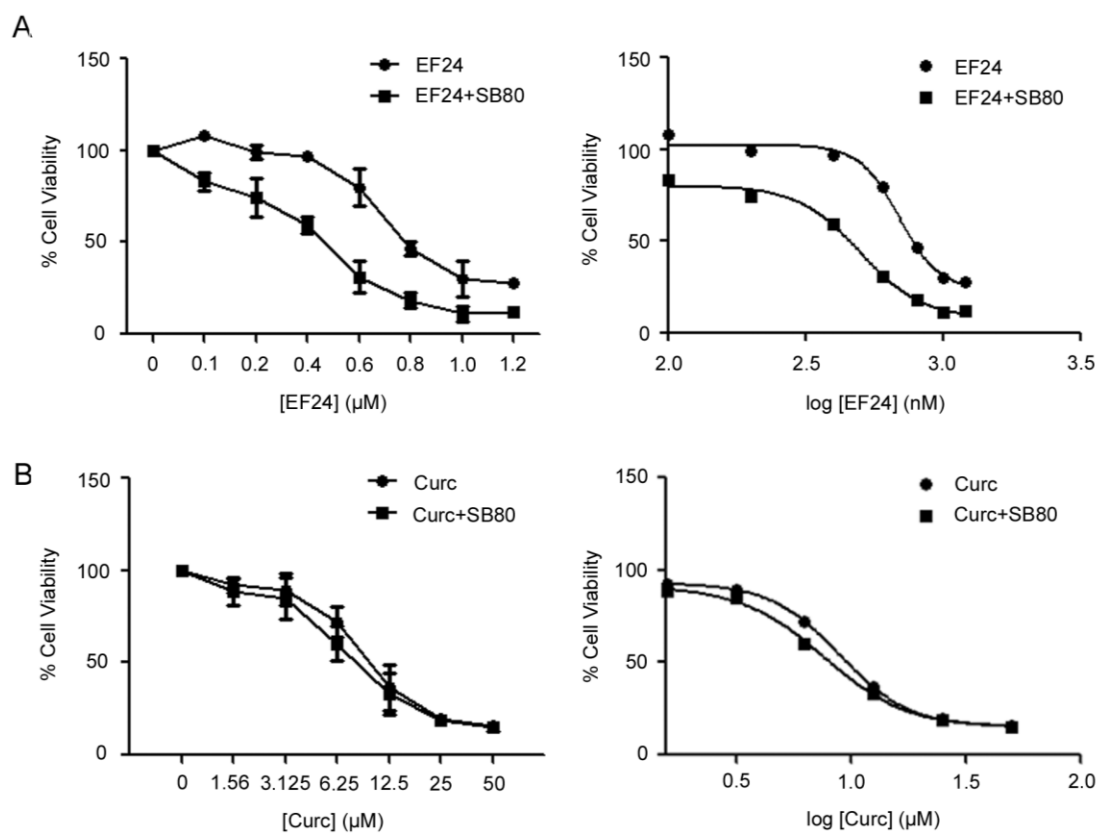
Analysis of dose-response curves show that the combination of EF24 and SB203580 is synergistic: To further determine the nature of the combination effect, we first graphed the dose response curve for EF24 by titrating increasing amounts of this compound into the media in combination with SB203580 and determining the percent cell viability at each concentration after 48 h (Fig. 3.3A). By transforming the dose-response curve for both curcumin and EF24 to a logarithmic scale, the IC_{50} values were determined to be for EF24 (0.7 μ M) and the EF24 combination (0.5 μ M), respectively. Similarly, curcumin combination with SB203580 was analyzed in comparison to the EF24 effect (Fig 3.3B), which gave rise to a much smaller difference with IC_{50} values of 8.9 μ M for curcumin and 7.6 μ M for the curcumin combination. While this data represented about a 30% reduction in IC_{50} for EF24, the addition of p38 MAPK inhibitors to curcumin only reduced the IC_{50} of EF24 by about 15%.

Scheduling of the addition of EF24 and SB203580 may affect the efficacy of the treatment combination: Data shows that the combination of EF24 and p38 inhibitors is highly effective in inhibiting the growth of cancer cells. In order to determine if scheduling the addition of these agents are important for the maximal anticancer activity, we first pretreated A549 cells with either EF24 (0.4 μ M) or SB202190 (12.5 μ M) for 30' before the addition of the other agent (Fig 3.4A). The time point for pretreatment was chosen due to the approximate time for activation of p38 by EF24. Cell viability was then assessed after 48h and compared to the simultaneous addition of the two agents. While the EF24/SB90 combination inhibited cell viability by approximately 30% below

FIG 3.3. Effect of SB203580 on dose-response growth curves of EF24 and curcumin.

A549 cells were treated with EF24 (**A**) or curcumin (**B**) in the presence or absence of SB203580 and their viability was measured after 48 h by the SRB assay.

FIG 3.3 (continued). Effect of SB203580 on dose-response growth curves of EF24 and curcumin.



the additive effect of these agents, no significant difference was noted in the regimes that included pretreatments. Additionally, studies were conducted to analyze how effective scheduling of EF24 and SB203580 similar to that in a clinical situation would compare to the concurrent treatment of these agents (Fig 3.4B). A549 cells were treated with EF24 for 24h before the addition of SB80 into the culture media for an additional 24h or vice versa. Both of these treatment schedules were not as active as the synergy noted with the concurrent treatment. Pretreated with EF24 for 24h before the addition of SB80 was however slightly synergistic (approximately 20% below additive effect) while the pretreatment of SB80 was closer to the combination additive level.

Genetic inhibition of p38 MAPK sensitizes A549 to EF24-induced loss of cell viability:

In order to determine if the inhibition of p38 is responsible for the enhanced EF24-induced cytotoxicity, we used a genetic rather than chemical approach to inhibit p38 MAPK. A549 cells were treated with siRNA targeting p38, which resulted in a 50-70% knockdown of p38. The siRNA was deemed fairly specific because no change in other kinases was observed as seen for ERK expression levels (Fig. 3.5A&B). The, these p38-knockdown cells were used to test the effect of reduced p38 on cell sensitivity to EF24 (0.4 μ M) (Fig. 3.5C). Cell viability was analyzed 48 h after treatment of cells with test agents. The effect of p38 knockdown was compared to a mock transfected control with a scramble siRNA. As shown in Fig. 3.5C, p38 silencing enhanced cell sensitivity to EF24, showing significantly loss of cell viability similar to that of the combination of EF24 and SB203580. These results suggest that upregulated p38 upon EF24 treatment

FIG 3.4. Scheduling of the EF24 and SB203580 combination. A SRB assay was used to determine the effects of the scheduling EF24 (0.4 μ M) and SB203580/SB202190 (12.5 μ M) treatments on A549 cell viability. **(A)** The concurrent addition of these two agents were compared to a pretreatment (30 min) of each agent before the addition of the other. Cell viability was accessed 48 h following the addition of the last drug treatment. **(B)** The effect of scheduling of regimes comprised of 24 h treatment of one agent before the addition of the second for an additional 24 h was compared to the 48 h treatment of EF24 and SB203580 added simultaneously.

FIG 3.4 (continued). Scheduling of the EF24 and SB203580 combination.

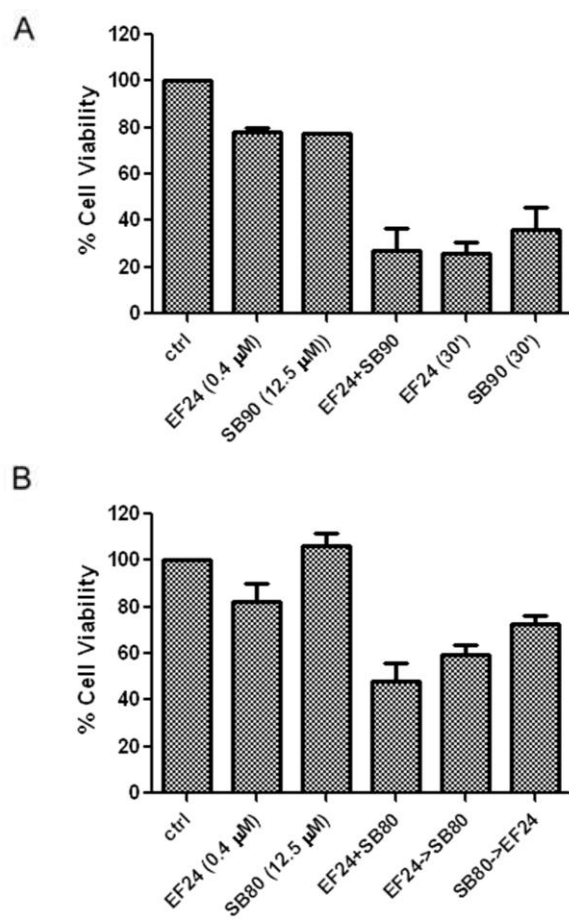
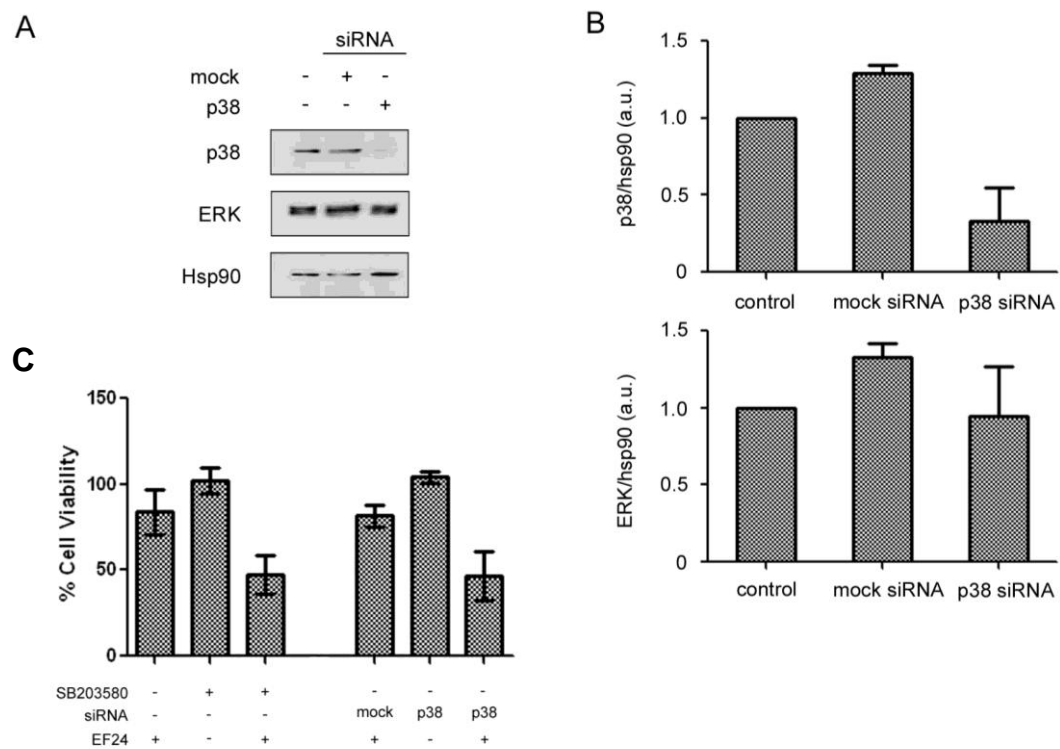


FIG 3.5. Knockdown of p38 sensitizes A549 cells to EF24-induced cytotoxicity. (A & B)

A549 cells were transiently transfected with p38 siRNA as outlined in Materials and Methods. p38 as well as total Hsp90 ERK protein expression was assessed by western blotting. (C) A549 cells were transiently transfected with mock or p38 siRNA and were incubated with or without 0.4 μ M of EF24 for 48 hr where indicated. Cell growth was assessed by SRB assay. Results were compared to mock transfected control.

FIG 3.5 (continued). Knockdown of p38 sensitizes A549 cells to EF24-induced cytotoxicity.



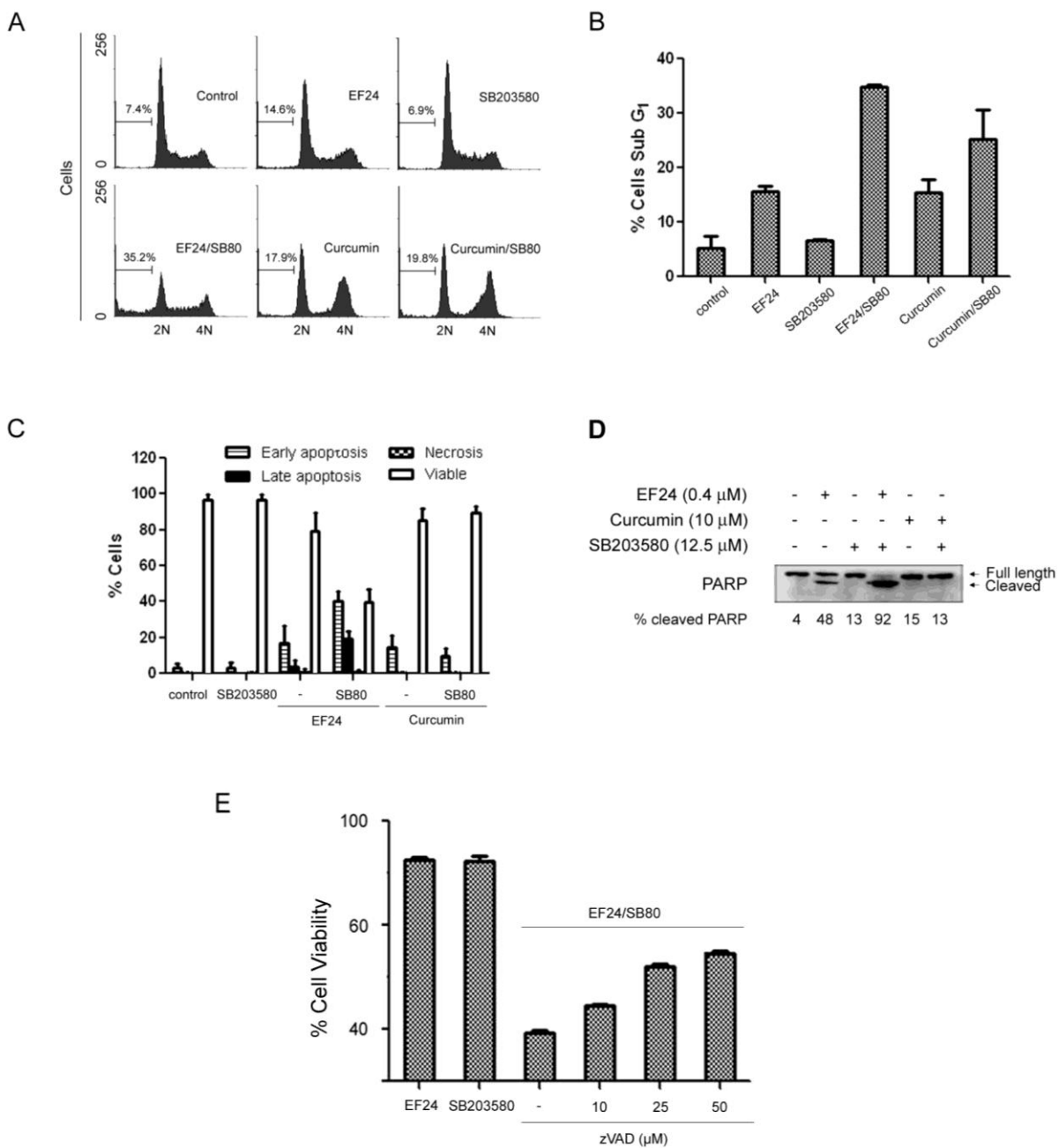
may provide a feedback loop in support of lung cancer survival. Disabling this p38-mediated negative feedback mechanism reduces the resistance to EF24, leading potentially to an enhanced therapeutic efficacy.

The induction of apoptosis by EF24 is potentiated by pharmacological p38 MAPK

inhibition: EF24 has already been demonstrated to induce apoptosis in a various panel of cancer cells (66, 68, 70, 184). We examined whether the combination of EF24 and SB203580 caused an increased apoptotic response by using flow cytometry analysis (Fig. 3.6A&B). The treatment of EF24 (0.4 μ M) or SB203580 (12.5 μ M) alone for 48 h resulted in no significant difference in the percent of apoptotic cells from the vehicle-control. However, when these two agents are combined, a synergistic accumulation of cells in the sub-G₁ fraction, an indication of cells undergoing apoptosis, was observed. A dramatic increase in sub-G₁ cells were not observed between the curcumin and curcumin plus SB203580 treatment groups (Fig. 3.6A&B). Moreover, differentiating between apoptotic and necrotic cells using double-staining techniques shows that the cells treated with the combination explicitly undergo apoptosis (Fig 3.6C). The trend was also seen using western blot analysis when examining combination drug-induced cleavage of PARP, another hallmark of the induction of apoptotic cell death (Fig. 3.6D). In all experiments, the same striking effect of the combination of EF24 and SB203580 was not observed with the curcumin combination. Since PARP cleavage suggests that the combination of EF24 and SB203580 induces caspase activation to elicit apoptosis, we wanted to determine whether inhibiting global caspase activity could attenuate the loss

FIG 3.6. Combination of EF24 and SB203580 synergistically induces apoptosis. (A) Cell cycle analysis of combined treatment of EF24 (0.4 μ M) and the SB203580 (12.5 μ M). A549 cells were exposed to the indicated compound treatment for 48 h. Flow cytometry was performed to define the cell cycle distribution based on nuclear content of cells as described in Materials and Methods. The data represents the cell cycle distribution for a representative experiment. (B) Summary of results with sub-G1 cells from three independent experiments. (C) Western blot analysis of A549 lysates treated with EF24 (0.4 μ M), SB203580 (12.5 μ M), curcumin (10 μ M) or the combination of two compounds after 48 h. The amount of full length and cleaved PARP was revealed by western blotting using an anti-PARP antibody. (D) Results of a cell health assay. A549 cells were plated in a 96 well plate at a density of 5000 cells/well. The following day, the cells were treated with the indicated concentrations of EF24, SB203580, curcumin, or the combinations of EF24 or curcumin with SB203580 for 48 h. The cellular stains DAPI, Yo-Pro-1, and PI were added to each well. Yo-Pro-1 positive cells are deemed early apoptotic, PI-positive cells are necrotic, and Yo-Pro-1 and PI-positive cells are late apoptotic (185). Cells that excluded both stains but had intact nuclear staining were deemed viable. A second concentration of EF24 (0.6 μ M) served as a control to ensure the assay could identify an increase in apoptosis. (E) Caspase inhibitor effect. A549 cells were pretreated with the caspase inhibitor zVAD-fmk at indicated concentrations for 1 h before treatment with the combination of EF24 (0.4 μ M) and SB203580 (12.5 μ M).

FIG 3.6 (continued). Combination of EF24 and SB203580 synergistically induces apoptosis.



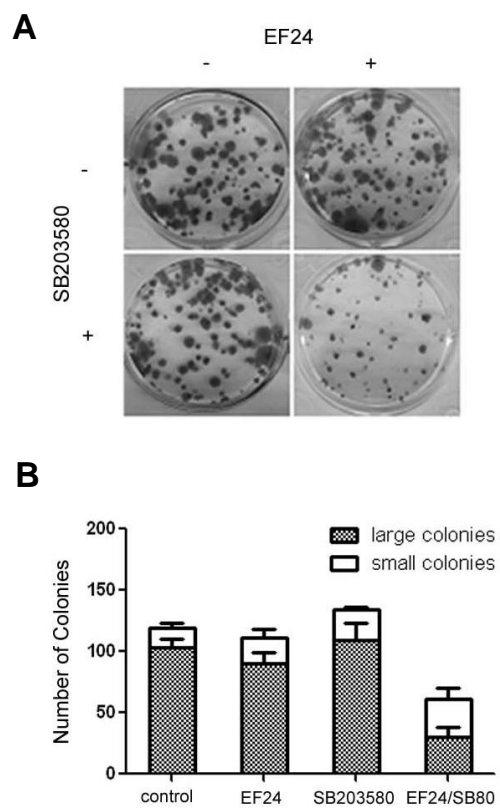
of cell viability induced by this combination. To do so, we pretreated A549 cells with the pan caspase inhibitor zVAD-fmk for 1h before a 48h treatment of cells with the combination of EF24 and SB203580. The pretreatment of caspase inhibitor significantly blocked the loss of cell viability by EF24 and SB203580 (Fig. 3.6E).

Combination of EF24 and SB203580 synergistically inhibits colony formation: To further investigate the synergistic activity of the combination of EF24 and pharmacological inhibition of p38 MAPK, we assessed whether this combination could inhibit relatively long term A549 cancer cell proliferation using a colony formation assay (Fig. 3.7A). We determined from previous data that the IC₅₀ for inhibition of colony formation for EF24 is about 150 nM and about 10 μM for SB203580 (data not shown). For the combination treatment for this experiment, 100nM of EF24 was used. To keep the EF24:SB203580 ratio similar to that used in cell viability experiments (1:32.5) we used 5 μM of SB203580 for this assay. As expected, the combination proved effective in decreasing the number of colonies between all treatment groups by approximately 50% and also inhibiting the overall size of the colonies (Fig. 3.7B).

EF24 does not enhance SB203580 in inhibiting p38 kinase activity in vitro: In order to determine whether EF24 enhances the inhibition of p38 MAPK kinase activity by SB203580 which could contribute, at least in part, to the synergistic effects with the combination of these two agents, we conducted a p38 *in vitro* kinase assay to analyze the

FIG 3.7. EF24 and SB203580 show a synergistic effect on the inhibition of A549 colony formation. (A) A549 cells were first plated at a density of 450 cells/well and then treated every 3 days with the indicated concentration test compounds. On day 10, the cells were fixed and stained with SRB. Colonies formed were counted using Image J. The effect of compound treatment on colony formation was compared to the vehicle-treated (0.5% DMSO) well. (B) Summary of data with both colony number and size included.

FIG 3.7 (continued). EF24 and SB203580 show a synergistic effect on the inhibition of A549 colony formation.



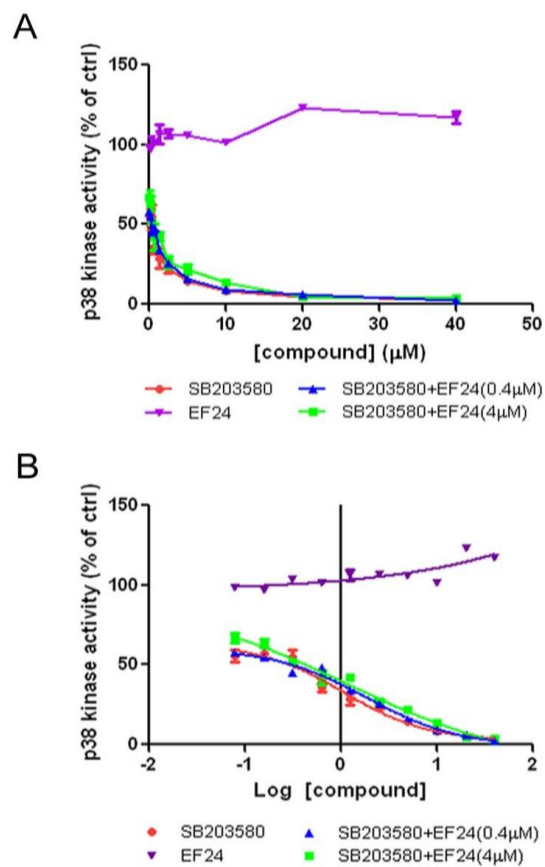
effects of these agents on p38 catalytic activity. The enzymatic activity of p38 was observed in the presence of SB203580, EF24, or the combination of the two agents (Fig 3.8A&B). As expected, the known p38 MAPK inhibitor SB203580 dramatically inhibited the activity of p38 with an IC_{50} of approximately 1 μ M. As we hypothesized, the presence of 0.4 μ M or even 4 μ M EF24 alone in the reaction mixture did not inhibit the kinase activity of p38. When the combination of EF24 (0.4 μ M or 4 μ M) was added to SB203580, no significant change in the IC_{50} of p38 inhibition was noted.

Combination of NF- κ B and p38 MAPK inhibition does not fully explain EF24 and

SB30580 synergy: We have previously shown that EF24, like curcumin, blocks TNF α -induced NF- κ B translocation in A549. Further investigation showed that EF24 directly interferes with the NF- κ B pathway by directly targeting IKK β . Consequently, it hinders phosphate transfer to the endogenous substrate I κ B in *in vitro* kinase assays, suggesting a unique anti-NF- κ B mechanism when compared with curcumin (52). To further examine whether the synergy elicited by the EF24 and SB203580 combination was simply due to the combined effect of IKK β and p38 MAPK inhibition, IKK β inhibitor IV, a specific inhibitor of IKK β , was combined with SB203580 and used to treat A549 cells. Three concentrations of the IKK inhibitor chosen for this study did inhibit TNF α -induced I κ B phosphorylation to a similar level to that of EF24 (data not shown). However, a 48h SRB cell viability assay was conducted with the combination of these agents and no dramatic loss of cell viability was observed (Fig. 3.9A). In order to ascertain whether this may be due to the lack of induction of p38 by the IKK β inhibitor,

FIG 3.8. EF24 does not potentiate SB203580-mediated inhibition of p38 activity *in vitro*. The ability of EF24, SB203580, and the combination of EF24 and SB203580 to attenuate p38 kinase activity was determined *in vitro* and graphed as the concentration of compound vs. % p38 activity (**A**) and as the log of the concentration vs. activity (**B**). The compounds were incubated with the kinase for 30 min before the addition of the reaction mixture including the substrate MBP as described in the Materials and Methods.

FIG 3.8 (continued). EF24 does not potentiate SB203580-mediated inhibition of p38 activity *in vitro*.



we compared 0.4 μ M EF24-induced phosphorylation of p38 MAPK to that induced by 10 μ M of this inhibitor (Fig 3.9B). Two different time points – 15' and 30' – were chosen based on high p38 activation by EF24 in previous time course experiments. Even at this high concentration exceeding its IKK β inhibition IC₅₀ (approximately 1 μ M), this inhibitor failed to induced significant p38 MAPK activation.

Differences in the efficacy of EF24/p38 inhibitor combination exist across various lung cancer cell lines. To determine whether the synergistic nature of the EF24 and SB203580 was confined to A549 lung cancer cells, the combination was tested against various lung cancer cells lines. Similar 48h SRB assays were conducted, and the IC₅₀ values for EF24 treatment alone and EF24 in combination with SB203580 were determined (Table 3.1). The A549 cell line was used as a control for synergism since previous experiments established the significant anticancer activity of the EF24 and SB203580 combination in this cell line. H1299 had a similar EF24 IC₅₀ profile to A549 and was the cell line where the treatment combination exerted similar synergistic activity. Three cell lines – H157, H460, and H358 – were slightly more sensitive to EF24 treatment over A549 (0.5 fold) and also had comparable degrees of synergism, which was closer to an additive effect.

FIG 3.9. Combination of the specific IKK inhibitor and SB203580 does not cause a dramatic effect on cell viability. (A) The simultaneous combination of the indicated concentrations of the IKK-2 inhibitor IV and SB203580 (12.5 μ M) was tested using a 48h SRB cell viability assay as previously described. (B) Western blot analysis was conducted to determine the activating phosphorylation status of p38 MAPK for EF24 or IKK inhibitor IV treatment after 30' and 1h.

FIG 3.9 (continued). Combination of the specific IKK inhibitor and SB203580 does not cause a dramatic effect on cell viability.

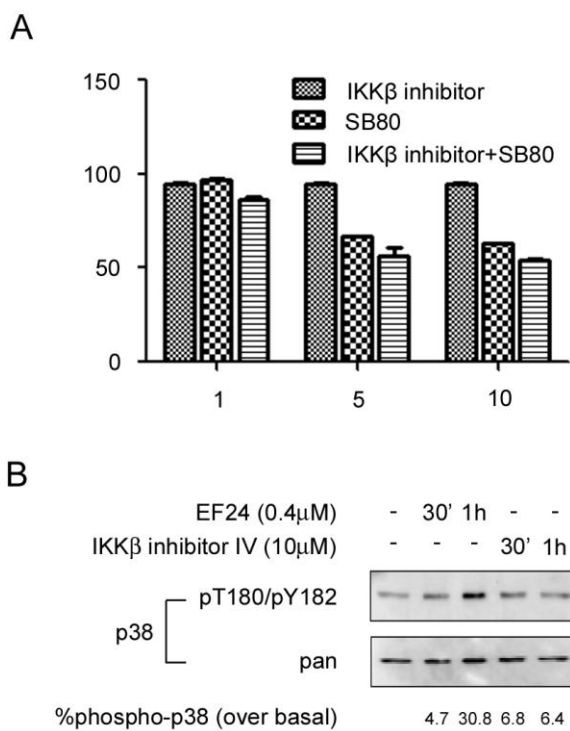


TABLE 3.1. EF24 and SB203580 cooperates to create cytotoxic synergism in multiple lung cancer cell lines. The IC₅₀ values for 48 hr drug treatments were determined for a panel of lung cancer cell lines (A549 H1299, H157, H460, H358) using a SRB assay as previously described. Each cell line was treated with EF24 alone and in combination with SB203580 and the IC₅₀ values were determined. The relative percent difference between the theoretical additive effect of the two agents and the experimental effect was used to determine the degree of synergy.

TABLE 3.1 (continued). EF24 and SB203580 cooperate to create cytotoxic synergism in multiple lung cancer cell lines.

Cell line	EF24 IC₅₀ (μM)	EF24/SB80IC₅₀ (μM)	IC₅₀ Difference (%)
A549	0.77	0.39	53.2
H1299	0.76	0.59	36.4
H157	0.44	0.38	13.2
H460	0.42	0.32	15.8
H358	0.45	0.39	11.9

Conclusions

Lung cancer is the leading cause of death worldwide, most people being diagnosed with advanced or metastatic non-small cell lung cancer (NSCLC). Currently, treatment options for this particular cancer are limited. In the present study, we used the A549 lung adenocarcinoma cell line, a cell model for NSCLC, to demonstrate that EF24 exhibits higher cytotoxicity than the lead compound curcumin. Interestingly, our work also reveals a negative feedback loop mediated by p38 that may restrict the efficacy of EF24. By disabling the EF24-induced upregulated p38, it may be possible to enhance the EF24 effect. Indeed, EF24 produces a dramatic synergistic growth inhibition of A549 cells and induction of apoptosis when combined with pyridinyl imidazole p38 MAPK inhibitors (Fig 3.2). The same is not true for the combination of curcumin and p38 MAPK pathway inhibitors, however. This study not only provides us with a potential combination that may be useful in a clinical setting, but also furnishes several important observations concerning the mechanism of action of EF24 against A549 cells.

The ERK, JNK, and p38 MAPK signaling pathways were activated in response to EF24 treatment as revealed by enhanced phosphorylation of the specific threonine and tyrosine motifs in the activation loops of each kinase. Though ERK has a widely accepted role in mediating cellular survival and proliferation, inhibiting the activation of ERK failed to potentiate the effect of EF24 to inhibit A549 cell growth. Furthermore, JNK is thought to act as a pro-apoptotic kinase, but our studies show that inhibition of JNK activity in combination with EF24 was slightly additive. We expected JNK inhibition to

attenuate the anti-cancer activity of EF24. One conclusion from this observation is that either activation of JNK is not imperative for EF24-mediated cell death, or EF24-induced JNK has a pro-survival function (193, 194). However, the non-specific nature of the chemical inhibitor SP600125 certainly complicates the interpretation of the data (195).

p38 MAPK has been implicated in survival pathways since there is often a link made between this MAPK pathway and NF- κ B transcriptional activation. The involvement of p38 in the induction of COX-2 and the biosynthesis of cytokines such as TNF α and IL-6 supports the importance of p38 in inflammation (196, 197). We demonstrated that SB203580, the prototypical p38 MAPK inhibitor used in the majority of our studies, blocks p38 activity induced by EF24 as evidenced by the inhibition of MAPKAPK-2 phosphorylation. SB203580 did not significantly affect A549 cell growth, indicating that inhibition of p38 MAPK alone does affect cell proliferation. Concurrent inhibition of p38 MAPK activity in combination with EF24 enhances A549 cell death and thereby suggests that p38 MAPK has a pro-survival function in A549 in response to EF24. Cellular staining in flow cytometry as well as an increase in cleaved PARP further verified the synergistic nature of this treatment combination.

In support of a potential role of the EF24 combination with a p38 inhibitor for the treatment of lung cancer, we have demonstrated a potent combination effect in the suppression of A549 cell clonogenic activity. In analyzing the data from the 10 day colony formation assay, there was a dramatic decrease in the number of colonies formed, which may be a result of the death of cells with colony-formation potential.

However, there was also a difference in the size of the colonies formed with the combination treatment, possibly suggesting growth suppression of cells in these colonies as well as apoptosis. This conclusion was supported by the experimental results with a pan caspase inhibitor zVAD-fmk, which showed significant reversal of cell death induced by EF24. However, it is interesting to note that even at the highest zVAD-fmk concentration used for pretreatment (50 μ M), full recovery of cell viability was not reached. The data are consistent with other published reports that EF24 induces cell death in part through a potentially caspase-independent mechanism (68).

Scheduling analysis of the addition of EF24 and the p38 inhibitor showed that short term (30 min) pretreatments of these agents do not affect the significant anticancer activity of the combination. However, further studies show that concurrent treatment is preferable against schedules with longer duration between agents and shorter treatment times. Additionally, genetic background of the tumor and the sensitivity of the cancer to EF24 alone may play a role in the efficacy of the combination. These results can ultimately benefit the design of clinical regimes and the determination of which tumor types may respond better to this proposed therapeutic combination.

To address the mechanism of the combination effect, we examined the possibility of a direct action of both EF24 and SB203580 on p38 and conducted a p38 *in vitro* kinase assay. The enzymatic activity of p38 was observed in the presences of SB203580, EF24, or the combination of the two agents. As expected, the known p38 MAPK inhibitor SB203580 dramatically inhibited the activity of p38 with an IC_{50} of approximately 1 μ M.

However, the presence of EF24 alone (0.4 μM or 4 μM) in the reaction mixture did not inhibit the kinase activity of p38. Furthermore, no significant change in the IC_{50} of p38 inhibition was noted when EF24 (0.4 μM or 4 μM) was added to the reaction in the presence of SB203580. These studies rule out a direct action of EF24 on p38, in further support of the model that the p38 inhibition lowered the threshold of A549 lung cancer cells for the EF24 action. It is likely due to a disabled negative feedback loop mediated by the upregulated p38 upon EF24 treatment.

A second hypothesis is that it is the inhibition of p38 MAPK with the inhibition of the NF- κB pathway that mediates significant anti-survival signals. Though EF24 is thought to be a pleiotropic agent, EF24 is known to target the NF- κB pathway by directly inhibiting IKK β . However, evidence showing the lack of dramatic effect of the anti-NF- κB agent curcumin and SB203580 on A549 cell growth argues against this idea. Though this could be due to the lack of potency of curcumin to inhibit IKK β , a range of curcumin concentrations up to 50 μM , a concentration more than 100 times that of EF24, was tested in combination with SB203580. A more specific IKK β inhibitor co-treated with SB203580 also failed to produce a significant combinational effect. This IKK β inhibitor, however, did not induce a high level of p38 MAPK activation as EF24 so it did not completely mimic EF24 in that respect, a factor that is undoubtedly important to the SB-mediated enhanced of the cytotoxicity of EF24. This could account for the lack of the synergistic effect since the induction of p38 by EF24 is possibly a major survival mechanism for this agent and may not be for the IKK β inhibitor. Nevertheless, this data

also suggests that the induction of p38 MAPK by EF24 is not a general consequence of IKK β inhibition. A more detailed mechanism responsible for this synergy will require additional investigation.

At the present time, p38 MAPK inhibitors are in clinical trial for a plethora of inflammatory diseases from arthritis to skin disorders such as psoriasis. Recently, these inhibitors have been found to also be efficacious against tumors but often fail due to increased toxicity at the effective doses (198). Development of combination treatments using these inhibitors could possibly decrease the dose needed to see a dramatic effect and therefore prevent side effects. We suggest that molecular-targeted agents like p38 MAPK inhibitors may serve as a companion agent to curcumin analogs with increased *in vivo* activity and bioavailability like EF24 in order to successfully treat lung cancer. Our work supports a combination strategy with EF24 and a specific p38 inhibitor for enhanced therapeutic efficacy in lung cancers.

CHAPTER 4

Induction of Hsp70 through EF24-mediated p38 signaling confers cancer survival advantage

Rationale

In our analysis, we observed the significant induction of Hsp70 protein levels in cancer cell lines in response to EF24 treatment. We hypothesize that the increase expression of Hsp70 is through EF24-induced p38 signaling and mediates a cellular survival advantage against the stress of this cytotoxic agent. This hypothesis was formulated based on the rationale stated below:

1. Hsp70 is one of the major heat shock proteins that assist in maintaining cellular homeostasis in the face of stress induced by heat shock, toxic chemical agents, and chemotherapeutics.
2. One proposed mechanism of Hsp70 from the literature is inhibiting the activity of several components of the apoptotic pathway (i.e. caspases, AIF) leading persistent cell survival.
3. Previous published studies have shown that p38 MAPK, which is induced by EF24, plays an important role in the regulation of Hsp70 through phosphorylation of transcription factors that control Hsp70 expression.

The purpose of this study is to determine the mechanism by which EF24 causes the accumulation of Hsp70 protein levels in cancer cells. Additionally, if this Hsp70 protects cells against EF24-induced apoptosis, we propose that inhibition of Hsp70 can enhance this cell death. Our objectives are to I) determine the mechanism of how EF24 treatment leads to induction of Hsp70, II) evaluate whether inhibition of upregulated Hsp70 can enhanced EF24-induced cancer cell death, and III) investigate if inhibition of EF24-

induced Hsp70 contributes to the synergistic nature of the combination of p38 inhibitors and EF24.

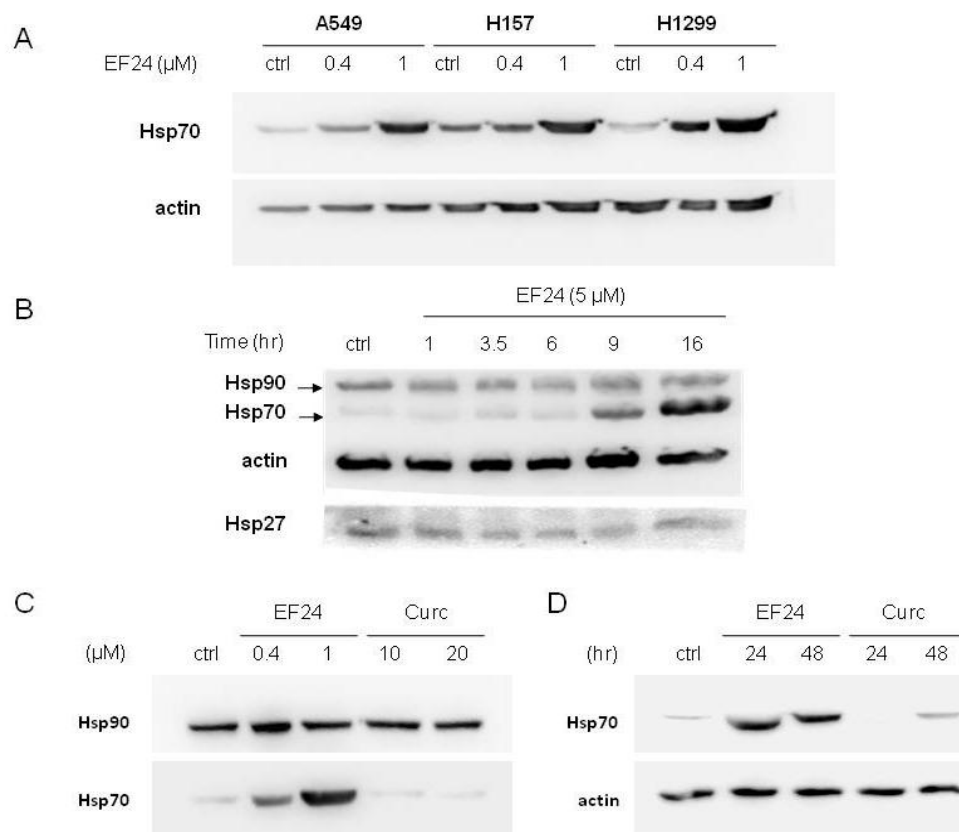
Results

EF24 specifically and dramatically induces Hsp70 protein levels: In our analysis of the mechanism of EF24, we observed the dose-dependent induction in A549 of a protein approximately 70 KD in western blot analysis with an IC_{50} of approximately 1 μ M. This band was later identified to be the heat shock protein, Hsp70. Further analysis revealed that EF24-mediated Hsp70 protein accumulation is not a cell line-specific response confined to A549 lung cancer cells. Induction of Hsp70 in H157 and H1299 cell lines by EF24 was also observed (Fig. 4.1A). Based on timecourse analysis, increased Hsp70 protein levels from basal levels were observed after approximately 9 hr of treatment and were persistent overnight (Fig. 4.1B). Additionally, levels of other heat shock proteins (Hsp90 and Hsp27) remained relatively unchanged in response to EF24, suggesting induction of Hsp70 is a specific response. Though induction of Hsp70 has been shown to occur with various cellular stresses, curcumin failed to induce detectable levels of Hsp70 to the same extent as EF24 after 9 hr, even at comparable cytotoxic concentrations (Fig 4.1C). Significant levels of Hsp70 following curcumin treatment was also not detected after 24 and 48 h (Fig 4.1D).

EF24-induced Hsp70 is due to increased transcription: Based on the timecourse studies, induction of Hsp70 is observed around 9 hr of EF24 treatment. Since the upregulation of Hsp70 is not immediate, it may be due to stimulation of Hsp70 transcription and protein synthesis. To rule out the possibility that the induced Hsp70 is due to the EF24-mediated effect on a post-translational regulation factor, the translation inhibitor cyclohexamide

FIG 4.1. EF24 specifically induces Hsp70 protein levels in a dose-dependent and time-dependent manner. (A) The lung cancer cell lines A549, H157, and H1299 were treated with various concentrations of EF24 (0.4, 1 μ M) overnight. Western blot analysis was conducted to assess levels of Hsp70 and actin. (B) A549 cells were treated with 5 μ M EF24 for 1, 3.5, 6, 9, and 18 hr. After the designated time period, lysates were collected and immunoblotting was performed using the specific antibodies indicated. (C) A549 cells were treated with EF24 (0.4, 1 μ M) or curcumin (Curc; 10, 20 μ M) overnight and the levels of Hsp70 in response to drug treatment were assessed using western blot analysis. (D) Hsp70 was detected following 24 and 48 hr of EF24 (1 μ M) or Curc (20 μ M) treatment.

FIG 4.1 (continued). EF24 specifically induces Hsp70 protein levels in a dose-dependent and time-dependent manner.



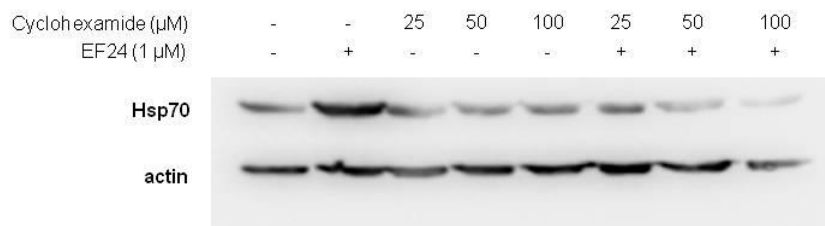
(CHX) was used to determine whether inhibiting protein synthesis could attenuate EF24-induced Hsp70 (Fig. 4.2A). Combining 25, 50, and 100 μ M of CHX with EF24 blocked EF24-induced Hsp70 in a dose-dependent manner. In order to determine if the increase in protein levels in response to EF24 is due to the upregulation of transcription, northern blot analysis was used (Fig 4.2B). Results show that in a dose-dependent manner, EF24 treatment leads to an increase in the Hsp70 mRNA. Northern blot analysis show a slight increase in Hsp70 transcription though not as significantly as EF24.

Upregulation of Hsp70 by EF24 conveys a survival advantage to cancer cells: To evaluate whether the Hsp70 induced by EF24 leads to a survival response, the combination of the flavanoid Hsp70 inhibitor quercetin (199-201) and EF24 was tested using a SRB cell viability assay. Previous western blot analysis shows that pretreatment with quercetin for 6 hours before addition of EF24 was sufficient to block EF24-induced Hsp70 (Fig. 4.3A). Consistent with published reports on the activity of quercetin, treatment with quercetin alone decreased A549 cell viability. When a pretreatment of quercetin (50,100 μ M) was combined with EF24 (0.4 μ M) this generally elicited a slightly synergistic effect (Fig 4.3B). Since the flavanoid may not be entirely specific for the Hsp70 inhibition, the same cell viability experiment was conducted using Hsp70 siRNA, which successfully inhibited EF24-induced Hsp70, in combination with EF24 (Fig 4.3C). The results showed that genetic silencing EF24-induced Hsp70 caused an additive decrease in cell viability (Fig 4.3D).

FIG 4.2. EF24 induces Hsp70 protein levels through increased transcription. (A) The protein translation inhibitor cyclohexamide (CHX) used to treat A549 cells simultaneously with EF24 at the indicated concentrations. Levels of Hsp70 in response to these treatments were assessed using western blotting analysis. (B) Northern blot analysis was used to evaluate the transcription of Hsp70 in response to treatment with EF24, curcumin (Curc), SB203580, and the combination of EF24 and SB203580. All drug treatments were for 5 hr. In the case of EF24 and SB203580 combination, SB203580 treatment was for an hour before the addition of EF24. Graphical data is represented as the average of two independent experiments.

FIG 4.2 (continued). EF24 induces Hsp70 protein levels through increased transcription.

A



B

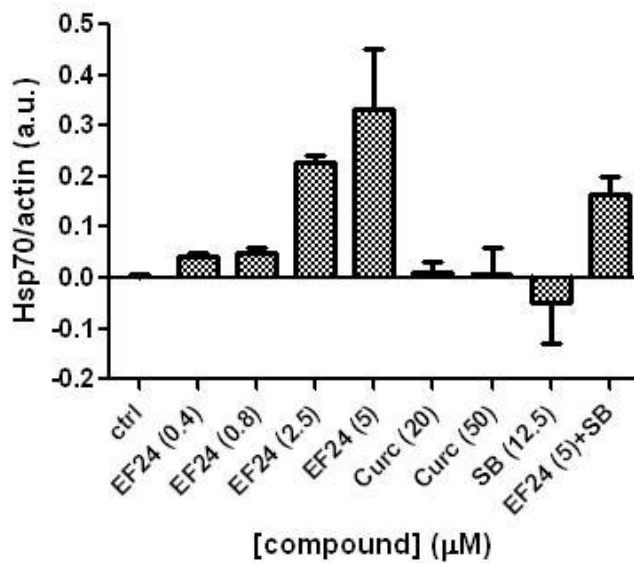
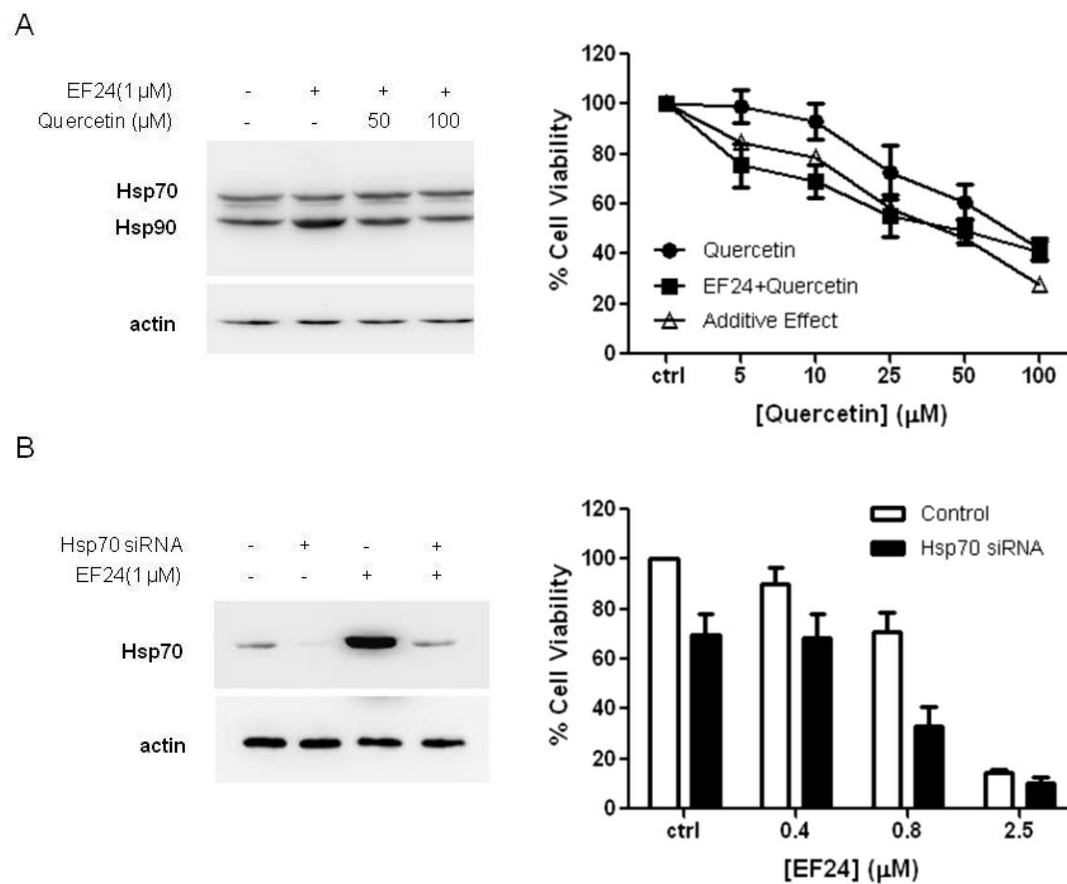


FIG 4.3. Inhibition of EF24-induced Hsp70 expression inhibits cancer cell viability and induces apoptosis. (A) Pretreatment of A549 cells with quercetin at the indicated concentrations was followed by treatment with EF24 overnight. Western blotting was used to evaluate induction of Hsp70 as well as Hsp90 and actin levels (B) The effect on cell viability by the combination of quercetin (6 hr pretreatment) and EF24 (0.4 μ M) was assessed using a SRB assay. A line is graphed to assess where the additive effect of the combination would lie. Any line graphed before this line was deemed synergistic. (C) A549 cells were transfected with Hsp70 siRNA for 24 hr before the EF24 treatment. To evaluate the level of Hsp70 knockdown, western blotting was utilized. (D) The combination of EF24 (0.4 μ M) and Hsp70 siRNA (24 hr transfection) was conducted in A549 and the effect on cell viability was assessed with a SRB assay.

FIG 4.3 (continued). Inhibition of EF24-induced Hsp70 expression inhibits cancer cell viability and induces apoptosis.

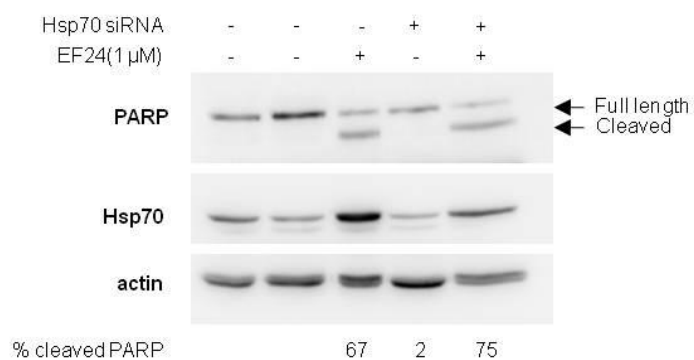


EF24-induced Hsp70 is associated with inhibition of apoptotic signaling: In order to determine whether the loss of cell viability when Hsp70 inhibition is combined with EF24 treatment is due to an increase in apoptotic signaling, western blot analysis was used to analyze PARP cleavage as a marker for the induction of caspase-mediated intrinsic apoptosis. Inhibition of Hsp70 with Hsp70 siRNA (Fig. 4.4A) additively increased the levels of cleaved PARP induced by 0.4 μ M EF24 without significantly inducing apoptosis alone. Published reports describe an anti-apoptotic function of Hsp70 in which Hsp70 prevents the cleavage and activation of pro-apoptotic factors through binding (100, 102). To determine if EF24-induced Hsp70 promotes cell survival through an enhanced interaction of Hsp70 with caspase 3, we performed an immunoprecipitation experiment using an anti-Hsp70 antibody (Fig. 4.4B). Results show a slight increase in the amount of full length caspase 3 coming down with Hsp70 in the EF24-treated cells. To further determine if EF24-induction of Hsp70 does enhance the interaction of Hsp70 with caspase, we also conducted a similar experiment using an anti-caspase 3 antibody for immunoprecipitation (Fig 4.4B). A significant amount of EF24-induced Hsp70 came down with caspase 3. To address whether Hsp70 non-specifically interacted with the caspase 3 antibody or beads due to the high levels of Hsp70 induced, we also evaluated levels of actin, a protein of high cellular abundance. Though actin did co-immunoprecipitate with Hsp70, actin was not detected in lanes without compound-induced Hsp70. Taken together, this suggests that the increased

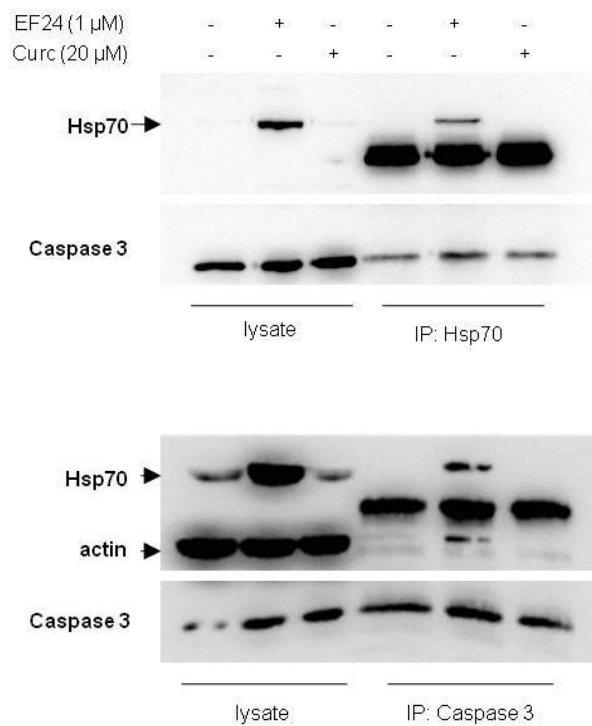
FIG 4.4. Decrease in caspase-mediated apoptosis linked to EF24-induced Hsp70. (A) A549 cells were transfected with Hsp70 siRNA 24 hr prior to treatment with 0.4 μ M EF24 . Levels of full length and cleaved PARP were detected by immunoblotting 48 h after the addition of EF24 in the culture media. (B) An anti-Hsp70 antibody and an anti-caspase 3 antibody was used to immunoprecipitate Hsp70 and caapase 3 from cells that were treated overnight with EF24 (1 μ M), curcumin (20 μ M), or vehicle control. Western blot analysis was used to evaluate level of co-immunoprecipitated proteins.

FIG 4.4 (continued). Decrease in caspase-mediated apoptosis linked to EF24-induced Hsp70.

A



B



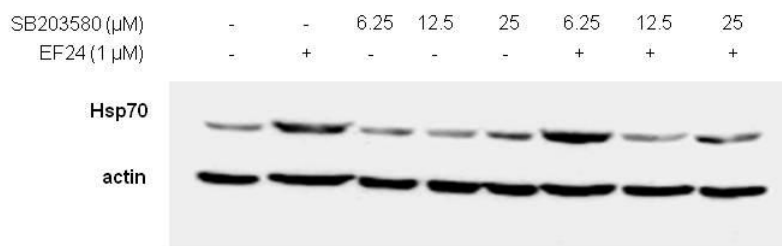
levels of Hsp70 induced by EF24 may bind to caspase 3, and we postulate that this then prevents caspase activation and caspase-dependent cell death.

Inhibition of Hsp70 induced by EF24 may contribute to the synergistic effects of EF24

and p38 MAPK inhibitors: Since previous data showed that p38 activation in response to EF24 occurred rapidly on the order of minutes, and the p38 pathway has been postulated to participate in transcription of the Hsp70 gene possibly through phosphorylation of major transcription factors (95, 96), we hypothesize that induction of Hsp70 by EF24 is at least in part due to activation of the p38 MAPK pathway. Western blot analysis has shown that the p38 inhibitor SB203580 attenuates EF24-induced Hsp70 protein levels (Fig. 4.5A). Additionally, northern blot analysis shows a slight reduction in EF24-induced Hsp70 mRNA levels (Fig. 4.2B), suggesting p38 MAPK activation by EF24 possibly contributes to upregulation of this transcript and may be one mechanism of the synergistic nature of EF24 and p38 MAPK inhibitors (Chapter 3).

FIG 4.5. Inhibition of p38 MAPK downregulates EF24-induced Hsp70. (A) EF24, SB203580, or the combination of the two agents were used to treat A549 cells. Cells were first pretreated for 1hr with SB203580 (6.25, 12.5, 25 μ M) or DMSO before treatment with EF24 (0.4 μ M) overnight. Immunoblotting with antibodies to Hsp70 was used to assess protein levels. Actin was used as a loading control.

FIG 4.5 (continued). Inhibition of p38 MAPK downregulates EF24-induced Hsp70.



Conclusions

In this current study, we examined the mechanism for the induction of Hsp70 protein levels in cancer cell lines by EF24 and the relationship between EF24-induced Hsp70 and the synergistic anticancer activity of the combination of EF24 and p38 MAPK inhibitors. We demonstrated that EF24 induces Hsp70 in various lung cancer cell lines as well as cancer cell lines of other origins (data not shown), suggesting a general mechanism of EF24 to induce increased expression of Hsp70. Additionally, we show that the increase in Hsp70 levels is due to the upregulation of transcription of the Hsp70 gene and represents another possibly survival response to EF24. More importantly, we provide one of the possible mechanisms for the synergy elicited by EF24 and p38 MAPK inhibitors. Our results show that treatment with SB203580 inhibits the induction of Hsp70 mediated by EF24 and also partially inhibited EF24-induced transcription of Hsp70.

Hsp70 has been demonstrated to promote cell survival and the development of cancer. Increased expression of Hsp70 has been correlated with resistance to a myriad of commonly used chemotherapeutics *in vitro* as well as in the clinical setting. This is mainly thought to be due to the link between Hsp70 and prevention of the initiation of apoptosis. Flavanoids, like quercetin, have been reported to inhibit Hsp70 transcription through its interaction with HSF-1 and preventing its activation from upstream pathways. Indeed, in our studies, quercetin sufficiently attenuated EF24-induced Hsp70 levels. Because of the mechanism of quercetin, we postulated that EF24-induced Hsp70

protein levels were due to increased transcription. This is based on the idea that in order for quercetin to inhibit Hsp70, EF24 must induce it on the level of transcription. Additionally, induction of Hsp70 protein levels took at least 8-9 h, which is also consistent with upregulation of transcription. Northern blot analysis confirmed the upregulated transcription of Hsp70 in response to EF24 treatment specifically when compared to treatment with curcumin or cisplatin. Though curcumin did not induce any significant changes in protein levels of Hsp70, a slight increase in transcription of Hsp70 was observed on the northern blot. This increase does not appear to translate into increased protein, which may be due to an additional mechanism of curcumin.

Since we propose that induction of Hsp70 is a survival response by the cell to offset EF24-induced cell death, we assessed various methods of Hsp70 inhibition in combination with EF24. We initially evaluated the small molecule quercetin or genetic silencing of Hsp70 mRNA in combination with EF24 to determine if there is a synergistic decrease in cell viability. Combinational analysis showed that the quercetin combination was relatively additive. However, flavanoids, like most natural products, are not entirely specific for one target so the most specific mechanism of Hsp70 siRNA was utilized to inhibit Hsp70. Genetic inhibition in combination with EF24 also elicited an additive effect.

Results from western blot and northern blot analysis suggest that the p38 MAPK pathway may participate in Hsp70 regulation. Other reports have demonstrated that p38 signals to HSF-1, a major transcription factor that controls the mRNA expression of

Hsp70. We suggested previously that p38 has a pro-survival function in the cellular context when its activation is induced by EF24. Signaling of this pathway to cellular factors like Hsp70 could explain this survival signaling. Though attenuation of the Hsp70 transcript was slight, this may be sufficient to decrease protein levels. It is also possible that the p38 pathway, or even EF24, inhibits Hsp70 post-transcriptionally. Since inhibition of Hsp70 only slightly enhanced the anticancer of EF24 and this was not nearly to the same extent as the combination of EF24 and p38 MAPK inhibitors, we hypothesize that there are more than one pathway downstream of p38 MAPK that is mediating the survival signaling induced by EF24. Discovering the mechanism of EF24 and p38 MAPK inhibitor synergy would be beneficial in personalizing medicine.

CHAPTER 5

EF24 disrupts the microtubule cytoskeleton and inhibits HIF-1

Rationale

Our hypothesis is that curcumin and the novel curcumin analog EF24 inhibits cancer cell proliferation and survival by disrupting the microtubule cytoskeleton and that the microtubule-disrupting ability of these agents lead to the inhibition of the HIF-1 pathway. This hypothesis was formulated based on the rationale stated below:

1. Curcumin is a natural product with a structure similar to a series of biaryl enones called chalcones, compounds that bind at the colchicine site on tubulin and induce microtubule depolymerization.
2. Published studies and preliminary data show that curcumin and EF24 induces some G₂/M arrest in the cell cycle, a property shared by all microtubule-targeting drugs.
3. Curcumin and EF24 also exhibit antiangiogenic activity in *in vitro* and *in vivo* models, and it has been previously shown that microtubule-targeting drugs exert antiangiogenic activity by inhibiting HIF-1 α and HIF transcriptome (e.g. VEGF) downstream of microtubule disruption.

In this study, we seek to investigate the potential mechanisms for the anticancer activity of EF24 and the parent compound curcumin. More specifically our objectives are to I) determine whether these agents inhibit the normal network of microtubules and II) investigate whether HIF activity is inhibited by these agents, which may contribute to the antiangiogenic properties of these agents.

Results

EF24, but not curcumin, disrupts normal mitosis, interphase microtubule organization and stabilizes cellular microtubules: Our results thus far show that curcumin and EF24, even though structurally related, exert their anti-HIF activities via distinct molecular mechanisms. Examination of both compounds' chemical structures revealed a structural resemblance to chalcones, a class of microtubule depolymerizing antimetabolic agents that bind to the colchicine site (202, 203). We have previously shown that microtubule-targeting drugs that bind to the colchicine site can exert antiangiogenic activity by inhibiting HIF-1 α and HIF transcriptomes (e.g., VEGF) downstream of microtubule disruption (147, 186). In addition, we have shown that microtubule-targeting drugs inhibit HIF protein post-transcriptionally, similar to the effects of EF24 described above (186). Thus, we hypothesized that EF24 might elicit its anti-HIF activity as a result of microtubule disruption. To evaluate potential cytoskeletal effects of EF24, we treated MCF-7 breast cancer (5.1A) or PC-3 prostate cancer cells (5.1B) with EF24 and curcumin and analyzed the cells' cytoskeletons by confocal microscopy. Treatment with EF24 resulted in aberrant mitotic figures (Fig. 5.1A, arrows), indicative of microtubule disruption. The drug's effects on interphase microtubules appeared to be stabilizing, as shown by the appearance of microtubule bundles (Fig. 5.1A and B). Compared with untreated control PC-3 cells, which maintain an intricate and organized network of microtubules, EF24 treatment caused microtubules to cluster (bundle) around the nucleus in a ring-like structure. No major effect on the actin cytoskeleton was observed.

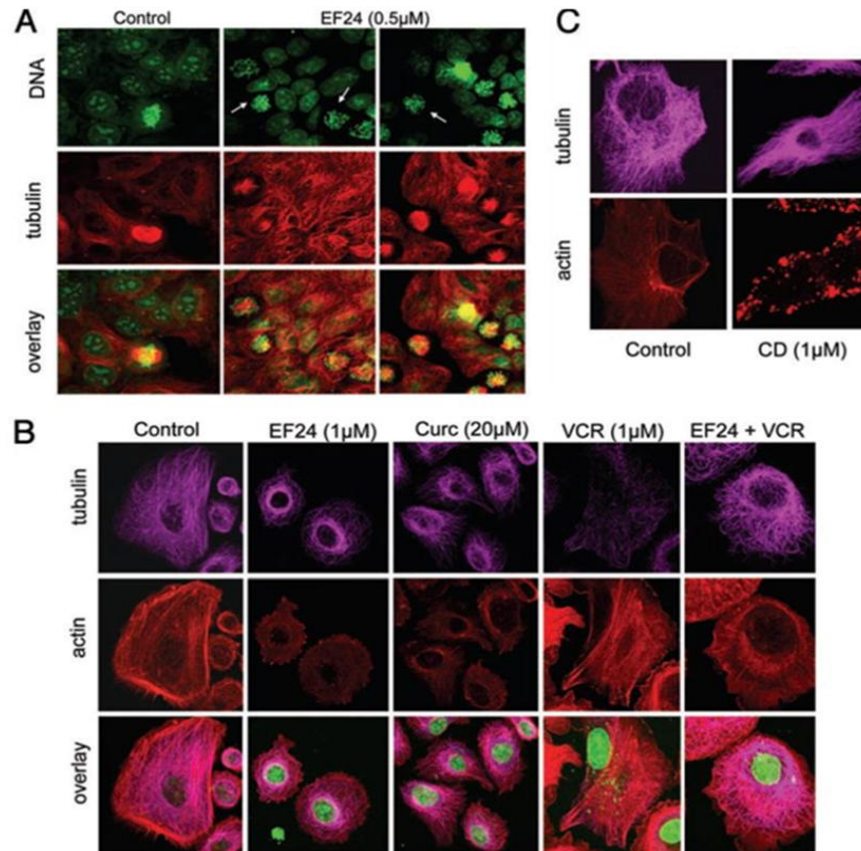
Treatment with cytochalasin D (17) is also shown as a control for actin depolymerization (Fig. 5.1C).

In contrast to EF24, curcumin had no detectable effect on the organization of either the microtubule or the actin cytoskeleton. To further probe the microtubule-stabilizing properties of EF24, we treated cells concomitantly with EF24 and the microtubule-depolymerizing drug vincristine (VCR). Vincristine alone completely depolymerized interphase microtubules (Fig. 5.1B). The presence of as little as 1 μ M EF24 protected microtubules from the depolymerizing effects of VCR, as evidenced by the extensive microtubule network that PC-3 cells retained. Collectively, these results suggest that EF24 has a significant stabilizing effect on the microtubule cytoskeleton, which appears to be distinct from the classic effect of taxanes and other well-characterized microtubule-stabilizing drugs.

To quantitatively assess the microtubule-stabilizing effects of EF24, we conducted a cell-based tubulin polymerization assay (204) (Fig. 5.2A). Treated and untreated PC-3 cells were lysed and fractionated into the soluble and polymer forms of tubulin. Lanes labeled "P" contained the polymerized form of tubulin (pelleted microtubule polymers), while those labeled "S" contained the soluble (α/β -tubulin dimers). Our results show that treatment with EF24 caused a dose-dependent increase in tubulin polymerization, as evidenced by the shift of tubulin from the soluble (S) to the polymerized fraction (P). To rule out non-specific sedimentation of tubulin, we reprobbed the same blot with an antibody specific for acetylated tubulin. Tubulin acetylation is a posttranslational

FIG 5.1. EF24 induced mitotic arrest and stabilized interphase microtubules. (A) MCF-7 breast cancer cells or (B) PC-3 prostate cancer cells were left untreated or treated with the indicated drug concentrations for 16 h. Cells were fixed and processed for immunofluorescence. Confocal laser scanning microscopy was used to analyze the images. Tubulin (A): red; (B and C): magenta), actin (23). DNA was counterstained with Sytox green. Arrows in (A) point to aberrant mitotic figures.

FIG 5.1 (continued). EF24 induced mitotic arrest and stabilized interphase microtubules.



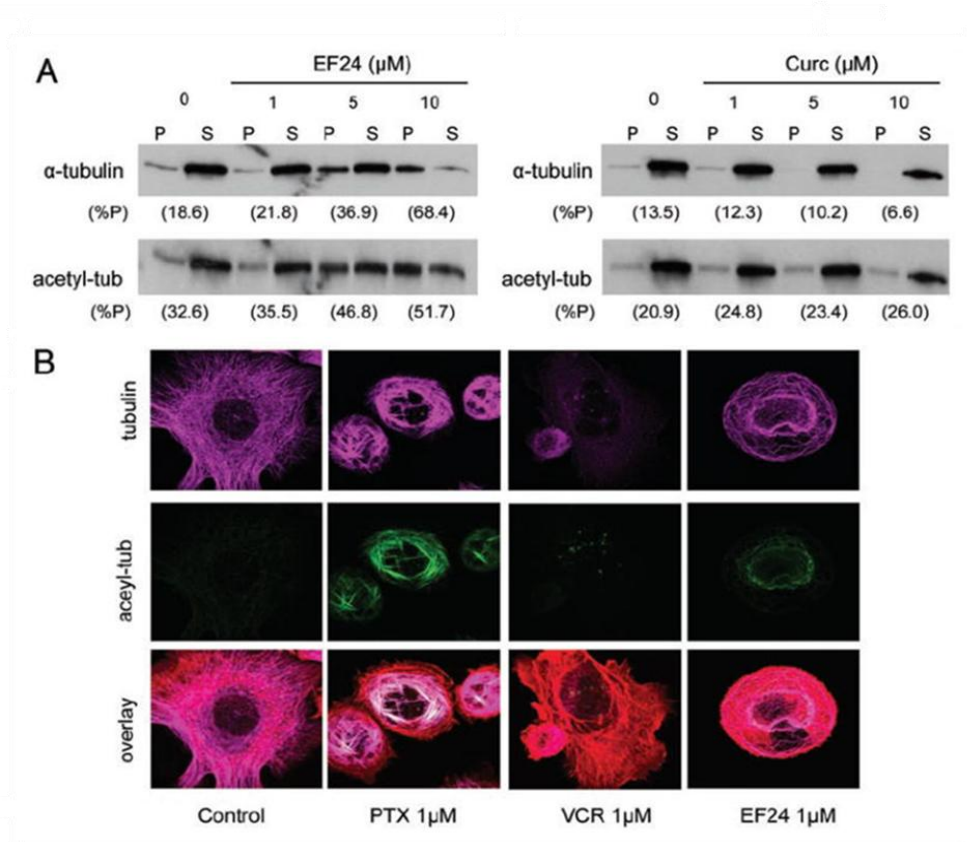
modification that occurs on the microtubule polymer, and its presence denotes stable, long-lived microtubule polymers (205). Similar to the results with total tubulin, EF24 treatment caused an incremental increase in tubulin acetylation, further attesting to the microtubule-stabilizing activity of EF24 (Fig. 5.2A). Curcumin, on the other hand, had no effect on tubulin polymerization nor on the proportion of acetylated tubulin, consistent with the immunofluorescence results presented in Figure 5.1B.

Immunofluorescence staining for total and acetylated tubulin following drug treatment with either paclitaxel (PTX), VCR or EF24 is shown in Figure 5.2B. As expected, treatment with paclitaxel produced characteristic needle-like bundles of microtubules and relatively heavy microtubule acetylation that co-localized with the bundles. On the other hand, treatment with the microtubule-depolymerizing vincristine did not enhance tubulin acetylation. EF24 treatment resulted once again in an increase in acetylated microtubules and microtubule polymerization as compared with untreated cells. The characteristic EF24-induced microtubule perinuclear ring was composed of acetylated microtubules, indicating that this ring is composed of stable microtubules. In summary, we have demonstrated by two independent assays that EF24 confers a stabilizing effect on microtubules in a dose-dependent manner, albeit distinct from that induced by paclitaxel.

EF24 remains active in taxol- and epothilone-resistant cells with acquired β -tubulin mutations: The clinical success of the microtubule-targeting drugs used in clinical oncology, such as the taxanes and the vinca alkaloids, is hampered by the development

FIG 5.2. EF24, but not curcumin, induced microtubule stabilization. (A) Relative levels of polymerized (P) and solubilized (S) tubulin from untreated or 16 h drug-treated PC-3 cells were analyzed by western blotting. The relative amount of tubulin in the pellet is represented by (%P). (B) Effects of drug treatment were analyzed by immunofluorescence using confocal microscopy. Tubulin (purple), acetyl- α -tubulin (5), actin (23).

FIG 5.2 (continued). EF24, but not curcumin, induced microtubule stabilization.



of drug-resistance—a serious treatment obstacle accounting for the majority of cancer related deaths. We have previously shown that drug-resistance to various microtubule-targeting drugs occurs following acquired tubulin mutations, which impair drug-tubulin interactions (204, 206). The microtubule-stabilizing effects induced by EF24 suggest that this drug may also bind directly to tubulin or microtubules. To examine whether EF24 binds to tubulin at the same site as other microtubule-stabilizing drugs, such as the taxanes and the epothilones, we tested the activity of EF24 in cells resistant to these drugs due to distinct mutations in the predominantly expressed β -tubulin gene M40 (Table 5.1). Results from 72-h cytotoxicity experiments revealed that EF24 retains activity against both cell lines, suggesting that either the effects of EF24 on the microtubule cytoskeleton are indirect or that EF24 may bind to tubulin at a location distinct from the taxane site.

EF24 demonstrates weak microtubule-depolymerizing activity in vitro: To investigate whether the activity of EF24 on cellular microtubules resulted from direct binding of the compound to tubulin, we examined the effects of EF24 on tubulin polymerization in vitro. Assembly of purified tubulin was induced by glutamate in the presence of GTP (Fig. 5.3). As control compounds, we also examined paclitaxel (data not shown), a powerful inducer of assembly, and combretastatin A-4, a powerful inhibitor of assembly (Fig. 5.3, curve 6). As shown in Figure 5.3, the latter compound nearly eliminated the assembly of 10 μ M tubulin when present at the substoichiometric concentration of 2 μ M (compare curve 6 with curve 1). We also examined curcumin, but found minimal effects

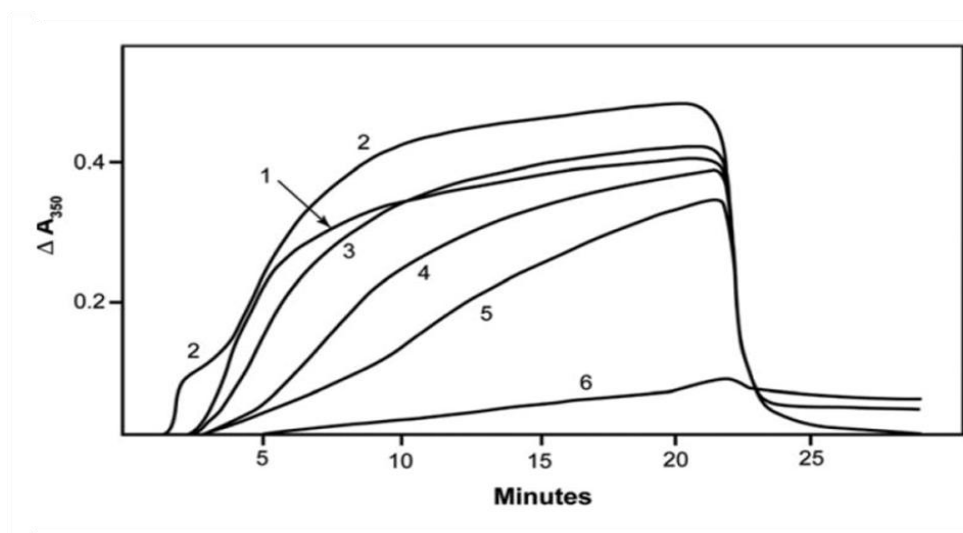
TABLE 5.1. EF24 and curcumin both retain cytotoxic activity against a panel of β -tubulin mutants specific for the taxane and the epothilone binding sites. Cytotoxicities of EF24, curcumin, and paclitaxel (PTX) against 1A9 ovarian cancer cells and cell lines that have mutations in β -tubulin (1A9/PTX10 - F270V, 1A9/A8 - A274T) selected for resistance with paclitaxel and epothilone A, respectively. PTX (nM) is used as a control. The cytotoxic potential of the compounds were assessed in a 72 hour growth inhibition SRB assay as described. IC_{50} values derived from the experiment are given for each compound in μ M. RR = relative resistance; equaled to the IC_{50} in resistant cell line divided by IC_{50} in 1A9 parental wildtype cells.

TABLE 5.1 (continued). EF24 and curcumin both retain cytotoxic activity against a panel of β -tubulin mutants specific for the taxane and the epothilone binding sites.

DRUG	CELL LINES				
	1A9 IC ₅₀	PTX10 (R270)		A8 (R274)	
		IC ₅₀	RR	IC ₅₀	RR
EF24	0.21	0.31	1.5	0.29	1.4
Curcumin	15.5	14.8	0.95	11.5	0.74
PTX	3.8	63	17	17.5	4.6

FIG 5.3. Weak inhibition of tubulin assembly by EF24. Assembly of purified tubulin (10 μM) was monitored turbidimetrically in the absence (curve 1) or presence of the following compounds: 80 μM curcumin (curve 2), 20 μM EF24 (curve 3), 40 μM EF24 (curve 4), 80 μM EF24 (curve 5) or 2.0 μM combretastatin A-4 (curve 6). The cuvettes were held at 0°C for 1 min, jumped to 30°C at the 1 min time point, held at 30°C until the 21 min time point, at which time they were jumped back to 0°C, and the reaction was followed for an additional 8 min. The 0 to 30°C jump takes less than 20 s, and the 30 to 0°C jump takes about 1 min.

FIG 5.3 (continued). Weak inhibition of tubulin assembly by EF24.

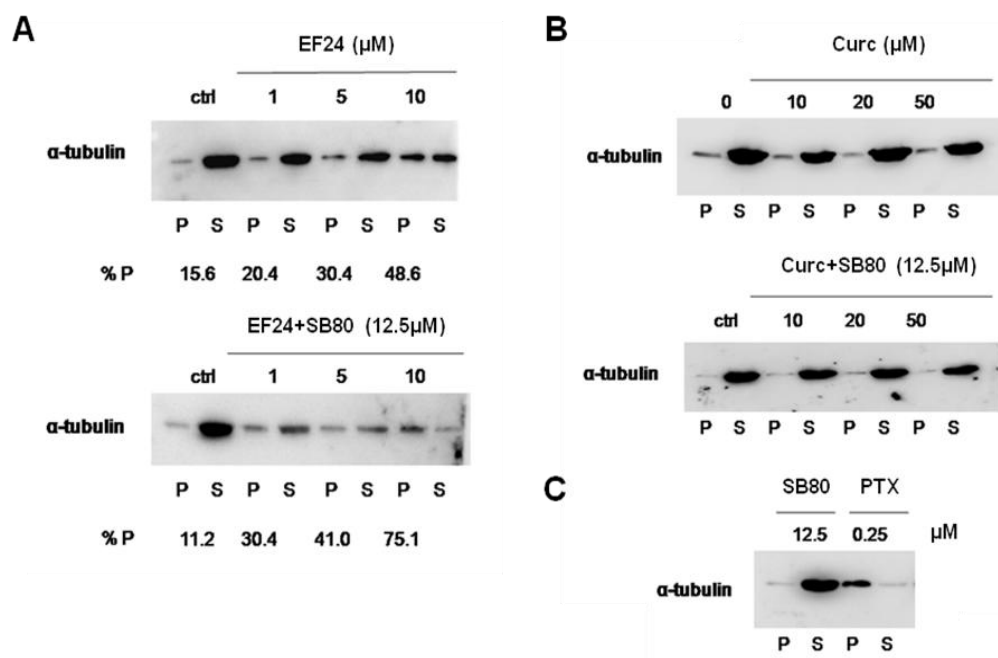


on the assembly reaction at concentrations up to 80 μM (curve 2). EF24, however, displayed weak, progressive partial inhibition of tubulin assembly, affecting most notably the onset of the reaction (nucleation phase) and its rate (elongation phase). Examination of the reaction rates in several experiments showed that a 50% reduction in the reaction rate occurred at about 40 μM EF24. Higher concentrations of both EF24 and curcumin produced optical distortions that were difficult to evaluate, and at 200 μM heavy precipitation of both compounds took place.

EF24-induced microtubule polymerization potentiated by SB203580: Previous data showed that the combination of EF24 and pyrimidyl imidazole p38 MAPK inhibitors is synergistic in inhibiting cancer cell proliferation and inducing cell death (Chapter 3). To determine whether this may be due to an increase in EF24-mediated microtubule stabilization by p38 MAPK inhibitors, a tubulin polymerization assay was conducted followed by western blot analysis. Since the synergistic effect of the combination of EF24 and SB203580 was greatest in A549, these lung cancer cells were used. The amount of polymerized tubulin induced by EF24 was compared to that induced by the combination of EF24 and SB20380 (Fig 5.4A). After approximately 16hr of EF24 treatment, a shift of tubulin from the soluble fraction to the polymerized fraction was noted in a dose-dependent manner. When A549 cells were co-treated with EF24 and SB203580 (12.5 μM), a 10-25% increase in the percentage of tubulin in the pellet was noted with no affect on tubulin polymerization with SB203580 alone (Fig 5.4C). Curcumin treatment, which previously has been shown to have little affect on tubulin

FIG 5.4. Inhibition of p38 MAPK pathway enhances EF24-induced microtubule stabilization. Relative levels of polymerized (P) and solubilized (S) tubulin from control untreated (0.5% DMSO) or 16 h drug-treated A549 cells were analyzed by western blotting. The effects on tubulin polymerization when A549 cells were co-treat with SB203580 and EF24 (A) or Curc (B) were compared with each corresponding single agent treatment. The relative amount of tubulin in the pellet is represented by (%P).

FIG 5.4 (continued). Inhibition of p38 MAPK pathway enhances EF24-induced microtubule stabilization.

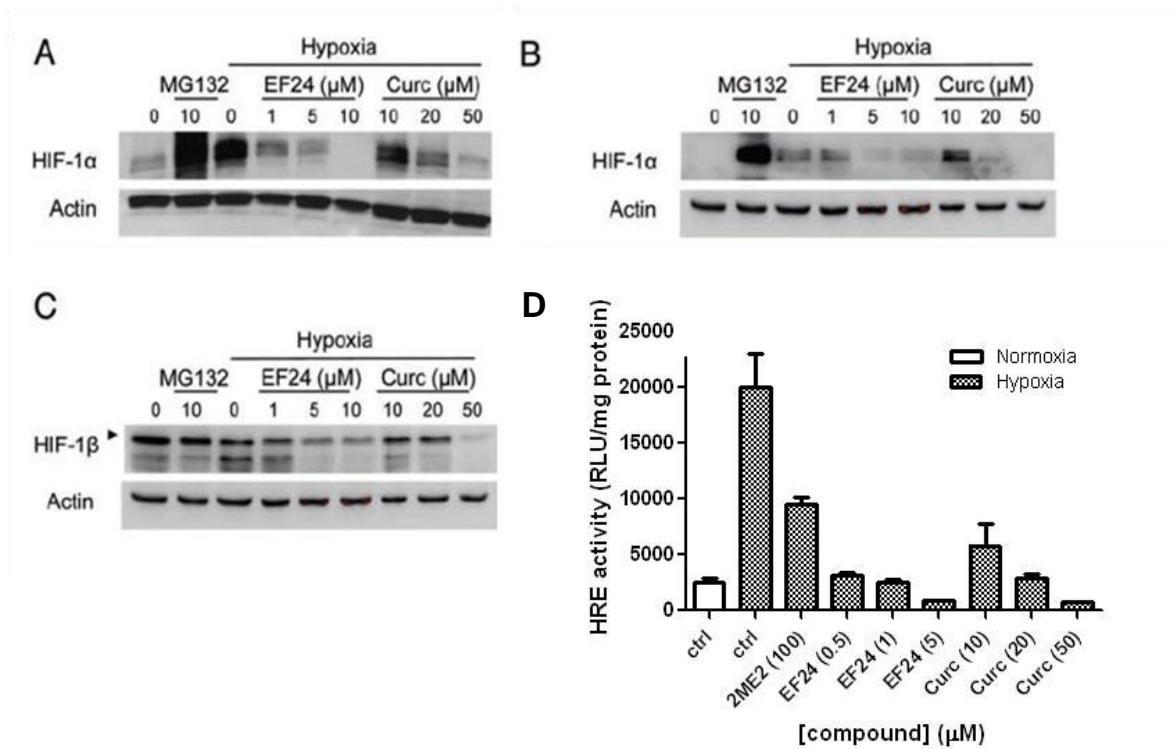


polymerization, and the non-synergistic combination of curcumin and SB203580 were used as a negative controls (Fig 5.4B). The known microtubule stabilizing agent paclitaxel was a positive control for tubulin polymerization (Fig 5.4C).

Both curcumin and EF24 downregulate HIF-1 α protein levels and HIF-1 transcriptional activity in a dose-dependent manner: Recently, curcumin has been reported to inhibit HIF-1 (207, 208). However, it is not clear how it exerts its anti-HIF activity. One group showed that curcumin affects only the HIF-1 β (ARNT) subunit (208), while another reported that curcumin inhibited HIF-1 α (207). We treated PC3 human prostate cancer (Fig. 5.5A) and MDA-MB-231 breast cancer cells (Fig. 5.5B and C) with curcumin or EF24 and measured HIF-1 α and HIF-1 β protein levels. Under normal oxygenated conditions, HIF-1 α protein is barely detectable due to its rapid proteasomal degradation. Hypoxia stabilizes HIF-1 α protein by preventing its association with the VHL protein and subsequent targeting to the proteasome for degradation. Treatment with either EF24 or curcumin resulted in a dose-dependent downregulation of HIF-1 α levels in both cell lines. In PC3 cells, treatment with as little as 1 μ M EF24 resulted in almost a 90% reduction in HIF-1 α protein, while 20–50 μ M curcumin was required to produce a similar effect (Fig. 5.5A). We found that both compounds reduced HIF-1 β levels (Fig. 5.5C), but higher concentrations than those required to reduce HIF-1 α levels were needed. For example, 20 μ M curcumin almost completely inhibited production of HIF-1 α protein but had little, if any, effect on the HIF-1 β level. These results suggested that HIF-1 α is more susceptible to the effects of EF24 and curcumin than HIF-1 β , and,

FIG 5.5. EF24 and curcumin downregulate HIF-1 α and HIF-1 β levels and impair the transcriptional activity of HIF. PC-3 (A) and MDA-MB231 (B and C) cells were treated with increasing concentrations of EF24 or curcumin (Curc) for 16 h and then subjected to hypoxia or remained in normoxia (N) for an additional 4 h. Whole cell extracts were analyzed by SDS-PAGE and immunoblotted with anti-HIF-1 α (A and B), anti-HIF-1 β (C) and actin antibodies. Treatment with the proteasome inhibitor MG132 at 10 μ M for 4 h was also included as a control for HIF-1 α protein stabilization resulting from inhibition of protein degradation, similar to the effects of hypoxia. (D) 1A9 cells transiently transfected with the HRE-luc construct pBI-GL V6L and treated to the indicated drug concentrations for 16 hr under normoxia or hypoxia. The cells were then harvested and analyzed for luciferase activity. Luciferase values were normalized to total cell protein content.

FIG 5.5 (continued). EF24 and curcumin downregulate HIF-1 α and HIF-1 β levels and impair the transcriptional activity of HIF.



therefore, we limited our further studies to the mechanism by which EF24 and curcumin affected the α subunit of the HIF complex.

Upon hypoxia-induced stabilization, HIF-1 α translocates to the nucleus, dimerizes with HIF-1 β , and activates genes containing hypoxia response elements (HREs). To determine whether EF24 or curcumin had any effect on HIF's transcriptional activity, we transiently transfected 1A9 human ovarian cancer cells with a reporter plasmid, which contains six tandem copies of the VEGF HREs and drives the expression of luciferase (187) (Fig. 5.5D). As expected, hypoxia induced HIF's transcriptional activity, as evidenced by the increase in the luciferase reporter activity. Treatment with either EF24 or curcumin resulted in a dose-dependent reduction of the transcriptional activity of HIF-1 consistent with the drug-induced reduction of HIF-1 α protein levels (Fig. 5.5A and B). 2ME2, a small molecule that inhibits HIF-1 α formation, was used as a positive control (186).

Curcumin and EF24 inhibited HIF formation by a VHL-dependent but proteasomal independent mechanism: To further investigate the mechanism by which EF24 treatment decreases HIF-1 α protein levels and its transcriptional activity, we examined the drug's ability to target HIF-1 α for proteosomal degradation. Thus, we treated PC-3 cells with 25 μ M EF24 for 4 h in the presence or absence of the proteasome inhibitor MG132 (Fig. 5.6A). As expected, treatment with MG132 resulted in increased HIF-1 α protein levels due to inhibition of HIF-1 α degradation. Interestingly, MG132 had no effect on the EF24-mediated reduction in HIF-1 α levels, even though it prevented HIF-

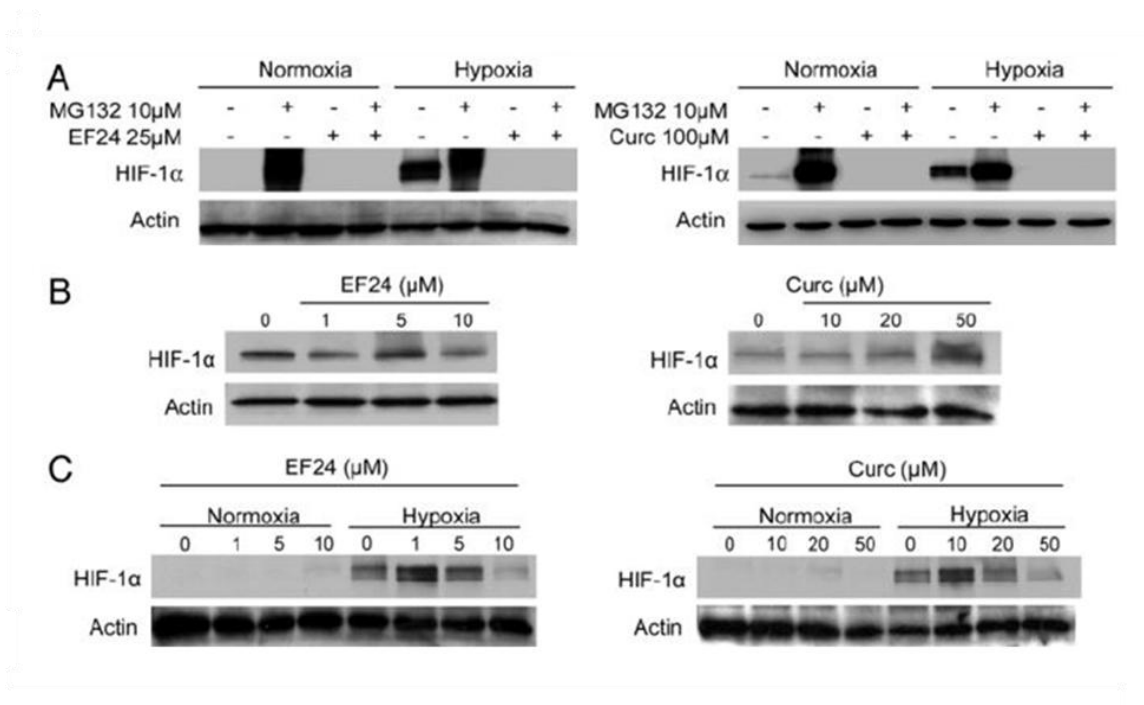
1 α degradation when used alone. Similar to the results with EF24, MG132 did not prevent the curcumin mediated reduction in HIF-1 α levels.

Since enhanced protein degradation did not appear to be the mechanism of action of EF24 or curcumin, we examined next the effects of these compounds in the context of VHL loss of function. It is well established that the VHL protein is a negative regulator of HIF-1 α by targeting it to the proteasome for degradation under normoxic conditions (209). VHL loss of function mutations occur in over 50% of human renal cancers, leading to constitutively high levels of HIF-1 α protein and activation of HIF-target genes. To examine the role of the VHL protein on the anti-HIF activities of EF24 and curcumin, we used an isogenic pair of renal cancer cell lines, RCC2 cells harboring high basal HIF levels due to VHL gene inactivation and RCC2-VHL cells in which the wild-type VHL gene was stably reintroduced. No decrease in HIF-1 α protein was observed in the RCC2 cells following treatment with either EF24 or curcumin (Fig. 5.6B). However, with wild-type VHL gene expression in the RCC2-VHL cells, the ability of EF24 and curcumin to inhibit HIF-1 α protein levels was restored (Fig. 5.6C). These results suggest that both EF24 and curcumin inhibit HIF-1 α in a VHL protein-dependent manner that likely does not require proteasome activity.

Curcumin, but not EF24, inhibited HIF-1 α transcription: To further explore the mechanism by which curcumin and EF24 reduced HIF-1 α levels, we examined their effects on HIF-1 α transcription, as assessed by northern blotting. Results in Figure 5.7A

FIG 5.6. Curcumin and EF24 inhibit HIF-1 α in a VHL protein-dependent but proteasome independent manner. (A) PC-3 cells were treated with 25 μ M EF24 or 100 μ M curcumin in the presence and absence of 10 μ M MG-132 for 4 h. RCC2 renal cells with loss of VHL protein function (B) or RCC2-VHL renal cells with reconstituted wild-type VHL (C) were treated with the indicated drug concentrations for 16 h. In (B), only cells treated under normoxic conditions are shown. Equal amounts of protein from each cell lysate were resolved by SDS-PAGE, transferred and immunoblotted with antibodies against HIF-1 α and actin.

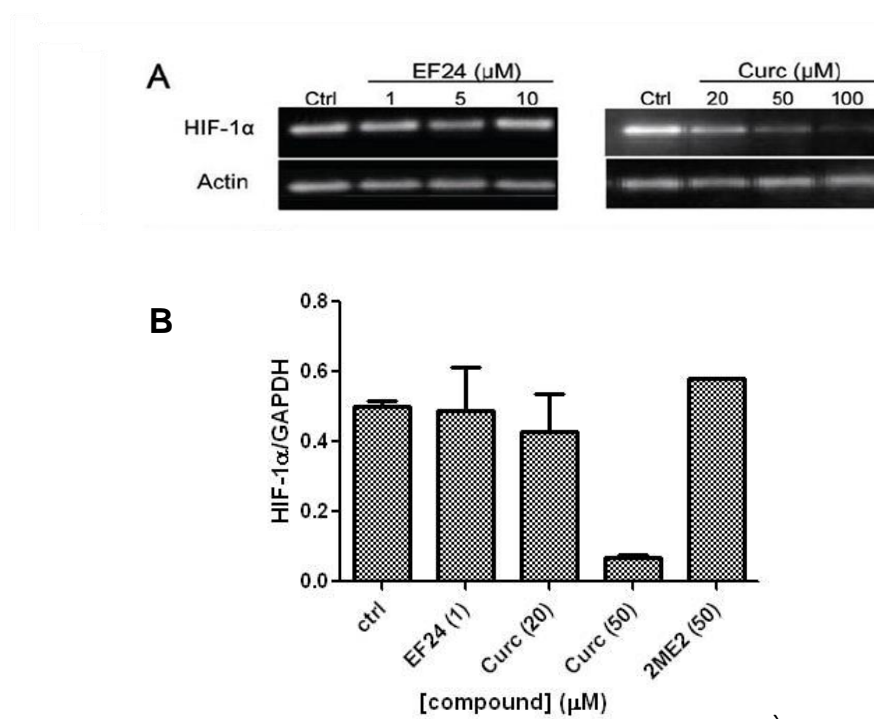
FIG 5.6 (continued). Curcumin and EF24 inhibit HIF-1 α in a VHL protein-dependent but proteasome independent manner.



show that EF24 treatment of PC-3 cells had no effect on HIF-1 α mRNA expression, while treatment with curcumin significantly downregulated HIF-1 α mRNA in a dose-dependent manner. Actin mRNA expression is shown as a loading control. To increase the sensitivity of our assay, we also assessed HIF-1 α expression by quantitative real-time RT-PCR in untreated and drug-treated PC3 cells. HIF-1 α expression was normalized to that of *GAPDH*, used here as an internal loading control (Fig. 5.7B). Curcumin significantly downregulated HIF-1 α gene expression, while EF24 treatment had no effect, in agreement with the northern blot analysis (Fig. 5.7A). Treatment with 2ME2 is included here as a negative control for lack of transcriptional inhibition of HIF-1 α , as we have previously shown that 2ME2 inhibits HIF-1 α protein at the level of translation (186) (Fig. 5.7B). Similar results were obtained in MDA-MB-231 breast cancer cells (data not shown), confirming that curcumin, but not EF24, inhibits HIF-1 α at the level of transcription.

FIG 5.7. Curcumin, but not EF24, inhibites *HIF-1 α* gene expression. Cultured PC-3 cells were treated with the indicated concentrations of EF24 or curcumin (Curc) for 16 h. Total mRNA was extracted as described in Materials and Methods. (A) *HIF-1 α* mRNA expression of drug-treated cells was analyzed by northern blotting. (B) Relative mRNA expression of *HIF-1 α* was determined by quantitative RT-PCR normalized to *GAPDH* expression.

FIG 5.7 (continued). Curcumin, but not EF24, inhibited *HIF-1 α* gene expression.



Conclusions

In this study we demonstrated that the synthetic curcumin congener EF24 is an effective antiproliferative agent that exerts its activity by stabilizing cellular microtubules and by inhibiting intracellular levels of the pro-angiogenic transcription factor HIF. The hypoxia inducible transcription factor HIF-1 is an important mediator of tumor angiogenesis and survival, and inhibition of HIF levels or HIF action is an attractive therapeutic strategy for cancer chemotherapy (152). Here we show that both curcumin and even more potent EF24 inhibit intracellular levels of both HIF-1 α and HIF-1 β proteins. This in turn results in the subsequent downregulation of HIF's transcriptional activity in various human epithelial cancer cell lines (Fig. 5.5). Our results demonstrated that inhibition of the HIF-1 α protein level occurred at a lower drug concentration than that required for the inhibition of the HIF-1 β protein. Thus, the oxygen-regulated α subunit of HIF was more sensitive to the effects of these compounds. Nevertheless, inhibition of the levels of both HIF subunits is a rather unique characteristic for the known HIF inhibitors, most of which have been reported to affect primarily HIF-1 α either directly or indirectly (210). However, since the transcriptional activation of HIF target genes requires interaction between both the α and β HIF subunits, a drug that achieves inhibition of both should have superior anti-HIF activity *in vivo*. Our data are in agreement with recent reports showing that curcumin exerted anti-HIF activity by inhibiting HIF-1 β (208) or HIF-1 α levels (207). Contrary to our results, Choi et al., reported that curcumin had no effect on HIF-1 α

levels This discrepancy may be due to the original source of curcumin used in each of the studies, since we found it necessary to repurify curcumin. Our original commercial curcumin sample contained a mixture of three different curcuminoids, each of which may have distinct effects on cellular levels of the HIF-1 subunits.

EF24 and curcumin inhibited HIF protein levels by two distinct mechanisms (5.5-5.7). Curcumin, on the one hand, inhibited HIF-1 α at the level of transcription, as evidenced by the dose-dependent decrease of HIF-1 α mRNA expression (5.7). In contrast, EF24 exerted its anti-HIF activity post-transcriptionally. We have previously shown that the microtubule inhibitors (i.e., 2ME2, paclitaxel) downregulated HIF-1 α downstream of microtubule disruption, regardless of drug structure, tubulin-binding site, and tubulin-stabilizing or -destabilizing activity (147, 186). In addition, we have shown that the anti-HIF effects of these inhibitors depend on their relative ability to disrupt microtubules, as evidenced by the loss of the drug-induced HIF inhibition in paclitaxel- or epothilone-resistant cells harboring β -tubulin mutations that impair drug-binding to tubulin (147, 186). Importantly, we showed that the tubulin inhibitors affected HIF-1 α post-transcriptionally, similar to the effects of EF24. In the case of the tubulin inhibitors we found that HIF-downregulation occurred via inhibition of its translation.

This led us to examine the effects of EF24 and curcumin on cellular microtubules. We found that EF24, but not curcumin, affects both interphase and spindle microtubules

in a variety of human epithelial cancer cell lines. We demonstrated that EF24 caused some cells to arrest in mitosis and stabilized interphase microtubules. The latter effect was documented by an increase in microtubule polymer mass and in tubulin acetylation in EF24-treated cells (Fig. 5.2). Increased acetylation of α -tubulin is a well-established marker for formation of stabilized microtubules (205). Additional evidence for formation of stabilized microtubules in EF24-treated cells were the bundled microtubules, particularly those surrounding the nucleus, as well as the EF24-mediated protection of microtubules from VCR-induced depolymerization (Figs. 5.1 and 5.2).

We wished to obtain evidence for the binding site for EF24 on tubulin by examining the compound's activity in a panel of cells harboring distinct mutations in a β -tubulin gene that confer resistance to either paclitaxel, epothilone A (Table 5.1), or 2ME2 (V β 236I, data not shown). EF24 retained its activity against all mutant lines examined, suggesting that EF24 either binds to tubulin at a different site or by a different mechanism not affected by the mutations examined. Alternatively, it is possible that EF24 does not interact directly with tubulin, despite its cellular effects on microtubules. The latter hypothesis is supported by the inability of EF24 to stabilize microtubules *in vitro* (Fig. 5.3). Unexpectedly, in these *in vitro* experiments EF24 showed a weak inhibitory effect on microtubule assembly, most notably on the nucleation phase of the reaction. This inhibitory effect required super-stoichiometric concentrations of EF24, in sharp contrast to the potent substoichiometric inhibition that occurred with combretastatin A-4. Although assembly studies with bovine brain tubulin typically

agrees with the mechanism of action of antitubulin drugs observed in cells, we cannot exclude that the different isotypes and/or post-translational modifications in cultured cells as compared with bovine brain tubulin could have caused the different effects we observed. Nor are we able to exclude a possible metabolic conversion of EF24 within the cells to a compound with a different mechanism of action.

We were unable to reproduce the apparent inhibition of tubulin assembly by curcumin reported by Gupta et al (211). Possible causes for our different results could be the use of different reaction conditions, different tubulin preparations, the methodology used to monitor turbidity development, or, perhaps most likely, by other curcuminoids in the material used by Gupta et al.

Taken together, the cellular and in vitro effects of EF24 on the microtubule cytoskeleton suggest that this compound may affect cellular microtubules indirectly by modulating pathways that influence microtubule formation and/or stability. For instance, one of the possible mechanisms for the synergistic anticancer activity of the combination of EF24 and p38 MAPK inhibitors is cell death caused by enhanced microtubule stabilization, suggesting that the induction of the p38 pathway by EF24 may contribute to the destabilization of the microtubule pathway to offset increased microtubule polymerization (Fig 5.4). Current reports suggest... Further investigation into the role of EF24-induced p38 activation in the maintenance of microtubule integrity is warranted.

Though the EF24-mediated effects on the microtubule cytoskeleton may not be direct, this microtubule stabilization in cells possibly results in the downstream inhibition of HIF-1 α and β levels, similar to the effects of the known microtubule inhibitors. Further studies are necessary to address the causal relationship between EF24-induced microtubule disruption and reduction in HIF protein levels.

Experiments with the proteasome inhibitor MG-132 with EF24 have increased our understanding of the mechanism by which EF24 reduces intracellular levels of HIF (Fig. 5.6A). Our data showed that the presence of MG-132 did not rescue HIF-1 α levels from the reduction caused by EF24, suggesting that EF24 is affecting HIF-1 α at a step prior to protein degradation. On the other hand, EF24 treatment of RCC2 renal cells expressing an inactive VHL protein, had no effect on HIF-1 α levels (Fig. 5.6B and C). Renal cancers are notorious for their loss of functional VHL protein, a condition that hinders the machinery necessary for HIF degradation and lead to accumulation of HIF-1 α , even under normoxic conditions. Indeed, when VHL was reconstituted in the RCC2 renal cell line, and HIF was targeted for proteasomal degradation, the anti-HIF activity of EF24 was restored. This result implies that functional VHL protein is most likely required for the EF24-mediated downregulation of HIF-1 α . Importantly, a recent study showed that VHL protein binds to and stabilizes cellular microtubules (212). This finding could explain the requirement for functional VHL protein for EF24 to exert its anti-HIF activity. It is possible that EF24 stabilizes microtubules in a VHL-dependent manner, and these results in downstream reduction of HIF-1 α levels. Furthermore, this

scenario could rationalize the apparent discrepancy between cellular microtubule stabilization and weak in vitro inhibition of microtubule assembly by EF24. The weak interaction of EF24 with tubulin would then play no role in the cellular effects of the compound.

In summary, our study has confirmed EF24 as a promising anticancer and antiangiogenic compound with a mechanism of action that is distinct than that of its parent compound, curcumin. Our results reveal that EF24 most likely affects the microtubule cytoskeleton indirectly and causes a sharp reduction HIF-1 α levels by a mechanism dependent on the VHL protein and not dependent on proteasomal degradation of HIF-1 α . EF24 also causes, but to a lesser extent, a reduction in HIF-1 β protein levels. In addition, EF24-mediated microtubule polymerization is further enhanced by inhibiting the p38 MAPK pathway, and this offers a mechanism for the synergistic potential of this combination. Further studies elucidating the relationship between EF24, p38, VHL protein, cellular microtubules and the HIF pathway will advance our molecular understanding of the mechanism of action of EF24 and should identify tumor types likely to be sensitive to EF24 and related compounds, based on their genetic make-up. Finally, this knowledge may be useful towards the development of combination therapies using EF24 with other microtubule- and HIF inhibitors with distinct, non-overlapping mechanisms of action.

CHAPTER 6

Discussion

Preclinical studies demonstrate that the fluorinated EF24, designed from the optimization of the curcumin structure, is a potent and effective anticancer agent in both *in vitro* and *in vivo* models (184). Like curcumin, EF24 has a favorable toxicity profile *in vivo* which suggests non-targeting to normal cells. Clinical safety becomes important when developing any agent as a potential chemotherapeutic. Though these two agents are highly tolerable, the anticancer activity of EF24 is far superior to curcumin. In cell culture studies, EF24 inhibited the proliferation of cancer cells with an IC₅₀ value at least 10-fold lower than curcumin (52, 184). This potent activity was consistent across multiple cancer cell lines derived from different physiological origins (i.e. breast, lung, ovaries, prostate). Similarly, in nude mouse models, EF24 inhibited tumor formation and decreased tumor volume of implanted cancer xenografts more potently than curcumin (66). Part of this increased *in vivo* activity of EF24 in comparison to curcumin may be due to the lack of the rapid inactivating metabolism and excretion associated with curcumin intake. Recent clinical trial studies show that curcumin has limited absorption and up to 95% of curcumin is readily cleared from the body after initial administration (59, 65). It is also important to note that the concentrations of curcumin used especially in *in vitro* studies do not represent concentrations that can be successfully achieved physiologically (59). This offers an advantage of using highly active curcumin analogs like EF24 that are retained more readily in the systemic circulation. Additionally, the development of EF24 conjugates will lead to even more selective delivering of EF24 to tumors and reduce effective dosages (70). Taken together,

EF24 represents a promising anticancer agent that potentially could surpass the clinical activity of curcumin as well as other commonly used chemotherapeutics.

The molecular mechanism of EF24 to explain its anticancer activity is currently under investigation. Published *in vitro* data demonstrates the EF24 induces apoptotic cell death by altering the function of the mitochondrial (69). Disturbances to the membrane potential of the mitochondria effectively lead to increase activation of caspases. Subsequently caspase-dependent apoptosis, characterized by externalization of phosphatidylserine and DNA fragmentation, is induced. Increases in the expression pro-apoptotic signaling molecules like Bax have also been noted in response to EF24. Various reports of cell cycle arrest in the G₂/M following EF24 treatment of various cancer cell lines have also been observed, leading to EF24-mediated cell death (68).

Additionally, EF24 also inhibits cellular proliferative and survival signaling. Inhibition of the activation of NF- κ B and subsequent downregulation of NF- κ B-mediated transcription is widely accepted to be a major mechanism of curcumin, and EF24 also shares this anti-NF- κ B property (52). Despite strong evidence the inhibition of IKK by curcumin, few experimental studies present evidence that curcumin directly targets this kinase. Recent studies from our group show that EF24 directly inhibits the kinase activity IKK and that this may be a key contributing mechanism to the potency of EF24. This differing anti-NF- κ B mechanism offers one possible explanation for the differences in activity between these two agents.

Our studies delve deeper into understanding how EF24 specifically inhibits cancer cell growth by analyzing EF24-modulated signaling pathways. We also attempt to show, in a chronological manner, the resulting molecular consequences. Though many published studies investigate the induction of cell death programs by EF24, few studies examine survival signaling induced in response to EF24. Increased cell survival signaling could effectively retard the induction of cancer cell death. Thus, studying these survival mechanisms becomes beneficial in understanding the cellular response to anticancer agents.

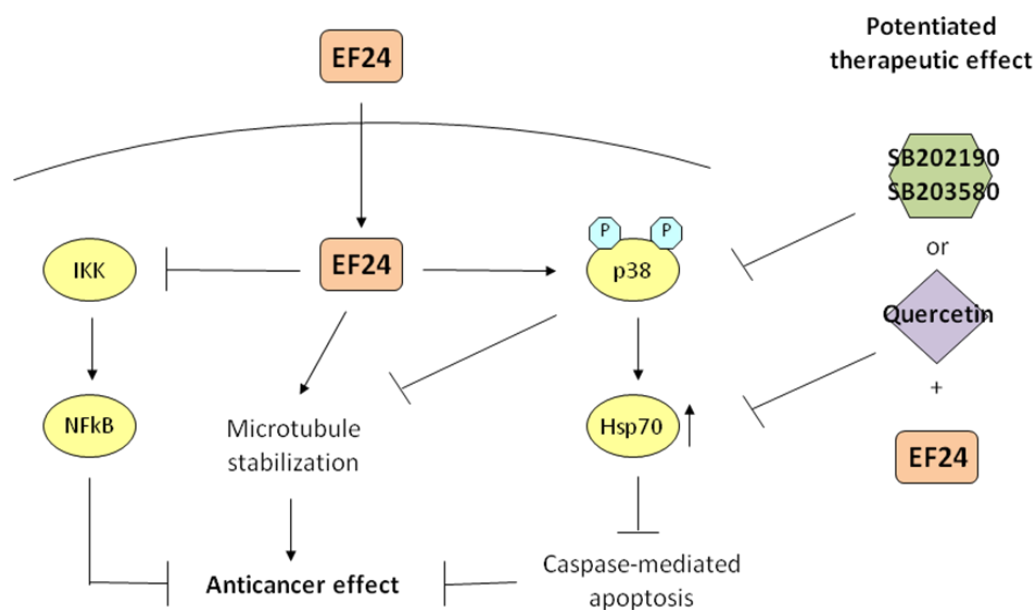


FIG 6.1. Working model of EF24-mediated activity and proposed EF24-based combinations to elicit potentiated therapeutic effects.

The preceding chapters present evidence showing that EF24 induces p38 signaling, which is believed to have pro-survival functions. In Chapter 3, we first show evidence the activation of p38 through EF24-induced dual phosphorylation is an early event, occurring in the first 30 minutes of EF24 treatment. Inhibition of p38, through pharmacological and genetic means, enhanced the anticancer activity of EF24 in a synergistic manner. We defined synergy here as an anticancer effect greater than the additive effect of each agent. Anticancer synergy was observed in both cell proliferation and apoptotic studies.

The combinational analysis of EF24 and p38 inhibitors presented here is data conducted almost exclusively in A549 cancer cells, an accepted model epithelial NSCLC, which showed the most dramatic cytotoxic activity of the combination of EF24 and p38 inhibitors. This combination was not as effective in a panel of other NSCLC cell lines including models of squamous cell carcinoma and large cell carcinoma (Table 3.1). There was also variability in the loss of cell viability with the test anticancer combination, which highlights the potential contribution of the genetic background of these cells to the activity of the combination. This then becomes important for the clinical development of this combination and how patient populations are stratified based on the postulated response to this therapy. p38 inhibitors were found to inhibit a greater percentage of the cytotoxicity of EF24 in A549 (30-50%) than in H157 (13%). In comparing the genetic profile of A549 and H157, it has been reported that H157 has known inactivating mutation in important tumor suppressor genes (i.e. PTEN) that may

cause increased survival signaling that onsets the anticancer effects of this combination (213). Additionally, since the work conducted here only focused on strategies to treat lung cancer, the genetic nature of the tumor also become important when you discuss therapeutic management across a variety of tumor types. For instance, A549 lung cancer cells harbor a constitutive activating K-Ras mutation in codon 12 that is also is present in other tumors like pancreatic cancers (214, 215). If this mutation plays a role in the synergistic activity of the EF24 and p38 combination, then this combination may also have potential therapeutic applications to this class of tumors. Further investigation, therefore, is warranted to further identify how certain genetic variability may impact the activity of this combination and to determine the far-reaching utility of this proposed combinational strategy in oncology.

Additionally, both NSCLC cell lines, especially A549, and tumors have been documented to have enhanced basal activation of p38 compared to normal lung cells (92). There is always a question of whether increase activation of a pathway will either increase or decrease sensitivity of cells to inhibitors of that pathway. Published reports show that this may be based on how dependent or “addicted” the cells are to that particular pathway. Previous data shows variable basal activation levels of p38 is present in the panel of NSCLC cell lines test. EF24 does not further enhance SB203580-induced p38 inhibition (Fig. 3.8), suggesting that the combination depends only on the p38 inhibitor to block activity of p38. Combinational analysis that showed a higher degree of synergism in A549 than other lung cancer used concentrations of p38

inhibitors optimized for A549 cells. Therefore, the basal activity of p38 should possibly be taken into consideration when determining the dose of p38 inhibitor used in combination with EF24 in the clinical setting.

Chapter 4 provides evidence that p38 activation plays a role in the upregulation of Hsp70. Accumulation of Hsp70 was noted after approximately 8 hours of EF24 treatment. Though we hypothesize that many downstream effectors of p38 mediate the survival signaling, we believe that the activity of Hsp70 to interact with and prevent the activation of apoptotic signaling molecules (i.e. caspase 3) contributes to this. Selective genetic silencing of Hsp70 in combination with EF24 led to an additive decrease in cancer cell viability.

Finally, in chapter 5, we provide evidence that EF24 treatment leads to disruption of the microtubule cytoskeleton important to cell shape, signal transduction, and cell division. Microtubule disruption was in the form of polymerized microtubules and was evident after overnight EF24 treatment. We believe that the microtubule stabilizing activity is not a direct effect of EF24 resulting from the interaction of EF24 with tubulin, but a potential consequence of EF24-modulated signaling. Signaling pathways, like p38, are known to regulate to the maintenance of microtubule integrity. This is consistent with our results showing that inhibition of p38 enhanced the EF24-induced microtubule polymerization, suggesting another role for p38-mediated survival

signaling. Further studies are necessary to determine what downstream p38 effector is responsible for this activity.

In conclusion, we have shown that the p38 MAPK activation, Hsp70 induction, and microtubule disruption occur within cancer cells upon treatment with EF24. Importantly, all of these molecular events were not cell line specific but appear to be a general mechanism of EF24 beyond a particular type of cancer. These molecular effects also occur specifically in response to EF24 when compared to the parent compound curcumin. Our findings thus suggest signaling responses that can be exploited clinically for the use of EF24 as a single agent and for the design of EF24-based combination therapeutic strategies. Based on our combinational analysis, concurrent administration of EF24 with pyridyl imidazole p38 inhibitors offers one potential clinical regime. Moreover, a specific Hsp70 inhibitor would likely also clinically enhance the activity of EF24, though no such inhibitor has been successfully developed to date. Additional exploration into whether these proposed combinations are beneficial for the treatment of cancers beyond lung cancer is warranted. However, since we believe that these EF24-induced survival mechanisms are generally attributed to EF24, we also believe that these combinations will be effective to some degree. Ultimately, continued studies into the mechanism of action of EF24 will ultimately benefit future clinical development of this curcumin analog.

CHAPTER 7

References

1. Krishnaswamy K. (2008) Traditional Indian spices and their health significance. *Asia Pac J Clin Nutr* **17 Suppl 1**: 265-268.
2. Hatcher H, Planalp R, Cho J, Torti FM, Torti SV. (2008) Curcumin: from ancient medicine to current clinical trials. *Cell Mol Life Sci* **65**: 1631-1652.
3. Wuthi-udomlert M, Grisanapan W, Luanratana O, Caichompoo W. (2000) Antifungal activity of *Curcuma longa* grown in Thailand. *Southeast Asian J Trop Med Public Health* **31 Suppl 1**: 178-182.
4. Srinivasan KR. (1953) A chromatographic study of the curcuminoids in *Curcuma longa*, L. *J Pharm Pharmacol* **5**: 448-457.
5. Sinha R, Anderson DE, McDonald SS, Greenwald P. (2003) Cancer risk and diet in India. *J Postgrad Med* **49**: 222-228.
6. Mohandas KM, Desai DC. (1999) Epidemiology of digestive tract cancers in India. V. Large and small bowel. *Indian J Gastroenterol* **18**: 118-121.
7. Rajakumar DV, Rao MN. (1995) Antioxidant properties of phenyl styryl ketones. *Free Radic Res* **22**: 309-317.
8. Amolins MW, Peterson LB, Blagg BS. (2008) Synthesis and evaluation of electron-rich curcumin analogues. *Bioorg Med Chem*.
9. Chignell CF, Bilski P, Reszka KJ, Motten AG, Sik RH, Dahl TA. (1994) Spectral and photochemical properties of curcumin. *Photochem Photobiol* **59**: 295-302.
10. Tayyem RF, Heath DD, Al-Delaimy WK, Rock CL. (2006) Curcumin content of turmeric and curry powders. *Nutr Cancer* **55**: 126-131.
11. Deshpande SS, Maru GB. (1995) Effects of curcumin on the formation of benzo[a]pyrene derived DNA adducts in vitro. *Cancer Lett* **96**: 71-80.
12. Rao CV, Rivenson A, Simi B, Reddy BS. (1995) Chemoprevention of colon carcinogenesis by dietary curcumin, a naturally occurring plant phenolic compound. *Cancer Res* **55**: 259-266.
13. Stoner GD, Mukhtar H. (1995) Polyphenols as cancer chemopreventive agents. *J Cell Biochem Suppl* **22**: 169-180.
14. Pari L, Tewas D, Eckel J. (2008) Role of curcumin in health and disease. *Arch Physiol Biochem* **114**: 127-149.
15. Nishino H, Satomi Y, Tokuda H, Masuda M. (2007) Cancer control by phytochemicals. *Curr Pharm Des* **13**: 3394-3399.
16. Desai AG, Qazi GN, Ganju RK, et al. (2008) Medicinal plants and cancer chemoprevention. *Curr Drug Metab* **9**: 581-591.
17. Singletary K, MacDonald C, Wallig M, Fisher C. (1996) Inhibition of 7,12-dimethylbenz[a]anthracene (DMBA)-induced mammary tumorigenesis and DMBA-DNA adduct formation by curcumin. *Cancer Lett* **103**: 137-141.
18. Pereira MA, Grubbs CJ, Barnes LH, et al. (1996) Effects of the phytochemicals, curcumin and quercetin, upon azoxymethane-induced colon cancer and 7,12-dimethylbenz[a]anthracene-induced mammary cancer in rats. *Carcinogenesis* **17**: 1305-1311.

19. Huang MT, Lou YR, Ma W, Newmark HL, Reuhl KR, Conney AH. (1994) Inhibitory effects of dietary curcumin on forestomach, duodenal, and colon carcinogenesis in mice. *Cancer Res* **54**: 5841-5847.
20. Limtrakul P, Lipigorngoson S, Namwong O, Apisariyakul A, Dunn FW. (1997) Inhibitory effect of dietary curcumin on skin carcinogenesis in mice. *Cancer Lett* **116**: 197-203.
21. Chuang SE, Kuo ML, Hsu CH, et al. (2000) Curcumin-containing diet inhibits diethylnitrosamine-induced murine hepatocarcinogenesis. *Carcinogenesis* **21**: 331-335.
22. Shalini VK, Srinivas L. (1987) Lipid peroxide induced DNA damage: protection by turmeric (*Curcuma longa*). *Mol Cell Biochem* **77**: 3-10.
23. Reddy AC, Lokesh BR. (1994) Effect of dietary turmeric (*Curcuma longa*) on iron-induced lipid peroxidation in the rat liver. *Food Chem Toxicol* **32**: 279-283.
24. Zhao BL, Li XJ, He RG, Cheng SJ, Xin WJ. (1989) Scavenging effect of extracts of green tea and natural antioxidants on active oxygen radicals. *Cell Biophys* **14**: 175-185.
25. Eybl V, Kotyzova D, Bludovska M. (2004) The effect of curcumin on cadmium-induced oxidative damage and trace elements level in the liver of rats and mice. *Toxicol Lett* **151**: 79-85.
26. Nishinaka T, Ichijo Y, Ito M, et al. (2007) Curcumin activates human glutathione S-transferase P1 expression through antioxidant response element. *Toxicol Lett* **170**: 238-247.
27. Nagabhushan M, Amonkar AJ, Bhide SV. (1987) In vitro antimutagenicity of curcumin against environmental mutagens. *Food Chem Toxicol* **25**: 545-547.
28. Iqbal M, Sharma SD, Okazaki Y, Fujisawa M, Okada S. (2003) Dietary supplementation of curcumin enhances antioxidant and phase II metabolizing enzymes in ddY male mice: possible role in protection against chemical carcinogenesis and toxicity. *Pharmacol Toxicol* **92**: 33-38.
29. Goud VK, Polasa K, Krishnaswamy K. (1993) Effect of turmeric on xenobiotic metabolising enzymes. *Plant Foods Hum Nutr* **44**: 87-92.
30. Jiang MC, Yang-Yen HF, Yen JJ, Lin JK. (1996) Curcumin induces apoptosis in immortalized NIH 3T3 and malignant cancer cell lines. *Nutr Cancer* **26**: 111-120.
31. Odot J, Albert P, Carlier A, Tarpin M, Devy J, Madoulet C. (2004) In vitro and in vivo anti-tumoral effect of curcumin against melanoma cells. *Int J Cancer* **111**: 381-387.
32. Chakraborty S, Ghosh U, Bhattacharyya NP, Bhattacharya RK, Roy M. (2006) Inhibition of telomerase activity and induction of apoptosis by curcumin in K-562 cells. *Mutat Res* **596**: 81-90.
33. Karunagaran D, Rashmi R, Kumar TR. (2005) Induction of apoptosis by curcumin and its implications for cancer therapy. *Curr Cancer Drug Targets* **5**: 117-129.

34. Deeb D, Xu YX, Jiang H, et al. (2003) Curcumin (diferuloyl-methane) enhances tumor necrosis factor-related apoptosis-inducing ligand-induced apoptosis in LNCaP prostate cancer cells. *Mol Cancer Ther* **2**: 95-103.
35. Hanif R, Qiao L, Shiff SJ, Rigas B. (1997) Curcumin, a natural plant phenolic food additive, inhibits cell proliferation and induces cell cycle changes in colon adenocarcinoma cell lines by a prostaglandin-independent pathway. *J Lab Clin Med* **130**: 576-584.
36. Lin SS, Huang HP, Yang JS, et al. (2008) DNA damage and endoplasmic reticulum stress mediated curcumin-induced cell cycle arrest and apoptosis in human lung carcinoma A-549 cells through the activation caspases cascade- and mitochondrial-dependent pathway. *Cancer Lett.*
37. Srivastava RK, Chen Q, Siddiqui I, Sarva K, Shankar S. (2007) Linkage of curcumin-induced cell cycle arrest and apoptosis by cyclin-dependent kinase inhibitor p21(WAF1/CIP1). *Cell Cycle* **6**: 2953-2961.
38. Srivastava KC, Bordia A, Verma SK. (1995) Curcumin, a major component of food spice turmeric (*Curcuma longa*) inhibits aggregation and alters eicosanoid metabolism in human blood platelets. *Prostaglandins Leukot Essent Fatty Acids* **52**: 223-227.
39. Hong J, Bose M, Ju J, et al. (2004) Modulation of arachidonic acid metabolism by curcumin and related beta-diketone derivatives: effects on cytosolic phospholipase A(2), cyclooxygenases and 5-lipoxygenase. *Carcinogenesis* **25**: 1671-1679.
40. Huang MT, Smart RC, Wong CQ, Conney AH. (1988) Inhibitory effect of curcumin, chlorogenic acid, caffeic acid, and ferulic acid on tumor promotion in mouse skin by 12-O-tetradecanoylphorbol-13-acetate. *Cancer Res* **48**: 5941-5946.
41. Singh S, Aggarwal BB. (1995) Activation of transcription factor NF-kappa B is suppressed by curcumin (diferuloylmethane) [corrected]. *J Biol Chem* **270**: 24995-25000.
42. Han SS, Keum YS, Seo HJ, Surh YJ. (2002) Curcumin suppresses activation of NF-kappaB and AP-1 induced by phorbol ester in cultured human promyelocytic leukemia cells. *J Biochem Mol Biol* **35**: 337-342.
43. Park C, Kim GY, Kim GD, Choi BT, Park YM, Choi YH. (2006) Induction of G2/M arrest and inhibition of cyclooxygenase-2 activity by curcumin in human bladder cancer T24 cells. *Oncol Rep* **15**: 1225-1231.
44. Limtrakul P, Anuchapreeda S, Lipigorngoson S, Dunn FW. (2001) Inhibition of carcinogen induced c-Ha-ras and c-fos proto-oncogenes expression by dietary curcumin. *BMC Cancer* **1**: 1.
45. Balasubramanyam M, Koteswari AA, Kumar RS, Monickaraj SF, Maheswari JU, Mohan V. (2003) Curcumin-induced inhibition of cellular reactive oxygen species generation: novel therapeutic implications. *J Biosci* **28**: 715-721.
46. Funk JL, Oyarzo JN, Frye JB, et al. (2006) Turmeric extracts containing curcuminoids prevent experimental rheumatoid arthritis. *J Nat Prod* **69**: 351-355.

47. Jackson JK, Higo T, Hunter WL, Burt HM. (2006) The antioxidants curcumin and quercetin inhibit inflammatory processes associated with arthritis. *Inflamm Res* **55**: 168-175.
48. Wang W, Bernard K, Li G, Kirk KL. (2007) Curcumin opens cystic fibrosis transmembrane conductance regulator channels by a novel mechanism that requires neither ATP binding nor dimerization of the nucleotide-binding domains. *J Biol Chem* **282**: 4533-4544.
49. Sharma C, Kaur J, Shishodia S, Aggarwal BB, Ralhan R. (2006) Curcumin down regulates smokeless tobacco-induced NF-kappaB activation and COX-2 expression in human oral premalignant and cancer cells. *Toxicology* **228**: 1-15.
50. Bremner P, Heinrich M. (2002) Natural products as targeted modulators of the nuclear factor-kappaB pathway. *J Pharm Pharmacol* **54**: 453-472.
51. Jobin C, Bradham CA, Russo MP, et al. (1999) Curcumin blocks cytokine-mediated NF-kappa B activation and proinflammatory gene expression by inhibiting inhibitory factor I-kappa B kinase activity. *J Immunol* **163**: 3474-3483.
52. Kasinski AL, Du Y, Thomas SL, et al. (2008) Inhibition of IkappaB kinase-nuclear factor-kappaB signaling pathway by 3,5-bis(2-fluorobenzylidene)piperidin-4-one (EF24), a novel monoketone analog of curcumin. *Mol Pharmacol* **74**: 654-661.
53. Bachmeier BE, Mohrenz IV, Mirisola V, et al. (2008) Curcumin downregulates the inflammatory cytokines CXCL1 and -2 in breast cancer cells via NFkappaB. *Carcinogenesis* **29**: 779-789.
54. Lee KW, Kim JH, Lee HJ, Surh YJ. (2005) Curcumin inhibits phorbol ester-induced up-regulation of cyclooxygenase-2 and matrix metalloproteinase-9 by blocking ERK1/2 phosphorylation and NF-kappaB transcriptional activity in MCF10A human breast epithelial cells. *Antioxid Redox Signal* **7**: 1612-1620.
55. Rajkumar SV, Richardson PG, Hideshima T, Anderson KC. (2005) Proteasome inhibition as a novel therapeutic target in human cancer. *J Clin Oncol* **23**: 630-639.
56. Orłowski RZ, Baldwin AS, Jr. (2002) NF-kappaB as a therapeutic target in cancer. *Trends Mol Med* **8**: 385-389.
57. Duan J, Friedman J, Nottingham L, Chen Z, Ara G, Van Waes C. (2007) Nuclear factor-kappaB p65 small interfering RNA or proteasome inhibitor bortezomib sensitizes head and neck squamous cell carcinomas to classic histone deacetylase inhibitors and novel histone deacetylase inhibitor PXD101. *Mol Cancer Ther* **6**: 37-50.
58. Joshi J, Ghaisas S, Vaidya A, et al. (2003) Early human safety study of turmeric oil (*Curcuma longa* oil) administered orally in healthy volunteers. *J Assoc Physicians India* **51**: 1055-1060.
59. Cheng AL, Hsu CH, Lin JK, et al. (2001) Phase I clinical trial of curcumin, a chemopreventive agent, in patients with high-risk or pre-malignant lesions. *Anticancer Res* **21**: 2895-2900.

60. Baum L, Lam CW, Cheung SK, et al. (2008) Six-month randomized, placebo-controlled, double-blind, pilot clinical trial of curcumin in patients with Alzheimer disease. *J Clin Psychopharmacol* **28**: 110-113.
61. Lao CD, Ruffin MTt, Normolle D, et al. (2006) Dose escalation of a curcuminoid formulation. *BMC Complement Altern Med* **6**: 10.
62. Sharma RA, Steward WP, Gescher AJ. (2007) Pharmacokinetics and pharmacodynamics of curcumin. *Adv Exp Med Biol* **595**: 453-470.
63. Lin JK, Pan MH, Lin-Shiau SY. (2000) Recent studies on the biofunctions and biotransformations of curcumin. *Biofactors* **13**: 153-158.
64. Yang KY, Lin LC, Tseng TY, Wang SC, Tsai TH. (2007) Oral bioavailability of curcumin in rat and the herbal analysis from *Curcuma longa* by LC-MS/MS. *J Chromatogr B Analyt Technol Biomed Life Sci* **853**: 183-189.
65. Anand P, Kunnumakkara AB, Newman RA, Aggarwal BB. (2007) Bioavailability of curcumin: problems and promises. *Mol Pharm* **4**: 807-818.
66. Subramaniam D, May R, Sureban SM, et al. (2008) Diphenyl difluoroketone: a curcumin derivative with potent in vivo anticancer activity. *Cancer Res* **68**: 1962-1969.
67. Mosley CA, Liotta DC, Snyder JP. (2007) Highly active anticancer curcumin analogues. *Adv Exp Med Biol* **595**: 77-103.
68. Selvendiran K, Tong L, Vishwanath S, et al. (2007) EF24 induces G2/M arrest and apoptosis in cisplatin-resistant human ovarian cancer cells by increasing PTEN expression. *J Biol Chem* **282**: 28609-28618.
69. Adams BK, Cai J, Armstrong J, et al. (2005) EF24, a novel synthetic curcumin analog, induces apoptosis in cancer cells via a redox-dependent mechanism. *Anticancer Drugs* **16**: 263-275.
70. Shoji M, Sun A, Kisiel W, et al. (2008) Targeting tissue factor-expressing tumor angiogenesis and tumors with EF24 conjugated to factor VIIa. *J Drug Target* **16**: 185-197.
71. Han J, Lee JD, Bibbs L, Ulevitch RJ. (1994) A MAP kinase targeted by endotoxin and hyperosmolarity in mammalian cells. *Science* **265**: 808-811.
72. Korb A, Tohidast-Akrad M, Cetin E, Axmann R, Smolen J, Schett G. (2006) Differential tissue expression and activation of p38 MAPK alpha, beta, gamma, and delta isoforms in rheumatoid arthritis. *Arthritis Rheum* **54**: 2745-2756.
73. Keesler GA, Bray J, Hunt J, et al. (1998) Purification and activation of recombinant p38 isoforms alpha, beta, gamma, and delta. *Protein Expr Purif* **14**: 221-228.
74. Raingeaud J, Gupta S, Rogers JS, et al. (1995) Pro-inflammatory cytokines and environmental stress cause p38 mitogen-activated protein kinase activation by dual phosphorylation on tyrosine and threonine. *J Biol Chem* **270**: 7420-7426.
75. Lin A, Minden A, Martinetto H, et al. (1995) Identification of a dual specificity kinase that activates the Jun kinases and p38-Mpk2. *Science* **268**: 286-290.

76. LoGrasso PV, Frantz B, Rolando AM, O'Keefe SJ, Hermes JD, O'Neill EA. (1997) Kinetic mechanism for p38 MAP kinase. *Biochemistry* **36**: 10422-10427.
77. Pomerance M, Quillard J, Chantoux F, Young J, Blondeau JP. (2006) High-level expression, activation, and subcellular localization of p38-MAP kinase in thyroid neoplasms. *J Pathol* **209**: 298-306.
78. Lee JC, Laydon JT, McDonnell PC, et al. (1994) A protein kinase involved in the regulation of inflammatory cytokine biosynthesis. *Nature* **372**: 739-746.
79. Kumar S, Boehm J, Lee JC. (2003) p38 MAP kinases: key signalling molecules as therapeutic targets for inflammatory diseases. *Nat Rev Drug Discov* **2**: 717-726.
80. Subbaramaiah K, Hart JC, Norton L, Dannenberg AJ. (2000) Microtubule-interfering agents stimulate the transcription of cyclooxygenase-2. Evidence for involvement of ERK1/2 AND p38 mitogen-activated protein kinase pathways. *J Biol Chem* **275**: 14838-14845.
81. Jijon H, Allard B, Jobin C. (2004) NF-kappaB inducing kinase activates NF-kappaB transcriptional activity independently of IkappaB kinase gamma through a p38 MAPK-dependent RelA phosphorylation pathway. *Cell Signal* **16**: 1023-1032.
82. Wang D, Richmond A. (2001) Nuclear factor-kappa B activation by the CXC chemokine melanoma growth-stimulatory activity/growth-regulated protein involves the MEKK1/p38 mitogen-activated protein kinase pathway. *J Biol Chem* **276**: 3650-3659.
83. Madrid LV, Mayo MW, Reuther JY, Baldwin AS, Jr. (2001) Akt stimulates the transactivation potential of the RelA/p65 Subunit of NF-kappa B through utilization of the Ikappa B kinase and activation of the mitogen-activated protein kinase p38. *J Biol Chem* **276**: 18934-18940.
84. Vanden Berghe W, Plaisance S, Boone E, et al. (1998) p38 and extracellular signal-regulated kinase mitogen-activated protein kinase pathways are required for nuclear factor-kappaB p65 transactivation mediated by tumor necrosis factor. *J Biol Chem* **273**: 3285-3290.
85. Smith JL, Collins I, Chandramouli GV, et al. (2003) Targeting combinatorial transcriptional complex assembly at specific modules within the interleukin-2 promoter by the immunosuppressant SB203580. *J Biol Chem* **278**: 41034-41046.
86. Boldt S, Weidle UH, Kolch W. (2002) The role of MAPK pathways in the action of chemotherapeutic drugs. *Carcinogenesis* **23**: 1831-1838.
87. Selimovic D, Hassan M, Haikel Y, Hengge UR. (2008) Taxol-induced mitochondrial stress in melanoma cells is mediated by activation of c-Jun N-terminal kinase (JNK) and p38 pathways via uncoupling protein 2. *Cell Signal* **20**: 311-322.
88. Holmes WF, Soprano DR, Soprano KJ. (2003) Early events in the induction of apoptosis in ovarian carcinoma cells by CD437: activation of the p38 MAP kinase signal pathway. *Oncogene* **22**: 6377-6386.

89. Wu GS. (2004) The functional interactions between the p53 and MAPK signaling pathways. *Cancer Biol Ther* **3**: 156-161.
90. Lin Z, Crockett DK, Jenson SD, Lim MS, Elenitoba-Johnson KS. (2004) Quantitative proteomic and transcriptional analysis of the response to the p38 mitogen-activated protein kinase inhibitor SB203580 in transformed follicular lymphoma cells. *Mol Cell Proteomics* **3**: 820-833.
91. Davidson B, Konstantinovskiy S, Kleinberg L, et al. (2006) The mitogen-activated protein kinases (MAPK) p38 and JNK are markers of tumor progression in breast carcinoma. *Gynecol Oncol* **102**: 453-461.
92. Greenberg AK, Basu S, Hu J, et al. (2002) Selective p38 activation in human non-small cell lung cancer. *Am J Respir Cell Mol Biol* **26**: 558-564.
93. Zhang D, Wong LL, Koay ES. (2007) Phosphorylation of Ser78 of Hsp27 correlated with HER-2/neu status and lymph node positivity in breast cancer. *Mol Cancer* **6**: 52.
94. Olson JM, Hallahan AR. (2004) p38 MAP kinase: a convergence point in cancer therapy. *Trends Mol Med* **10**: 125-129.
95. Hung JJ, Cheng TJ, Lai YK, Chang MD. (1998) Differential activation of p38 mitogen-activated protein kinase and extracellular signal-regulated protein kinases confers cadmium-induced HSP70 expression in 9L rat brain tumor cells. *J Biol Chem* **273**: 31924-31931.
96. Kim J, Nueda A, Meng YH, Dynan WS, Mivechi NF. (1997) Analysis of the phosphorylation of human heat shock transcription factor-1 by MAP kinase family members. *J Cell Biochem* **67**: 43-54.
97. Burston SG, Clarke AR. (1995) Molecular chaperones: physical and mechanistic properties. *Essays Biochem* **29**: 125-136.
98. Baneyx F. (1994) Chaperonins and protein folding. *Ann N Y Acad Sci* **745**: 383-394.
99. Calvaruso G, Giuliano M, Portanova P, Pellerito O, Vento R, Tesoriere G. (2007) Hsp72 controls bortezomib-induced HepG2 cell death via interaction with pro-apoptotic factors. *Oncol Rep* **18**: 447-450.
100. Komarova EY, Afanasyeva EA, Bulatova MM, Cheetham ME, Margulis BA, Guzhova IV. (2004) Downstream caspases are novel targets for the antiapoptotic activity of the molecular chaperone hsp70. *Cell Stress Chaperones* **9**: 265-275.
101. Ravagnan L, Gurbuxani S, Susin SA, et al. (2001) Heat-shock protein 70 antagonizes apoptosis-inducing factor. *Nat Cell Biol* **3**: 839-843.
102. Gurbuxani S, Schmitt E, Cande C, et al. (2003) Heat shock protein 70 binding inhibits the nuclear import of apoptosis-inducing factor. *Oncogene* **22**: 6669-6678.
103. Vargas-Roig LM, Gago FE, Tello O, Aznar JC, Ciocca DR. (1998) Heat shock protein expression and drug resistance in breast cancer patients treated with induction chemotherapy. *Int J Cancer* **79**: 468-475.
104. Karlseder J, Wissing D, Holzer G, et al. (1996) HSP70 overexpression mediates the escape of a doxorubicin-induced G2 cell cycle arrest. *Biochem Biophys Res Commun* **220**: 153-159.

105. Ciocca DR, Fuqua SA, Lock-Lim S, Toft DO, Welch WJ, McGuire WL. (1992) Response of human breast cancer cells to heat shock and chemotherapeutic drugs. *Cancer Res* **52**: 3648-3654.
106. Jackson PF, Bullington JL. (2002) Pyridinylimidazole based p38 MAP kinase inhibitors. *Curr Top Med Chem* **2**: 1011-1020.
107. Cuenda A, Rouse J, Doza YN, et al. (1995) SB 203580 is a specific inhibitor of a MAP kinase homologue which is stimulated by cellular stresses and interleukin-1. *FEBS Lett* **364**: 229-233.
108. Wang SW, Pawlowski J, Wathen ST, Kinney SD, Lichenstein HS, Manthey CL. (1999) Cytokine mRNA decay is accelerated by an inhibitor of p38-mitogen-activated protein kinase. *Inflamm Res* **48**: 533-538.
109. Tong L, Pav S, White DM, et al. (1997) A highly specific inhibitor of human p38 MAP kinase binds in the ATP pocket. *Nat Struct Biol* **4**: 311-316.
110. Young PR, McLaughlin MM, Kumar S, et al. (1997) Pyridinyl imidazole inhibitors of p38 mitogen-activated protein kinase bind in the ATP site. *J Biol Chem* **272**: 12116-12121.
111. English JM, Cobb MH. (2002) Pharmacological inhibitors of MAPK pathways. *Trends Pharmacol Sci* **23**: 40-45.
112. Wilson KP, McCaffrey PG, Hsiao K, et al. (1997) The structural basis for the specificity of pyridinylimidazole inhibitors of p38 MAP kinase. *Chem Biol* **4**: 423-431.
113. Davies SP, Reddy H, Caivano M, Cohen P. (2000) Specificity and mechanism of action of some commonly used protein kinase inhibitors. *Biochem J* **351**: 95-105.
114. Sack JS, Kish KF, Pokross M, et al. (2008) Structural basis for the high-affinity binding of pyrrolotriazine inhibitors of p38 MAP kinase. *Acta Crystallogr D Biol Crystallogr* **D64**: 705-710.
115. Sullivan JE, Holdgate GA, Campbell D, et al. (2005) Prevention of MKK6-dependent activation by binding to p38alpha MAP kinase. *Biochemistry* **44**: 16475-16490.
116. Margutti S, Laufer SA. (2007) Are MAP kinases drug targets? Yes, but difficult ones. *ChemMedChem* **2**: 1116-1140.
117. Peifer C, Wagner G, Laufer S. (2006) New approaches to the treatment of inflammatory disorders small molecule inhibitors of p38 MAP kinase. *Curr Top Med Chem* **6**: 113-149.
118. Badger AM, Bradbeer JN, Votta B, Lee JC, Adams JL, Griswold DE. (1996) Pharmacological profile of SB 203580, a selective inhibitor of cytokine suppressive binding protein/p38 kinase, in animal models of arthritis, bone resorption, endotoxin shock and immune function. *J Pharmacol Exp Ther* **279**: 1453-1461.
119. Lee MR, Dominguez C. (2005) MAP kinase p38 inhibitors: clinical results and an intimate look at their interactions with p38alpha protein. *Curr Med Chem* **12**: 2979-2994.

120. Schett G, Zwerina J, Firestein G. (2008) The p38 mitogen-activated protein kinase (MAPK) pathway in rheumatoid arthritis. *Ann Rheum Dis* **67**: 909-916.
121. Clark JE, Sarafraz N, Marber MS. (2007) Potential of p38-MAPK inhibitors in the treatment of ischaemic heart disease. *Pharmacol Ther* **116**: 192-206.
122. Barnes PJ. (2003) New treatments for chronic obstructive pulmonary disease. *Ann Ist Super Sanita* **39**: 573-582.
123. Newton R, Holden N. (2003) Inhibitors of p38 mitogen-activated protein kinase: potential as anti-inflammatory agents in asthma? *BioDrugs* **17**: 113-129.
124. Wittmann T, Hyman A, Desai A. (2001) The spindle: a dynamic assembly of microtubules and motors. *Nat Cell Biol* **3**: E28-34.
125. Luduena RF. (1998) Multiple forms of tubulin: different gene products and covalent modifications. *Int Rev Cytol* **178**: 207-275.
126. Orr GA, Verdier-Pinard P, McDaid H, Horwitz SB. (2003) Mechanisms of Taxol resistance related to microtubules. *Oncogene* **22**: 7280-7295.
127. Nicoletti MI, Valoti G, Giannakakou P, et al. (2001) Expression of beta-tubulin isoforms in human ovarian carcinoma xenografts and in a sub-panel of human cancer cell lines from the NCI-Anticancer Drug Screen: correlation with sensitivity to microtubule active agents. *Clin Cancer Res* **7**: 2912-2922.
128. Westermann S, Weber K. (2003) Post-translational modifications regulate microtubule function. *Nat Rev Mol Cell Biol* **4**: 938-947.
129. Mallik R, Carter BC, Lex SA, King SJ, Gross SP. (2004) Cytoplasmic dynein functions as a gear in response to load. *Nature* **427**: 649-652.
130. Thyberg J, Moskalewski S. (1999) Role of microtubules in the organization of the Golgi complex. *Exp Cell Res* **246**: 263-279.
131. King SJ, Brown CL, Maier KC, Quintyne NJ, Schroer TA. (2003) Analysis of the dynein-dynactin interaction in vitro and in vivo. *Mol Biol Cell* **14**: 5089-5097.
132. Quintyne NJ, Gill SR, Eckley DM, Crego CL, Compton DA, Schroer TA. (1999) Dynactin is required for microtubule anchoring at centrosomes. *J Cell Biol* **147**: 321-334.
133. Kikkawa M, Sablin EP, Okada Y, Yajima H, Fletterick RJ, Hirokawa N. (2001) Switch-based mechanism of kinesin motors. *Nature* **411**: 439-445.
134. Nangaku M, Sato-Yoshitake R, Okada Y, et al. (1994) KIF1B, a novel microtubule plus end-directed monomeric motor protein for transport of mitochondria. *Cell* **79**: 1209-1220.
135. Gundersen GG, Cook TA. (1999) Microtubules and signal transduction. *Curr Opin Cell Biol* **11**: 81-94.
136. Jordan MA, Wilson L. (1998) Microtubules and actin filaments: dynamic targets for cancer chemotherapy. *Curr Opin Cell Biol* **10**: 123-130.
137. Downing KH. (2000) Structural basis for the interaction of tubulin with proteins and drugs that affect microtubule dynamics. *Annu Rev Cell Dev Biol* **16**: 89-111.
138. Rowinsky EK. (1997) The development and clinical utility of the taxane class of antimicrotubule chemotherapy agents. *Annu Rev Med* **48**: 353-374.

139. Schiff PB, Fant J, Horwitz SB. (1979) Promotion of microtubule assembly in vitro by taxol. *Nature* **277**: 665-667.
140. Hung DT, Chen J, Schreiber SL. (1996) (+)-Discodermolide binds to microtubules in stoichiometric ratio to tubulin dimers, blocks taxol binding and results in mitotic arrest. *Chem Biol* **3**: 287-293.
141. Bollag DM, McQueney PA, Zhu J, et al. (1995) Epothilones, a new class of microtubule-stabilizing agents with a taxol-like mechanism of action. *Cancer Res* **55**: 2325-2333.
142. Mooberry SL, Tien G, Hernandez AH, Plubrukarn A, Davidson BS. (1999) Laulimalide and isolaulimalide, new paclitaxel-like microtubule-stabilizing agents. *Cancer Res* **59**: 653-660.
143. Duflos A, Kruczynski A, Barret JM. (2002) Novel aspects of natural and modified vinca alkaloids. *Curr Med Chem Anticancer Agents* **2**: 55-70.
144. Borisy GG, Taylor EW. (1967) The mechanism of action of colchicine. Binding of colchicine-3H to cellular protein. *J Cell Biol* **34**: 525-533.
145. Fotsis T, Zhang Y, Pepper MS, et al. (1994) The endogenous oestrogen metabolite 2-methoxyoestradiol inhibits angiogenesis and suppresses tumour growth. *Nature* **368**: 237-239.
146. Quasthoff S, Hartung HP. (2002) Chemotherapy-induced peripheral neuropathy. *J Neurol* **249**: 9-17.
147. Escuin D, Kline ER, Giannakakou P. (2005) Both microtubule-stabilizing and microtubule-destabilizing drugs inhibit hypoxia-inducible factor-1alpha accumulation and activity by disrupting microtubule function. *Cancer Res* **65**: 9021-9028.
148. Gray LH, Conger AD, Ebert M, Hornsey S, Scott OC. (1953) The concentration of oxygen dissolved in tissues at the time of irradiation as a factor in radiotherapy. *Br J Radiol* **26**: 638-648.
149. Brown JM, Wilson WR. (2004) Exploiting tumour hypoxia in cancer treatment. *Nat Rev Cancer* **4**: 437-447.
150. Wang GL, Jiang BH, Rue EA, Semenza GL. (1995) Hypoxia-inducible factor 1 is a basic-helix-loop-helix-PAS heterodimer regulated by cellular O₂ tension. *Proc Natl Acad Sci U S A* **92**: 5510-5514.
151. Wiener CM, Booth G, Semenza GL. (1996) In vivo expression of mRNAs encoding hypoxia-inducible factor 1. *Biochem Biophys Res Commun* **225**: 485-488.
152. Semenza GL. (2003) Targeting HIF-1 for cancer therapy. *Nat Rev Cancer* **3**: 721-732.
153. Harris AL. (2002) Hypoxia--a key regulatory factor in tumour growth. *Nat Rev Cancer* **2**: 38-47.
154. Iyer NV, Kotch LE, Agani F, et al. (1998) Cellular and developmental control of O₂ homeostasis by hypoxia-inducible factor 1 alpha. *Genes Dev* **12**: 149-162.
155. Ryan HE, Lo J, Johnson RS. (1998) HIF-1 alpha is required for solid tumor formation and embryonic vascularization. *EMBO J* **17**: 3005-3015.

156. Jaakkola P, Mole DR, Tian YM, et al. (2001) Targeting of HIF-alpha to the von Hippel-Lindau ubiquitylation complex by O₂-regulated prolyl hydroxylation. *Science* **292**: 468-472.
157. Ivan M, Kondo K, Yang H, et al. (2001) HIFalpha targeted for VHL-mediated destruction by proline hydroxylation: implications for O₂ sensing. *Science* **292**: 464-468.
158. Masson N, Willam C, Maxwell PH, Pugh CW, Ratcliffe PJ. (2001) Independent function of two destruction domains in hypoxia-inducible factor-alpha chains activated by prolyl hydroxylation. *EMBO J* **20**: 5197-5206.
159. Bruick RK, McKnight SL. (2001) A conserved family of prolyl-4-hydroxylases that modify HIF. *Science* **294**: 1337-1340.
160. Epstein AC, Gleadle JM, McNeill LA, et al. (2001) C. elegans EGL-9 and mammalian homologs define a family of dioxygenases that regulate HIF by prolyl hydroxylation. *Cell* **107**: 43-54.
161. Richard DE, Berra E, Gothie E, Roux D, Pouyssegur J. (1999) p42/p44 mitogen-activated protein kinases phosphorylate hypoxia-inducible factor 1alpha (HIF-1alpha) and enhance the transcriptional activity of HIF-1. *J Biol Chem* **274**: 32631-32637.
162. Park JH, Kim TY, Jong HS, et al. (2003) Gastric epithelial reactive oxygen species prevent normoxic degradation of hypoxia-inducible factor-1alpha in gastric cancer cells. *Clin Cancer Res* **9**: 433-440.
163. Brune B, Zhou J. (2003) The role of nitric oxide (NO) in stability regulation of hypoxia inducible factor-1alpha (HIF-1alpha). *Curr Med Chem* **10**: 845-855.
164. Chandel NS, McClintock DS, Feliciano CE, et al. (2000) Reactive oxygen species generated at mitochondrial complex III stabilize hypoxia-inducible factor-1alpha during hypoxia: a mechanism of O₂ sensing. *J Biol Chem* **275**: 25130-25138.
165. Bouvet M, Ellis LM, Nishizaki M, et al. (1998) Adenovirus-mediated wild-type p53 gene transfer down-regulates vascular endothelial growth factor expression and inhibits angiogenesis in human colon cancer. *Cancer Res* **58**: 2288-2292.
166. Zhong H, De Marzo AM, Laughner E, et al. (1999) Overexpression of hypoxia-inducible factor 1alpha in common human cancers and their metastases. *Cancer Res* **59**: 5830-5835.
167. Talks KL, Turley H, Gatter KC, et al. (2000) The expression and distribution of the hypoxia-inducible factors HIF-1alpha and HIF-2alpha in normal human tissues, cancers, and tumor-associated macrophages. *Am J Pathol* **157**: 411-421.
168. Sivridis E, Giatromanolaki A, Gatter KC, Harris AL, Koukourakis MI. (2002) Association of hypoxia-inducible factors 1alpha and 2alpha with activated angiogenic pathways and prognosis in patients with endometrial carcinoma. *Cancer* **95**: 1055-1063.
169. Bos R, Zhong H, Hanrahan CF, et al. (2001) Levels of hypoxia-inducible factor-1 alpha during breast carcinogenesis. *J Natl Cancer Inst* **93**: 309-314.

170. Bos R, van der Groep P, Greijer AE, et al. (2003) Levels of hypoxia-inducible factor-1alpha independently predict prognosis in patients with lymph node negative breast carcinoma. *Cancer* **97**: 1573-1581.
171. Schindl M, Schoppmann SF, Samonigg H, et al. (2002) Overexpression of hypoxia-inducible factor 1alpha is associated with an unfavorable prognosis in lymph node-positive breast cancer. *Clin Cancer Res* **8**: 1831-1837.
172. Kurokawa T, Miyamoto M, Kato K, et al. (2003) Overexpression of hypoxia-inducible-factor 1alpha(HIF-1alpha) in oesophageal squamous cell carcinoma correlates with lymph node metastasis and pathologic stage. *Br J Cancer* **89**: 1042-1047.
173. Zundel W, Schindler C, Haas-Kogan D, et al. (2000) Loss of PTEN facilitates HIF-1-mediated gene expression. *Genes Dev* **14**: 391-396.
174. Jiang BH, Jiang G, Zheng JZ, Lu Z, Hunter T, Vogt PK. (2001) Phosphatidylinositol 3-kinase signaling controls levels of hypoxia-inducible factor 1. *Cell Growth Differ* **12**: 363-369.
175. Zhong H, Semenza GL, Simons JW, De Marzo AM. (2004) Up-regulation of hypoxia-inducible factor 1alpha is an early event in prostate carcinogenesis. *Cancer Detect Prev* **28**: 88-93.
176. Richard S, Campello C, Taillandier L, Parker F, Resche F. (1998) Haemangioblastoma of the central nervous system in von Hippel-Lindau disease. French VHL Study Group. *J Intern Med* **243**: 547-553.
177. Escuin D, Simons JW, Giannakakou P. (2004) Exploitation of the HIF axis for cancer therapy. *Cancer Biol Ther* **3**: 608-611.
178. Rapisarda A, Uranchimeg B, Scudiero DA, et al. (2002) Identification of small molecule inhibitors of hypoxia-inducible factor 1 transcriptional activation pathway. *Cancer Res* **62**: 4316-4324.
179. Minet E, Mottet D, Michel G, et al. (1999) Hypoxia-induced activation of HIF-1: role of HIF-1alpha-Hsp90 interaction. *FEBS Lett* **460**: 251-256.
180. Isaacs JS, Jung YJ, Mimnaugh EG, Martinez A, Cuttitta F, Neckers LM. (2002) Hsp90 regulates a von Hippel Lindau-independent hypoxia-inducible factor-1 alpha-degradative pathway. *J Biol Chem* **277**: 29936-29944.
181. Mabeesh NJ, Post DE, Willard MT, et al. (2002) Geldanamycin induces degradation of hypoxia-inducible factor 1alpha protein via the proteasome pathway in prostate cancer cells. *Cancer Res* **62**: 2478-2482.
182. Jones MK, Szabo IL, Kawanaka H, Husain SS, Tarnawski AS. (2002) von Hippel Lindau tumor suppressor and HIF-1alpha: new targets of NSAIDs inhibition of hypoxia-induced angiogenesis. *FASEB J* **16**: 264-266.
183. Palayoor ST, Tofilon PJ, Coleman CN. (2003) Ibuprofen-mediated reduction of hypoxia-inducible factors HIF-1alpha and HIF-2alpha in prostate cancer cells. *Clin Cancer Res* **9**: 3150-3157.

184. Adams BK, Ferstl EM, Davis MC, et al. (2004) Synthesis and biological evaluation of novel curcumin analogs as anti-cancer and anti-angiogenesis agents. *Bioorg Med Chem* **12**: 3871-3883.
185. Gawlitta D, Oomens CW, Baaijens FP, Bouten CV. (2004) Evaluation of a continuous quantification method of apoptosis and necrosis in tissue cultures. *Cytotechnology* **46**: 139-150.
186. Mabeesh NJ, Escuin D, LaVallee TM, et al. (2003) 2ME2 inhibits tumor growth and angiogenesis by disrupting microtubules and dysregulating HIF. *Cancer Cell* **3**: 363-375.
187. Post DE, Van Meir EG. (2001) Generation of bidirectional hypoxia/HIF-responsive expression vectors to target gene expression to hypoxic cells. *Gene Ther* **8**: 1801-1807.
188. Hamel E, Lin CM. (1984) Separation of active tubulin and microtubule-associated proteins by ultracentrifugation and isolation of a component causing the formation of microtubule bundles. *Biochemistry* **23**: 4173-4184.
189. Hamel E. (2003) Evaluation of antimitotic agents by quantitative comparisons of their effects on the polymerization of purified tubulin. *Cell Biochem Biophys* **38**: 1-22.
190. Chen YR, Tan TH. (1998) Inhibition of the c-Jun N-terminal kinase (JNK) signaling pathway by curcumin. *Oncogene* **17**: 173-178.
191. Squires MS, Hudson EA, Howells L, et al. (2003) Relevance of mitogen activated protein kinase (MAPK) and phosphatidylinositol-3-kinase/protein kinase B (PI3K/PKB) pathways to induction of apoptosis by curcumin in breast cells. *Biochem Pharmacol* **65**: 361-376.
192. Chen YR, Tan TH. (2000) The c-Jun N-terminal kinase pathway and apoptotic signaling (review). *Int J Oncol* **16**: 651-662.
193. Bost F, McKay R, Bost M, Potapova O, Dean NM, Mercola D. (1999) The Jun kinase 2 isoform is preferentially required for epidermal growth factor-induced transformation of human A549 lung carcinoma cells. *Mol Cell Biol* **19**: 1938-1949.
194. Bost F, McKay R, Dean N, Mercola D. (1997) The JUN kinase/stress-activated protein kinase pathway is required for epidermal growth factor stimulation of growth of human A549 lung carcinoma cells. *J Biol Chem* **272**: 33422-33429.
195. Bain J, McLauchlan H, Elliott M, Cohen P. (2003) The specificities of protein kinase inhibitors: an update. *Biochem J* **371**: 199-204.
196. Craig R, Larkin A, Mingo AM, et al. (2000) p38 MAPK and NF-kappa B collaborate to induce interleukin-6 gene expression and release. Evidence for a cytoprotective autocrine signaling pathway in a cardiac myocyte model system. *J Biol Chem* **275**: 23814-23824.
197. Singer CA, Baker KJ, McCaffrey A, AuCoin DP, Dechert MA, Gerthoffer WT. (2003) p38 MAPK and NF-kappaB mediate COX-2 expression in human airway myocytes. *Am J Physiol Lung Cell Mol Physiol* **285**: L1087-1098.

198. Fabian MA, Biggs WH, 3rd, Treiber DK, et al. (2005) A small molecule-kinase interaction map for clinical kinase inhibitors. *Nat Biotechnol* **23**: 329-336.
199. Hansen RK, Oesterreich S, Lemieux P, Sarge KD, Fuqua SA. (1997) Quercetin inhibits heat shock protein induction but not heat shock factor DNA-binding in human breast carcinoma cells. *Biochem Biophys Res Commun* **239**: 851-856.
200. Hosokawa N, Hirayoshi K, Nakai A, et al. (1990) Flavonoids inhibit the expression of heat shock proteins. *Cell Struct Funct* **15**: 393-401.
201. Hosokawa N, Hirayoshi K, Kudo H, et al. (1992) Inhibition of the activation of heat shock factor in vivo and in vitro by flavonoids. *Mol Cell Biol* **12**: 3490-3498.
202. Kim do Y, Kim KH, Kim ND, et al. (2006) Design and biological evaluation of novel tubulin inhibitors as antimetabolic agents using a pharmacophore binding model with tubulin. *J Med Chem* **49**: 5664-5670.
203. Lawrence NJ, McGown AT, Ducki S, Hadfield JA. (2000) The interaction of chalcones with tubulin. *Anticancer Drug Des* **15**: 135-141.
204. Giannakakou P, Sackett DL, Kang YK, et al. (1997) Paclitaxel-resistant human ovarian cancer cells have mutant beta-tubulins that exhibit impaired paclitaxel-driven polymerization. *J Biol Chem* **272**: 17118-17125.
205. Piperno G, LeDizet M, Chang XJ. (1987) Microtubules containing acetylated alpha-tubulin in mammalian cells in culture. *J Cell Biol* **104**: 289-302.
206. Giannakakou P, Gussio R, Nogales E, et al. (2000) A common pharmacophore for epothilone and taxanes: molecular basis for drug resistance conferred by tubulin mutations in human cancer cells. *Proc Natl Acad Sci U S A* **97**: 2904-2909.
207. Bae MK, Kim SH, Jeong JW, et al. (2006) Curcumin inhibits hypoxia-induced angiogenesis via down-regulation of HIF-1. *Oncol Rep* **15**: 1557-1562.
208. Choi H, Chun YS, Kim SW, Kim MS, Park JW. (2006) Curcumin inhibits hypoxia-inducible factor-1 by degrading aryl hydrocarbon receptor nuclear translocator: a mechanism of tumor growth inhibition. *Mol Pharmacol* **70**: 1664-1671.
209. Kim WY, Kaelin WG. (2004) Role of VHL gene mutation in human cancer. *J Clin Oncol* **22**: 4991-5004.
210. Semenza GL. (2007) Evaluation of HIF-1 inhibitors as anticancer agents. *Drug Discov Today* **12**: 853-859.
211. Gupta KK, Bharne SS, Rathinasamy K, Naik NR, Panda D. (2006) Dietary antioxidant curcumin inhibits microtubule assembly through tubulin binding. *FEBS J* **273**: 5320-5332.
212. Hergovich A, Lisztwan J, Barry R, Ballschmieter P, Krek W. (2003) Regulation of microtubule stability by the von Hippel-Lindau tumour suppressor protein pVHL. *Nat Cell Biol* **5**: 64-70.
213. Kohno T, Takahashi M, Manda R, Yokota J. (1998) Inactivation of the PTEN/MMAC1/TEP1 gene in human lung cancers. *Genes Chromosomes Cancer* **22**: 152-156.

214. Martinez A, Lehman TA, Modali R, Mulshine JL. (2003) Screening of mutations in the ras family of oncogenes by polymerase chain reaction-based ligase chain reaction. *Methods Mol Med* **74**: 187-200.
215. Slebos RJ, Hoppin JA, Tolbert PE, et al. (2000) K-ras and p53 in pancreatic cancer: association with medical history, histopathology, and environmental exposures in a population-based study. *Cancer Epidemiol Biomarkers Prev* **9**: 1223-1232.